SECTION 15
CABLE-SUSPENDED BRIDGES

Walter Podolny, Jr., P.E.
Senior Structural Engineer, Office of Bridge Technology,
Federal Highway Administration,
U.S. Department of Transportation, Washington, D.C.

Few structures are as universally appealing as cable-supported bridges. The origin of the concept of bridging large spans with cables, exerting their strength in tension, is lost in antiquity and undoubtedly dates back to a time before recorded history. Perhaps primitive humans, wanting to cross natural obstructions such as deep gorges and large streams, observed a spider spinning a web or monkeys traveling along hanging vines.

15.1 EVOLUTION OF CABLE-SUSPENDED BRIDGES

Early cable-suspended bridges were footbridges consisting of cables formed from twisted vines or hide drawn tightly to reduce sag. The cable ends were attached to trees or other permanent objects located on the banks of rivers or at the edges of gorges or other natural obstructions to travel. The deck, probably of rough-hewn plank, was laid directly on the cable. This type of construction was used in remote ages in China, Japan, India, and Tibet. It was used by the Aztecs of Mexico, the Incas of Peru, and by natives in other parts of South America. It can still be found in remote areas of the world.

From the sixteenth to nineteenth centuries, military engineers made effective use of rope suspension bridges. In 1734, the Saxon army built an iron-chain bridge over the Oder River at Glorywitz, reportedly the first use in Europe of a bridge with a metal suspension system. However, iron chains were used much earlier in China. The first metal suspension bridge in North America was the Jacob's Creek Bridge in Pennsylvania, designed and erected by James Finley in 1801. Supported by two suspended chains of wrought-iron links, its 70-ft span was stiffened by substantial trussed railing and timber planks.

Chains and flat wrought-iron bars dominated suspension-bridge construction for some time after that. Construction of this type was used by Thomas Telford in 1826 for the noted Menai Straits Bridge, with a main span of 580 ft. But 10 years before, in 1816, the first wire suspension bridges were built, one at Galashiels, Scotland, and a second over the Schuylkill River in Philadelphia.

A major milestone in progress with wire cable was passed with erection of the 1,010-ft suspended span of the Ohio River Bridge at Wheeling, Va. (later W.Va.), by Charles Ellet, Jr., in 1849. A second important milestone was the opening in 1883 of the 1,595.5-ft wire-cable-supported span of the Brooklyn Bridge, built by the Roeblings.

In 1607, a Venetian engineer named Faustus Verantius published a description of a suspended bridge partly supported with several diagonal chain stays (Fig. 15.1*a*). The stays in that case were used in combination with a main supporting suspension (catenary) cable. The first use of a pure stayed bridge is credited to Löscher, who built a timber-stayed bridge in 1784 with a span of 105 ft (Fig. 15.2*a*). The pure-stayed-bridge concept was apparently not used again until 1817 when two British engineers, Redpath and Brown, constructed the King's Meadow Footbridge (Fig. 15.1*b*) with a span of about 110 ft. This structure utilized sloping wire cable stays attached to cast-iron towers. In 1821, the French architect, Poyet, suggested a pure cable-stayed bridge (Fig. 15.2*b*) using bar stays suspended from high towers.

The pure cable-stayed bridge might have become a conventional form of bridge construction had it not been for an unfortunate series of circumstances. In 1818, a composite suspension and stayed pedestrian bridge crossing the Tweed River near Dryburgh-Abbey, England (Fig. 15.1*c*) collapsed as a result of wind action. In 1824, a cable-stayed bridge crossing the Saale River near Nienburg, Germany (Fig. 15.1*d*) collapsed, presumably from overloading. The famous French engineer C. L. M. H. Navier published in 1823 a prestigious work wherein his adverse comments on the failures of several cable-stayed bridges virtually condemned the use of cable stays to obscurity.

Despite Navier's adverse criticism of stayed bridges, a few more were built shortly after the fatal collapses of the bridges in England and Germany, for example, the Gischlard-Arnodin cable bridge (Fig. 15.2*c*) with multiple sloping cables hung from two masonry towers. In 1840, Hatley, an Englishman, used chain stays in a parallel configuration resembling harp strings (Fig. 15.2*d*). He maintained the parallel spacing of the main stays by using a closely spaced subsystem anchored to the deck and perpendicular to the principal load-carrying cables.

The principle of using stays to support a bridge superstructure did not die completely in the minds of engineers. John Roebling incorporated the concept in his suspension bridges, such as his Niagara Falls Bridge (Fig. 15.3); the Old St. Clair Bridge in Pittsburgh (Fig. 15.4); the Cincinnati Bridge across the Ohio River, and the Brooklyn Bridge in New York. The stays were used in addition to vertical suspenders to support the bridge superstructure. Observations of performance indicated that the stays and suspenders were not efficient partners. Consequently, although the stays were comforting safety measures in the early bridges, in the later development of conventional catenary suspension bridges the stays were omitted. The conventional suspension bridge was dominant until the latter half of the twentieth century.

The virtual banishment of stayed bridges during the nineteenth and early twentieth centuries can be attributed to the lack of sound theoretical analyses for determination of the internal forces of the total system. The failure to understand the behavior of the stayed system and the lack of methods for controlling the equilibrium and compatibility of the various highly indeterminate structural components appear to have been the major drawback to further development of the concept. Furthermore, the materials of the period were not suitable for stayed bridges.

Rebirth of stayed bridges appears to have begun in 1938 with the work of the German engineer Franz Dischinger. While designing a suspension bridge to cross the Elbe River near Hamburg (Fig. 15.5), Dischinger determined that the vertical deflection of the bridge under railroad loading could be reduced considerably by incorporating cable stays in the suspension system. From these studies and his later design of the Strömsund Bridge in Sweden (1955) evolved the modern cable-stayed bridge. However, the biggest impetus for cable-stayed bridges came in Germany after World War II with the design and construction of bridges to replace those that had been destroyed in the conflict.

(W. Podolny, Jr., and J. B. Scalzi, "Construction and Design of Cable-Stayed Bridges," 2d ed., John Wiley & Sons, Inc., New York; R. Walther et al., "Cable-Stayed Bridges," Thomas Telford, London; D. P. Billington and A. Nazmy, "History and Aesthetics of Cable-Stayed Bridges," *Journal of Structural Engineering,* vol. 117, no. 10, October 1990, American Society of Civil Engineers.)

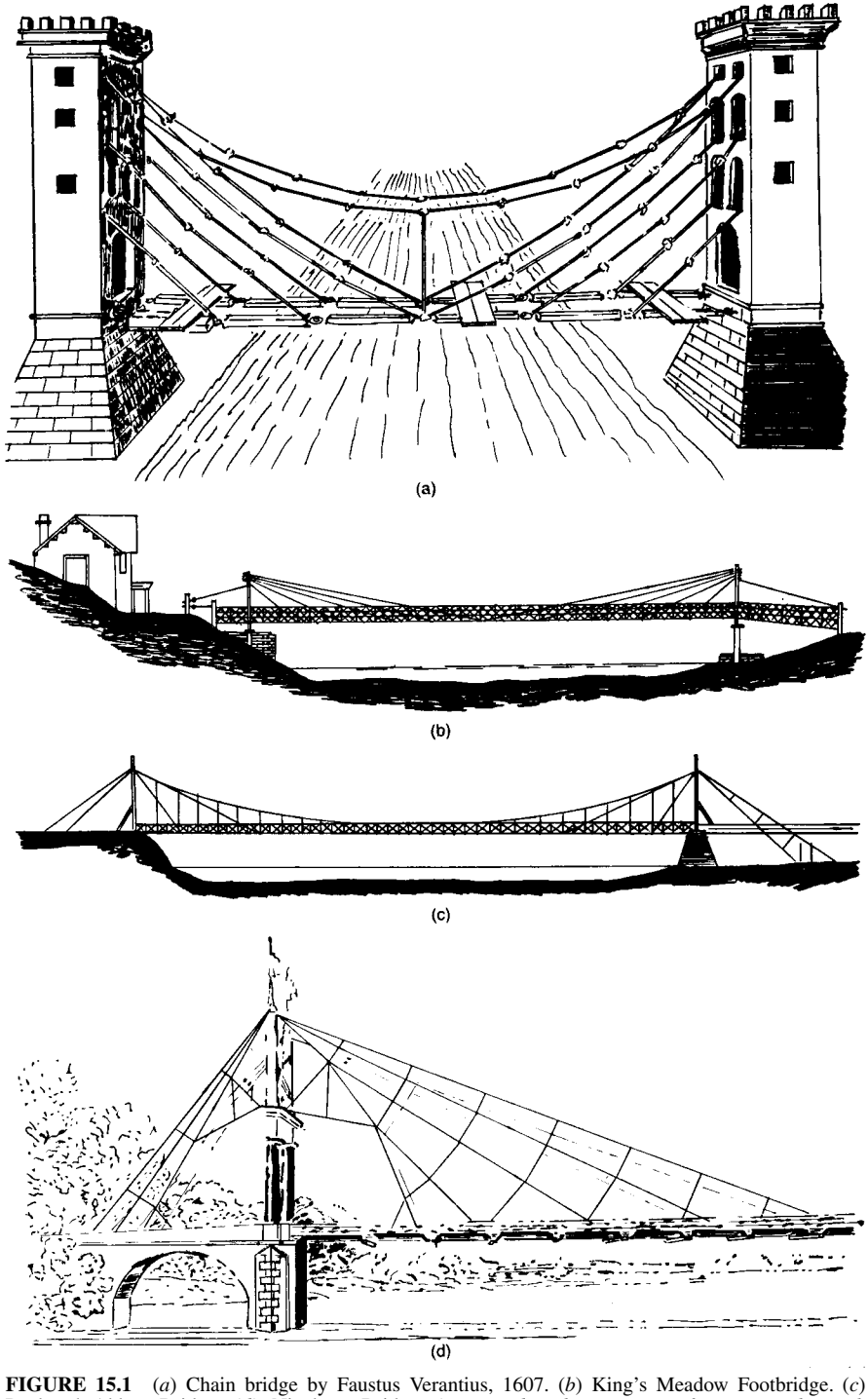

FIGURE 15.1 (*a*) Chain bridge by Faustus Verantius, 1607. (*b*) King's Meadow Footbridge. (*c*) Dryburgh-Abbey Bridge. (*d*) Nienburg Bridge. (*Reprinted with permission from K. Roik et al. "Schrägseilbrüchen," Wilhelm Ernst & Sohn, Berlin.*)

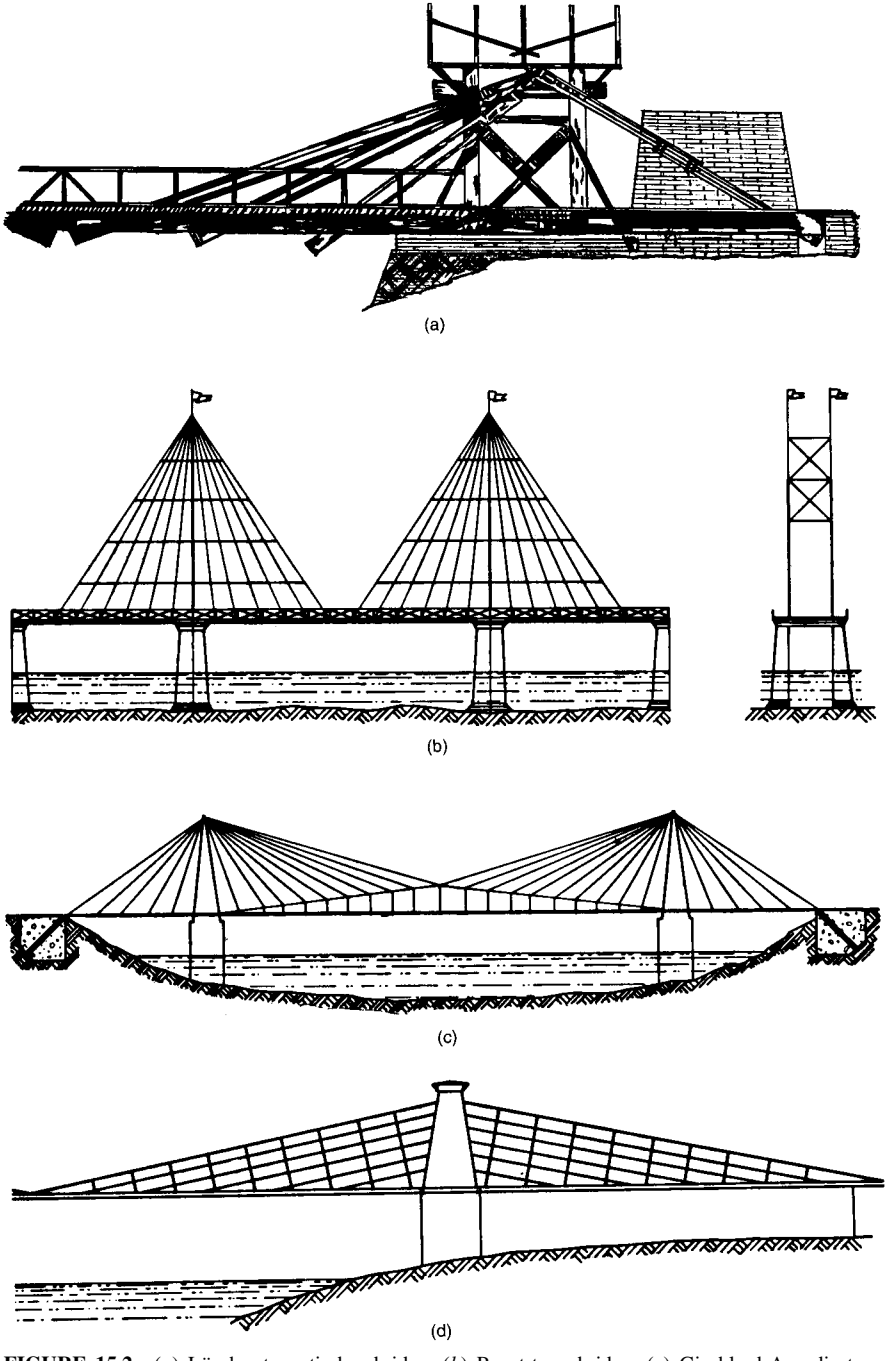

FIGURE 15.2 (*a*) Löscher-type timber bridge. (*b*) Poyet-type bridge. (*c*) Gischlard-Arnodin-type sloping-cable bridge. (*d*) Hatley chain bridge. (*Reprinted with permission from H. Thul, "Cable-Stayed Bridges in Germany," Proceedings of the Conference on Structural Steelwork, 1966. The British Constructional Steelwork Association, Ltd., London.*)

FIGURE 15.3 Niagara Falls Bridge.

15.2 CLASSIFICATION OF CABLE-SUSPENDED BRIDGES

Cable-suspended bridges that rely on very high strength steel cables as major structural elements may be classified as suspension bridges or cable-stayed bridges. The fundamental difference between these two classes is the manner in which the bridge deck is supported by the cables. In suspension bridges, the deck is supported at relatively short intervals by

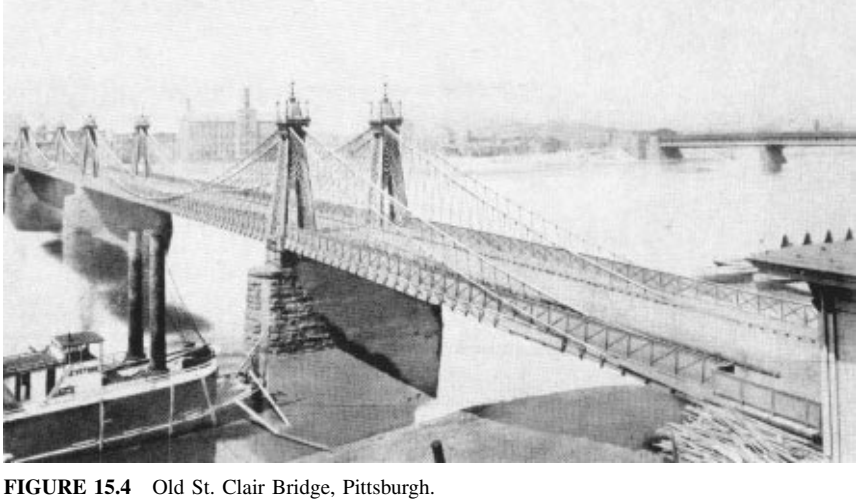

FIGURE 15.4 Old St. Clair Bridge, Pittsburgh.

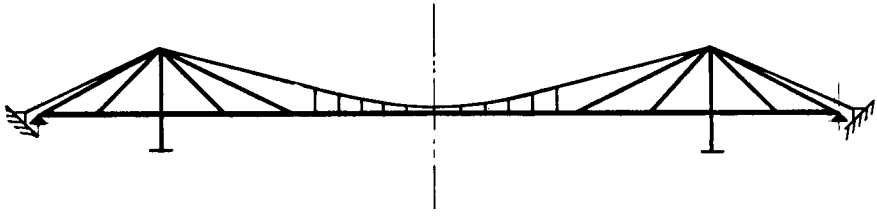

FIGURE 15.5 Bridge system proposed by Dischinger. (*Reprinted with permission from F. Dischinger, "Hangebrüchen for Schwerste Verkehrslasten," Der Bauingenieur, Heft 3 and 4, 1949.*)

vertical suspenders, which, in turn, are supported from a main cable (Fig. 15.6*a*). The main cables are relatively flexible and thus take a profile shape that is a function of the magnitude and position of loading. Inclined cables of the cable-stayed bridge (Fig. 15.6*b*), support the bridge deck directly with relatively taut cables, which, compared to the classical suspension bridge, provide relatively inflexible supports at several points along the span. The nearly linear geometry of the cables produces a bridge with greater stiffness than the corresponding suspension bridge.

Cable-suspended bridges are generally characterized by economy, lightness, and clarity of structural action. These types of structures illustrate the concept of form following function and present graceful and esthetically pleasing appearance. Each of these types of cable-suspended bridges may be further subclassified; those subclassifications are presented in articles that follow.

Many early cable-suspended bridges were a combination of the suspension and cable-stayed systems (Art. 15.1). Such combinations can offer even greater resistance to dynamic loadings and may be more efficient for very long spans than either type alone. The only contemporary bridge of this type is Steinman's design for the Salazar Bridge across the Tagus River in Portugal. The present structure, a conventional suspension bridge, is indicated in Fig. 15.7*a* In the future, cable stays are to be installed to accommodate additional rail traffic (Fig. 15.7*b*).

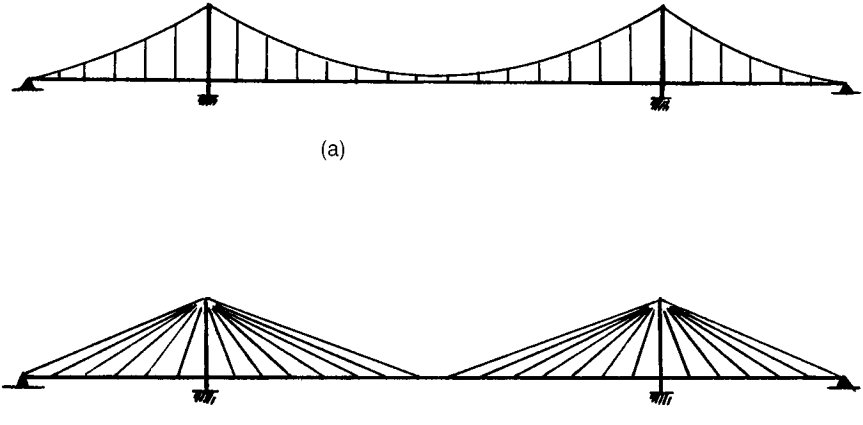

FIGURE 15.6 Cable-suspended bridge systems: (*a*) suspension and (*b*) cable-stayed. (*Reprinted with permission from W. Podolny, Jr. and J. B. Scalzi, "Construction and Design of Cable-Stayed Bridges," 2d ed., John Wiley & Sons, Inc., New York.*)

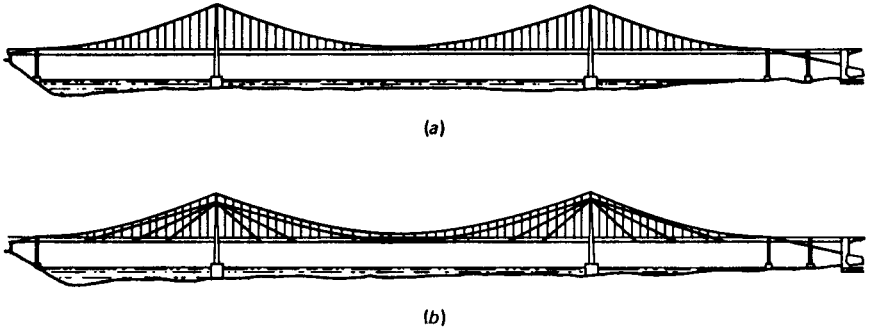

FIGURE 15.7 The Salazar Bridge. (*a*) elevation of the bridge in 1993; (*b*) elevation of future bridge. (*Reprinted with permission from W. Podolny, Jr., and J. B. Scalzi, "Construction and Design of Cable-Stayed Bridges," John Wiley & Sons, Inc., New York.*)

(W. Podolny, Jr., and J. B. Scalzi, "Construction and Design of Cable-Stayed Bridges," 2nd ed., John Wiley & Sons, Inc., New York.)

15.3 CLASSIFICATION AND CHARACTERISTICS OF SUSPENSION BRIDGES

Suspension bridges with cables made of high-strength, zinc-coated, steel wires are suitable for the longest of spans. Such bridges usually become economical for spans in excess of 1000 ft, depending on specific site constraints. Nevertheless, many suspension bridges with spans as short as 300 or 400 ft have been built, to take advantage of their esthetic features.

The basic economic characteristic of suspension bridges, resulting from use of high-strength materials in tension, is lightness, due to relatively low dead load. But this, in turn, carries with it the structural penalty of flexibility, which can lead to large deflections under live load and susceptibility to vibrations. As a result, suspension bridges are more suitable for highway bridges than for the more heavily loaded railroad bridges. Nevertheless, for either highway or railroad bridges, care must be taken in design to provide resistance to wind- or seismic-induced oscillations, such as those that caused collapse of the first Tacoma Narrows Bridge in 1940.

15.3.1 Main Components of Suspension Bridges

A pure suspension bridge is one without supplementary stay cables and in which the main cables are anchored externally to anchorages on the ground. The main components of a suspension bridge are illustrated in Fig. 15.8. Most suspension bridges are stiffened; that is, as shown in Fig. 15.8, they utilize horizontal stiffening trusses or girders. Their function is to equalize deflections due to concentrated live loads and distribute these loads to one or more main cables. The stiffer these trusses or girders are, relative to the stiffness of the cables, the better this function is achieved. (Cables derive stiffness not only from their cross-sectional dimensions but also from their shape between supports, which depends on both cable tension and loading.)

For heavy, very long suspension spans, live-load deflections may be small enough that stiffening trusses would not be needed. When such members are omitted, the structure is an unstiffened suspension bridge. Thus, if the ratio of live load to dead load were, say, 1:4, the midspan deflection would be of the order of $\frac{1}{100}$ of the sag, or 1/1,000 of the span, and the

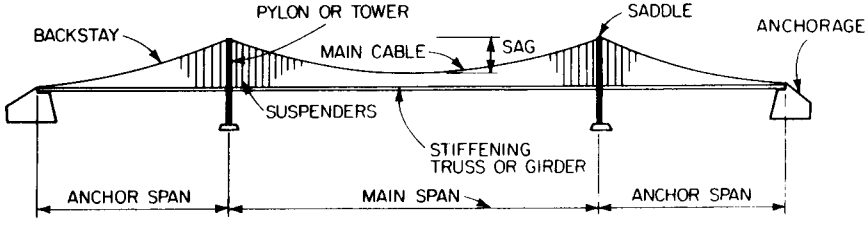

FIGURE 15.8 Main components of a suspension bridge.

use of stiffening trusses would ordinarily be unnecessary. (For the George Washington Bridge as initially constructed, the ratio of live load to dead load was approximately 1:6. Therefore, it did not need a stiffening truss.)

15.3.2 Types of Suspension Bridges

Several arrangements of suspension bridges are illustrated in Fig. 15.9. The main cable is continuous, over saddles at the pylons, or towers, from anchorage to anchorage. When the main cable in the side spans does not support the bridge deck (side spans independently supported by piers), that portion of the cable from the saddle to the anchorage is virtually straight and is referred to as a straight backstay. This is also true in the case shown in Fig. 15.9*a* where there are no side spans.

Figure 15.9*d* represents a multispan bridge. This type is not considered efficient, because its flexibility distributes an undesirable portion of the load onto the stiffening trusses and may make horizontal ties necessary at the tops of the pylons. Ties were used on several French multispan suspension bridges of the nineteenth century. However, it is doubtful whether tied towers would be esthetically acceptable to the general public. Another approach to multispan suspension bridges is that used for the San Francisco–Oakland Bay Bridge (Fig.

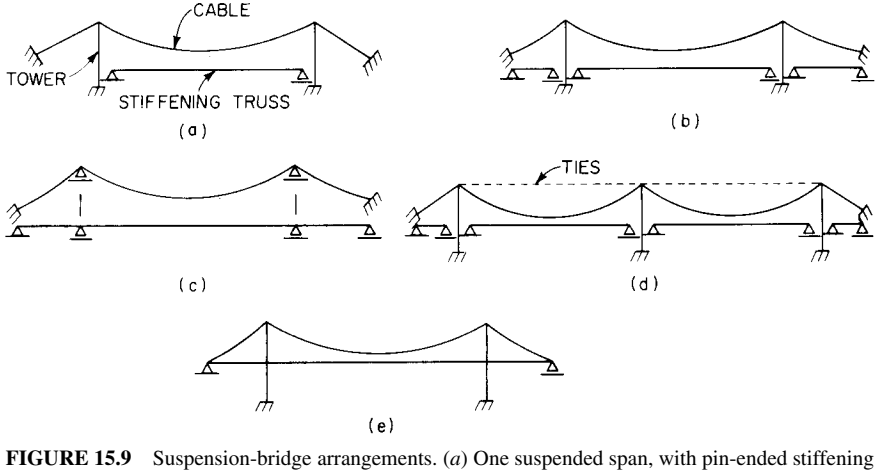

FIGURE 15.9 Suspension-bridge arrangements. (*a*) One suspended span, with pin-ended stiffening truss. (*b*) Three suspended spans, with pin-ended stiffening trusses. (*c*) Three suspended spans, with continuous stiffening truss. (*d*) Multispan bridge, with pin-ended stiffening trusses. (*e*) Self-anchored suspension bridge.

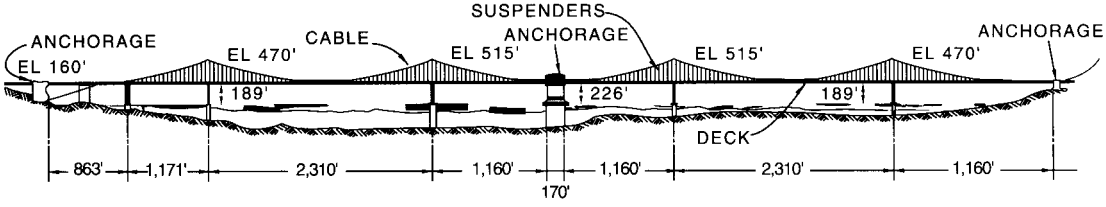

FIGURE 15.10 San Francisco-Oakland Bay Bridge.

15.10). It is essentially composed of two three-span suspension bridges placed end to end. This system has the disadvantage of requiring three piers in the central portion of the structure where water depths are likely to be a maximum.

Suspension bridges may also be classified by type of cable anchorage, external or internal. Most suspension bridges are *externally anchored* (earth-anchored) to a massive external anchorage (Fig. 15.9*a* to *d*). In some bridges, however, the ends of the main cables of a suspension bridge are attached to the stiffening trusses, as a result of which the structure becomes *self-anchored* (Fig. 15.9*e*). It does not require external anchorages.

The stiffening trusses of a self-anchored bridge must be designed to take the compression induced by the cables. The cables are attached to the stiffening trusses over a support that resists the vertical component of cable tension. The vertical upward component may relieve or even exceed the dead-load reaction at the end support. If a net uplift occurs, a pendulum-link tie-down should be provided at the end support.

Self-anchored suspension bridges are suitable for short to moderate spans (400 to 1,000 ft) where foundation conditions do not permit external anchorages. Such conditions include poor foundation-bearing strata and loss of weight due to anchorage submergence. Typical examples of self-anchored suspension bridges are the Paseo Bridge at Kansas City, with a main span of 616 ft, and the former Cologne-Mülheim Bridge (1929) with a 1,033-ft span.

Another type of suspension bridge is referred to as a *bridle-chord bridge.* Called by Germans *Zügelgurtbrücke,* these structures are typified by the bridge over the Rhine River at Ruhrort-Homberg (Fig. 15.11), erected in 1953, and the one at Krefeld-Urdingen, erected in 1950. It is a special class of bridge, intermediate between the suspension and cable-stayed types and having some of the characteristics of both. The main cables are curved but not continuous between towers. Each cable extends from the tower to a span, as in a cable-stayed bridge. The span, however, also is suspended from the cables at relatively short intervals over the length of the cables, as in suspension bridges.

A distinction to be made between some early suspension bridges and modern suspension bridges involves the position of the main cables in profile at midspan with respect to the stiffening trusses. In early suspension bridges, the bottom of the main cables at maximum sag penetrated the top chord of the stiffening trusses and continued down to the bottom chord (Fig. 15.5, for example). Because of the design theory available at the time, the depth of the stiffening trusses was relatively large, as much as 1/40 of the span. Inasmuch as the height of the pylons is determined by the sag of the cables and clearance required under the stiffening trusses, moving the midspan location of the cables from the bottom chord to the

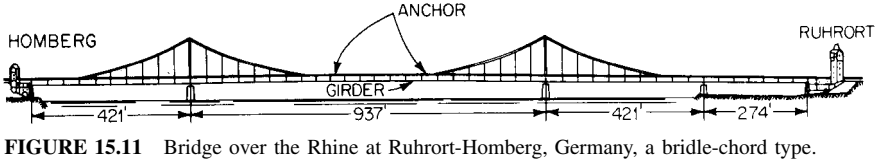

FIGURE 15.11 Bridge over the Rhine at Ruhrort-Homberg, Germany, a bridle-chord type.

top chord increases the pylon height by the depth of the stiffening trusses. In modern suspension bridges, stiffening trusses are much shallower than those used in earlier bridges and the increase in pylon height due to midspan location of the cables is not substantial (as compared with the effect in the Williamsburg Bridge in New York City where the depth of the stiffening trusses is 25% of the main-cable sag).

Although most suspension bridges employ vertical suspender cables to support the stiffening trusses or the deck structural framing directly (Fig. 15.8), a few suspension bridges, for example, the Severn Bridge in England and the Bosporus Bridge in Turkey, have inclined or diagonal suspenders (Fig. 15.12). In the vertical-suspender system, the main cables are incapable of resisting shears resulting from external loading. Instead, the shears are resisted by the stiffening girders or by displacement of the main cables. In bridges with inclined suspenders, however, a truss action is developed, enabling the suspenders to resist shear. (Since the cables can support loads only in tension, design of such bridges should ensure that there always is a residual tension in the suspenders; that is, the magnitude of the compression generated by live-load shears should be less than the dead-load tension.) A further advantage of the inclined suspenders is the damping properties of the system with respect to aerodynamic oscillations.

(N. J. Gimsing, ''Cable-Supported Bridges—Concept and Design,'' John Wiley & Sons, Inc., New York.)

15.3.3 Suspension Bridge Cross Sections

Figure 15.13 shows typical cross sections of suspension bridges. The bridges illustrated in Fig. 15.13*a*, *b*, and *c* have stiffening trusses, and the bridge in Fig. 15.13*d* has a steel box-girder deck. Use of plate-girder stiffening systems, forming an H-section deck with horizontal web, was largely superseded after the Tacoma Narrows Bridge failure by truss and box-girder stiffening systems for long-span bridges. The H deck, however, is suitable for short spans.

The Verrazano Narrows Bridge (Fig. 15.13*a*), employs 6-in-deep, concrete-filled, steel-grid flooring on steel stringers to achieve strength, stiffness, durability, and lightness. The double-deck structure has top and bottom lateral trusses. These, together with the transverse beams, stringers, cross frames, and stiffening trusses, are conceived to act as a tube resisting vertical, lateral, and torsional forces. The cross frames are rigid frames with a vertical member in the center.

The Mackinac Bridge (Fig. 15.13*b*) employs a 4¼-in. steel-grid flooring. The outer two lanes were filled with lightweight concrete and topped with bituminous-concrete surfacing. The inner two lanes were left open for aerodynamic venting and to reduce weight. The single deck is supported by stiffening trusses with top and bottom lateral bracing as well as ample cross bracing.

The Triborough Bridge (Fig. 15.13*c*) has a reinforced-concrete deck carried by floorbeams supported at the lower panel points of through stiffening trusses.

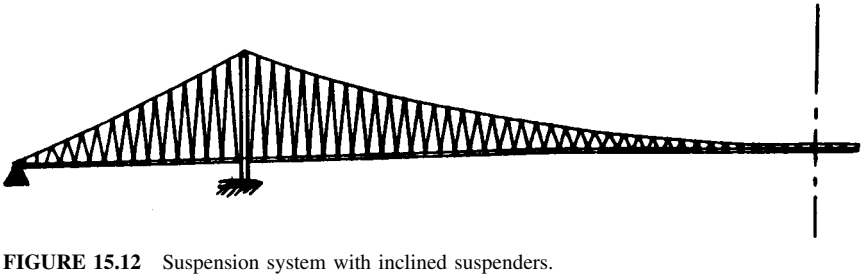

FIGURE 15.12 Suspension system with inclined suspenders.

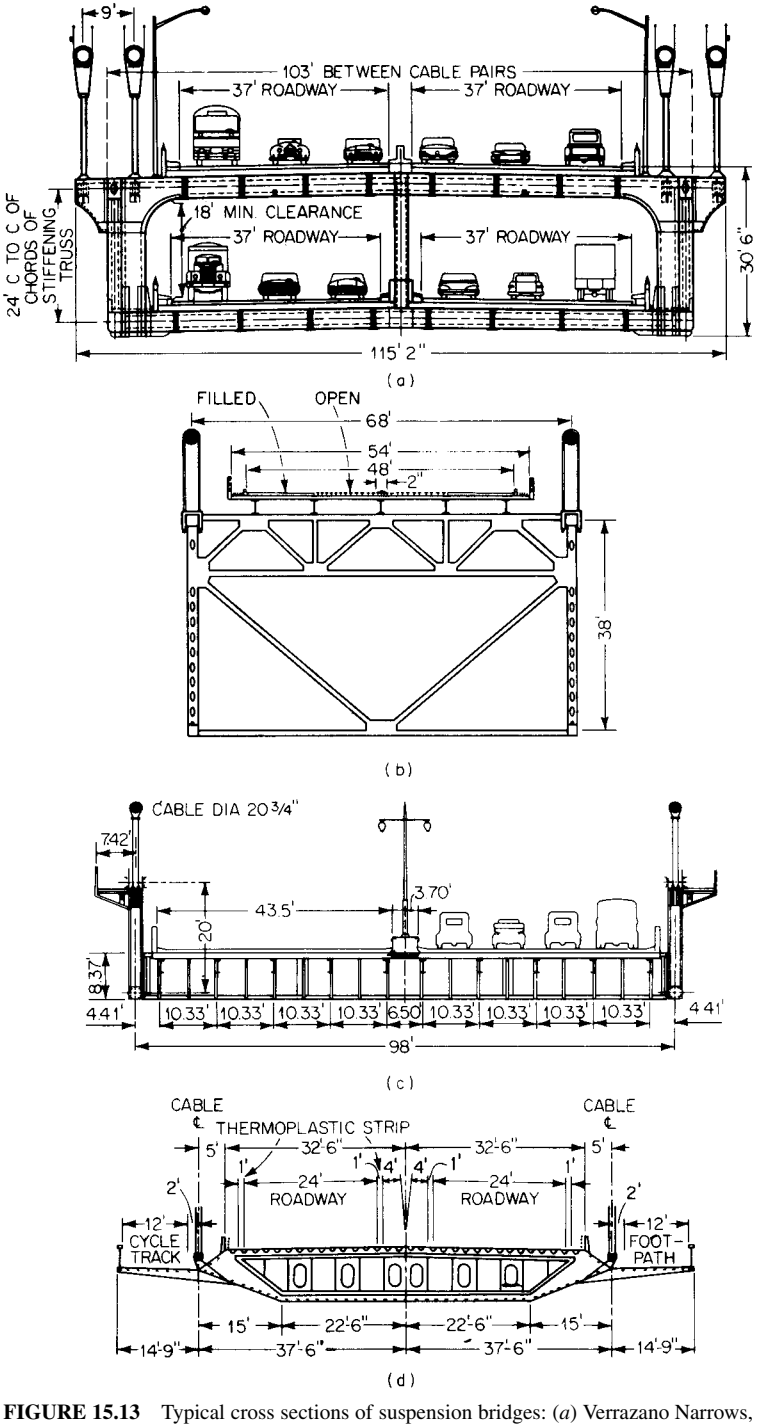

FIGURE 15.13 Typical cross sections of suspension bridges: (*a*) Verrazano Narrows, (*b*) Mackinac, (*c*) Triborough, (*d*) Severn.

The Severn Bridge (Fig. 15.13*d*) employs a 10-ft-deep torsion-resisting box girder to support an orthotropic-plate deck. The deck plate is stiffened by steel trough shapes, and the remaining plates, by flat-bulb stiffeners. The box was faired to achieve the best aerodynamic characteristics.

15.3.4 Suspension Bridge Pylons

Typical pylon configurations, shown in Fig. 15.14, are portal frames. For economy, pylons should have the minimum width in the direction of the span consistent with stability but sufficient width at the top to take the cable saddle.

Most suspension bridges have cables fixed at the top of the pylons. With this arrangement, because of the comparative slenderness of pylons, top deflections do not produce large stresses. It is possible to use rocker pylons, pinned at the base and top, but they are restricted to use with short spans. Also, pylons fixed at the base and with roller saddles at the top are possible, but limited to use with medium spans. The pylon legs may, in any event, be tapered to allow for the decrease in area required toward the top.

The statical action of the pylon and the design of details depend on the end conditions.

Simply supported, main-span stiffening trusses are frequently suspended from the pylons on short pendulum hangers. Dependence is placed primarily on the short center-span suspenders to keep the trusses centered. In this way, temperature effects on the pylon can be reduced by half.

A list of major modern suspension bridges is provided in Table 15.1.

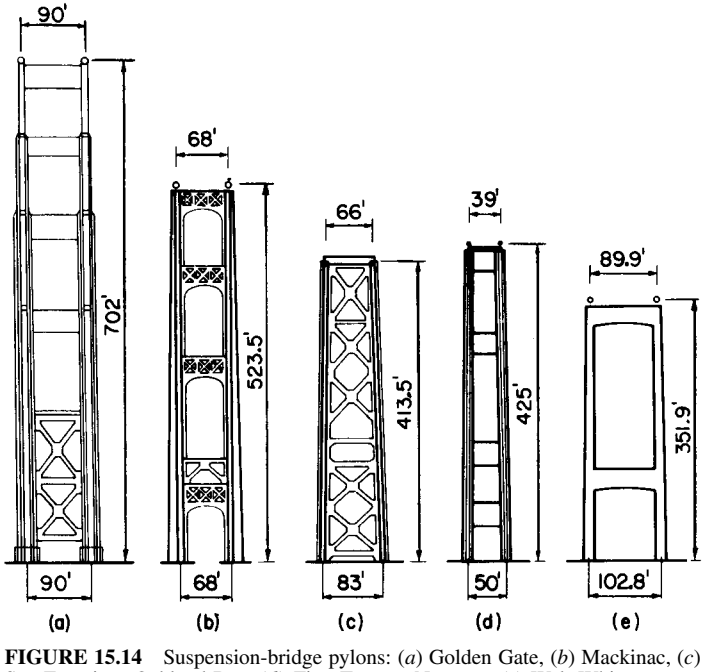

FIGURE 15.14 Suspension-bridge pylons: (*a*) Golden Gate, (*b*) Mackinac, (*c*) San Francisco-Oakland Bay, (*d*) First Tacoma Narrows, (*e*) Walt Whitman.

TABLE 15.1 Major Suspension Bridges

Name	Location	Length of main span		Year completed
		ft.	m	
Akashi Kaiko	Japan	6529	1990	1998
Storebelt	Zealand-Sprago, Denmark	5328	1624	1997
Humber River	Hull, England	4626	1410	1981
Jiangyin Bridge	Yangtze R., Jiangsu Prov., China	4544	1385	
Tsing Ma Bridge	Hong Kong	4518	1377	1997
Hardanger Fjord	Norway	4347	1325	
Verranzano-Narrows	New York, NY, USA	4260	1298	1964
Golden Gate	San Francisco, USA	4200	1280	1937
Höga Kusten	400 km N. Stockholm, Sweden	3970	1210	1997
Mackinac Straits	Michigan, USA	3800	1158	1957
Minami Bisan-Seto	Japan	3609	1100	1988
2nd Bosphorus	Istanbul, Turkey	3576	1090	1988
1st Bosphorus	Istanbul, Turkey	3524	1074	1973
George Washington	New York, NY, USA	3500	1067	1931
3rd Kurushima Bridge[1]	Japan	3379	1030	(1999)
2nd Kurushima Bridge[1]	Japan	3346	1020	(1999)
Tagus River[2]	Lisbon, Portugal	3323	1013	1966
Forth Road	Queensferry, Scotland	3300	1006	1964
Kita Bisan-Seto	Japan	3248	990	1988
Severn	Beachley, England	3240	988	1966
Shimotsui Straits	Japan	3084	940	1988
Xiling Bridge	over Yangtze R., Xiling Gorge, China	2953	900	1996
Tigergate (Humen)	Pearl R., Guangdon Prov., China	2913	888	1997
Ohnaruto	Japan	2874	876	1985
Tacoma Narrows I[3]	Tacoma, Washington, USA	2800	853	1940
Tacoma Narrows II	Tacoma, Washington, USA	2800	853	1950
Askøy	Near Bergen, Norway	2787	850	1992
Innoshima	Japan	2526	770	1983
Akinada[1]	Japan	2461	750	
Hakucho[1]	Japan	2362	720	
Kanmon Straits	Kyushu-Honshu, Japan	2336	712	1973
Angostura	Ciudad Bolivar, Venezuela	2336	712	1967
San Francisco-Oakland Bay[4]	San Francisco, California, USA	2310	704	1936
Bronx-Whitestone	New York, NY, USA	2300	701	1939
Pierre Laporte	Quebec, Canada	2190	668	1970
Delaware Memorial[5]	Wilmington, DE, USA	2150	655	1951 1968
Seaway Skyway	Ogdensburg, NY, USA	2150	655	1960
Gjemnessund	Norway	2044	623	1992
Walt Whitman	Philadelphia, PA, USA	2000	610	1957
Tancarville	Tancarville, France	1995	608	1959
1st Kurushima Bridge[1]	Japan	1969	600	(1999)
Lillebaelt	Lillebaelt Strait, Denmark	1969	600	1970
Kvisti[1]	Bergen, Hordland, Norway	1952	592	
Tokyo Port Connect. Br.	Tokyo, Japan	1870	570	1993
Ambassador	Detroit, MI, USA-Canada	1850	564	1929
Skyway[3]	(Chicago World's Fair) USA	1850	564	1933
Hakata-Ohshima	Japan	1837	560	1988
Throgs Neck	New York, NY, USA	1800	549	1961

TABLE 15.1 Major Suspension Bridges (*Continued*)

Name	Location	Length of main span		Year completed
		ft.	m	
Benjamin Franklin[2]	Philadelphia, PA, USA	1750	533	1926
Skjomen	Narvik, Norway	1722	525	1972
Kvalsund	Hammerfest, Norway	1722	525	1977
Dazi Bridge	Lasa, Xizang Region, China	1640	500	1984
Kleve-Emmerich	Emmerich, Germany	1640	500	1965
Bear Mountain	Peckskill, NY, USA	1632	497	1924
Wm. Preston Lane, Jr.[5]	near Annapolis, MD, USA	1600	488	1952
Williamsburg[2]	New York, NY, USA	1600	488	1903
Newport	Newport, RI, USA	1600	488	1969
Chesapeake Bay	Sandy Point, MD, USA	1600	488	1952
Brooklyn[7]	New York, NY, USA	1595	486	1883
Lions Gate	Vancouver, B.C., Canada	1550	472	1939
Hirato Ohashi	Hirato, Japan	1536	468	1977
Sotra	Bergen, Norway	1535	468	1971
Hirato	Japan	1526	465	1977
Vincent Thomas	San Pedro-Terminal Is., CA, USA	1500	457	1963
Mid-Hudson	Poughkeepsie, NY, USA	1495	457	1930
Shantou Bay Bridge	Shantou, Guangdong Prov., China	1483	452	1995
Manhattan[2]	New York, NY, USA	1470	448	1909
MacDonald Bridge	Halifax, Nova Scotia, Canada	1447	441	1955
A. Murray Mackay	Halifax, Nova Scotia, Canada	1400	426	1970
Triborough	New York, NY, USA	1380	421	1936
Alvsborg	Goteburg, Sweden	1370	418	1966
Hadong-Namhae	Pusan, South Korea	1325	404	1973
Aquitaine	Bordeaux, France	1292	394	
Baclan	Garrone R., Bordeaux, France	1292	394	1967
Ame-Darja R.	Buhara-Ural, Russia	1280	390	1964
Clifton[3]	Niagara Falls, NY, USA	1268	386	1869
Cologne-Rodenkirchen I[3]	Cologne, Germany	1240	378	1941
Cologne-Rodenkirchen II[10]	Cologne, Germany	1240	378	1955
St. Johns	Portland, OR, USA	1207	368	1931
Wakato	Kita-Kyushu City, Japan	1205	367	1962
Mount Hope	Bristol, RI, USA	1200	366	1929
St Lawrence R.,	Ogdensburg, NY–Prescot, Ont.	1150	351	1960
Ponte Hercilio[2,6]	Florianapolis, Brazil	1114	340	1926
Bidwell Bar Bridge	Oroville, CA, USA	1108	338	1965
Middle Fork Feather R.	California, USA	1105	337	1964
Varodd, Topdalsfjord	Kristiansand, Norway	1105	337	1956
Tamar Road	Plymouth, Great Britain	1100	335	1961
Deer Isle	Deer Isle, ME, USA	1080	329	1939
Rombaks	Narvik, Nordland, Norway	1066	325	1964
Maysville	Maysville, KY, USA	1060	323	1931
Ile d'Orleans	St. Lawrence R., Quebec, Canada	1059	323	1936
Ohio River	Cincinnati, OH, USA	1057	322	1867
Otto Beit	Zambezi R., Rodesia	1050	320	1939
Dent	N. Fork, Clearwater R., ID, USA	1050	320	1971
Niagra[3]	Lewiston, NY, USA	1040	317	1850
Cologne-Mulheim I[3]	Cologne, Germany	1033	315	1929
Cologne-Mulheim II	Cologne, Germany	1033	315	1951

TABLE 15.1 Major Suspension Bridges (*Continued*)

Name	Location	Length of main span		Year completed
		ft.	m	
Miampimi	Mexico	1030	314	1900
Wheeling	West Virginia, USA	1010	308	1848
(Wheeling Bridge reconstructed after collapse)				1856
Yong Jong[1]	Seoul, Korea	984	300	(2001)
Konohana[8,9]	Osaka, Japan	984	300	1990
Elisabeth[6]	Budapest, Hungary	951	290	1903
Tjeldsund	Harstad, Norway	951	290	1967
Grand' Mere	Quebec, Canada	948	289	1929
Cauca River	Columbia	940	287	1894
Jinhu Bridge	Taining, Fujian Prov., China	932	284	1989
Peach River	British Columbia, Canada	932	284	1950
Aramon	France	902	275	1901
Cornwall-Masena	St. Lawrence R., NY-Ontario	900	274	1958
Fribourg[3]	Switzerland	896	273	1834
Brevik	Telemark, Norway	892	272	1962
Royal George	Arkansas R., Canon City, CO, USA	880	268	1929
Kjerringstraumen	Nordland, Norway	853	260	1975
Vranov Lake Bridge	Czech Republic	827	252	1993
Railway Bridge[3]	Niagara River, NY, USA	821	250	1854
Dome, Grand Canyon	Dome, AZ, USA	800	244	1929
Point[3,6]	Pittsburgh, PA, USA	800	244	1877
Rochester	Rochester, PA, USA	800	244	1896
Niagara River	Lewiston, Nyn USA	800	244	1899
Thousand Is., Int.	St. Lawrence R., USA-Canada	800	244	1938
Waldo Hancock	Penobscot R., Bucksport, ME, USA	800	244	1931
Anthony Wayne	Maumee R., Toledo, OH, USA	785	239	1931
Parkersburg	Parkersburg, WV, USA	755	236	1916
Footbridge[3]	Niagara R., NY, USA	770	235	1847
Vernaison	France	764	233	1902
Cannes Ecluse	France	760	232	1900
Ohio River	E. Liverpool, OH, USA	750	229	1905
Gotteron	Freiburg, Switzerland	746	227	1840
Iowa-Illinois Mem. I[3]	Moline, IL, USA	740	226	1934
Iowa-Illinois Mem. II	Moline, IL, USA	740	226	1959
Davenport	Davenport, IL, USA	740	226	1935
Monongahela R.	So. 10th St., Pittsburgh, PA, USA	725	221	1933
Rondout	Kingston, NY, USA	705	215	1922
Ohio River	E. Liverpool, OH, USA	705	215	1896
Clifton[3,6]	Bristol, England	702	214	1864
Ohio River[6]	St. Marys, OH, USA	700	213	1929
Ohio River[3,6]	Point Pleasant, OH, USA	700	213	1928
Sixth Street	Pittsburgh, PA, USA	700	213	1928
General U.S. Grant	Ohio R., Portsmouth, OH, USA	700	213	1927
Airline	St. JO, Texas, USA	700	213	1927
Red River	Nocona, Texas, USA	700	213	1924
Ohio River	Steubenville, OH, USA	700	213	1904
Ohio River	Steubenville, OH, USA	689	210	1928
Isere	Veurey, France	688	210	1934
Hungerford[3,6]	London, England	676	206	1845

TABLE 15.1 Major Suspension Bridges (*Continued*)

Name	Location	Length of main span ft.	Length of main span m	Year completed
Mississippi R.[3]	Minneapolis, MN, USA	675	206	1877
Meixihe Bridge	Fengjie, Sichuan Prov., China	673	205	1990
Lancz[6]	Budapest, Hungary	663	202	1845
White River	Des Arc, Arkansas, USA	650	198	1928
Roche Bernard[3]	Vilaine, France	650	198	1836
Missouri River	Illinois, USA	643	196	1956
Caille[3]	Annecy, France	635	194	1839
Columbia R.	Beegee, WA, USA	632	193	1919

[1] Under Construction. [2]Railroad & Highway. [3]Not Standing. [4]Twin Spans. [5]Twin Bridges. [6]Eyebar Chain. [7]Includes cable stays. [8]Self-anchored. [10]Structure widened by addition of third cable. (1994)

15.4 CLASSIFICATION AND CHARACTERISTICS OF CABLE-STAYED BRIDGES

The cable-stayed bridge has come into wide use since the 1950s for medium- and long-span bridges, because of its economy, stiffness, esthetic qualities, and ease of erection without falsework. Cable-stayed bridges utilize taut cables connecting pylons to a span to provide intermediate support for the span. This principle has been understood by bridge engineers for at least two centuries, as indicated in Art. 15.1.

Cable-stayed bridges are economical for bridge spans intermediate between those suited for deck girders (usually up to 600 to 800 ft but requiring extreme depths, up to 33 ft) and the longer-span suspension bridges (over 1,000 ft). The cable-stayed bridge, thus, finds application in the general range of 600- to 1,600-ft spans, but spans as long as 2,600 ft may be economically feasible.

A cable-stayed bridge has the advantage of greater stiffness over a suspension bridge. Cable-stayed single or multiple box girders possess large torsional and lateral rigidity. These factors make the structure stable against wind and aerodynamic effects.

15.4.1 Structural Characteristics of Cable-Stayed Bridges

The true action of a cable-stayed bridge is considerably different from that of a suspension bridge. As contrasted with the relatively flexible main cables of the latter, the inclined, taut cables of the cable-stayed structure furnish relatively stable point supports in the main span. Deflections are thus reduced. The structure, in effect, becomes a continuous girder over the piers, with additional intermediate, elastic (yet relatively stiff) supports in the span. As a result, the stayed girder may be shallow. Depths usually range from $\frac{1}{60}$ to $\frac{1}{80}$ of the main span, sometimes even as small as $\frac{1}{100}$ of the span.

Cable forces are usually balanced between the main and flanking spans, and the structure is internally anchored; that is, it requires no massive masonry anchorages. Second-order effects of the type requiring analysis by a deflection theory are of relatively minor importance for the common, self-anchored type of cable-stayed bridge, characterized by compression in the main bridge girders.

15.4.2 Types of Cable-Stayed Bridges

Cable-stayed bridges may be classified by the type of material they are constructed of, by the number of spans stay-supported, by transverse arrangement of cable-stay planes, and by the longitudinal stay geometry.

A concrete cable-stayed bridge has both the superstructure girder and the pylons constructed of concrete. Generally, the pylons are cast-in-place, although in some cases, the pylons may be precast-concrete segments above the deck level to facilitate the erection sequence. The girder may consist of either precast or cast-in-place concrete segments. Examples are the Talmadge Bridge in Georgia and the Sunshine Skyway Bridge in Florida.

All-steel cable-stayed bridges consist of structural steel pylons and one or more stayed steel box girders with an orthotropic deck (Fig. 15.15). Examples are the Luling Bridge in Louisiana and the Meridian Bridge in California (also constructed as a swing span).

Other so-called steel cable-stayed bridges are, in reality, composite structures with concrete pylons, structural-steel edge girders and floorbeams (and possibly stringers), and a composite cast-in-place or precast plank deck. The precast deck concept is illustrated in Fig. 15.16.

In general, span arrangements are single span; two spans, symmetrical or asymmetrical; three spans; or multiple spans. Single-span cable-stayed bridges are a rarity, usually dictated by unusual site conditions. An example is the Ebro River Bridge at Navarra, Spain (Fig. 15.17). Generally, back stays are anchored to deadman anchorage blocks, analogous to the simple-span suspension bridge (Fig. 15.9*a*).

15.4.3 Span Arrangements in Cable-Stayed Bridges

A few examples of two-span cable-stayed bridges are illustrated in Fig. 15.18. In two-span, asymmetrical, cable-stayed bridges, the major spans are generally in the range of 60 to 70% of the total length of stayed spans. Exceptions are the Batman Bridge (Fig. 15.18*g*) and Bratislava Bridge (Fig. 15.18*h*), where the major spans are 80% of the total length of stayed spans. The reason for the longer major span is that these bridges have a single back stay anchored to the abutment rather than several back stays distributed along the side span.

Three-span cable-stayed bridges (Fig. 15.19) generally have a center span with a length about 55% of the total length of stayed spans. The remainder is usually equally divided between the two anchor spans.

Multiple-span cable-stayed bridges (Fig. 15.20) normally have equal length spans with the exception of the two end spans, which are adjusted to connect with approach spans or the abutment. The cable-stay arrangement is symmetrical on each side of the pylons. For convenience of fabrication and erection, the girder has ''drop-in'' sections at the center of the span between the two leading stays. The ratio of drop-in span length to length between pylons varies from 20%, when a single stay emanates from each side of the pylon, to 8% when multiple stays emanate from each side of the pylon.

15.4.4 Cable-Stay Configurations

Transverse to the longitudinal axis of the bridge, the cable stays may be arranged in a single or double plane with respect to the longitudinal centerline of the bridge and may be positioned in vertical or inclined planes (Fig. 15.21). Single-plane systems, located along the longitudinal centerline of the structure (Fig. 15.21*a*) generally require a torsionally stiff stayed box girder to resist the torsional forces developed by unbalanced loading. The laterally displaced vertical system (Fig. 15.21*b*) has been used for a pedestrian bridge. The V-shaped arrangement (Fig. 15.21*e*), has been used for cable-stayed bridges supporting pipelines. This

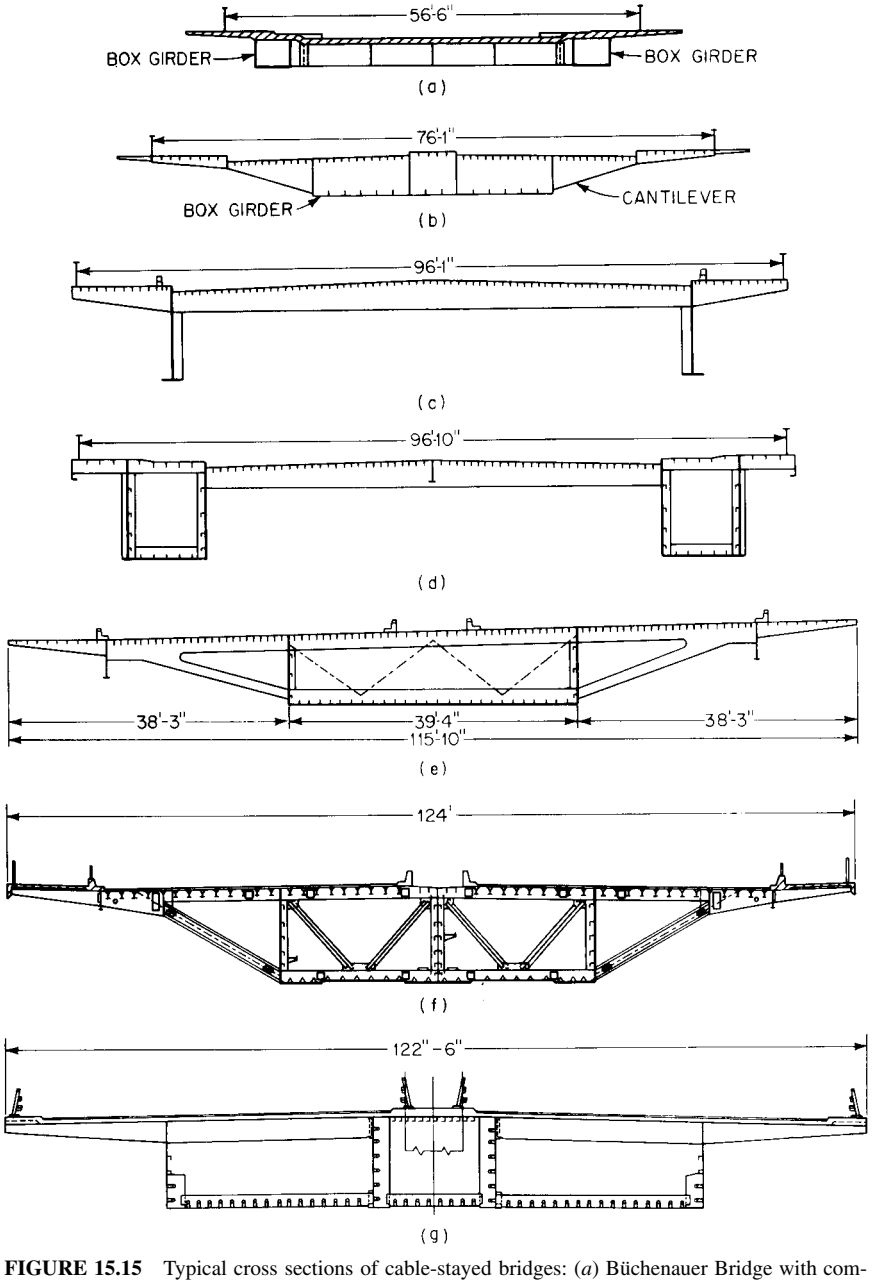

FIGURE 15.15 Typical cross sections of cable-stayed bridges: (*a*) Büchenauer Bridge with composite concrete deck and two steel box girders, (*b*) Julicherstrasse crossing with orthotropic-plate deck, box girder, and side cantilevers. (*c*) Kniebrucke with orthotropic-plate deck and two solid-web girders. (*d*) Severn Bridge with orthotropic-plate deck and two box girders. (*e*) Bridge near Maxau with orthotropic-plate deck, box girder, and side cantilevers. (*f*) Leverkusen Bridge with orthotropic-plate deck, box girder, and side cantilevers. (*g*) Lower Yarra Bridge with composite concrete deck, two box girders, and side cantilevers. (*Adapted from A. Feige, "The Evolution of German Cable-Stayed Bridges—An Overall Survey," Acier-Stahl-Steel* (*English version*)*, no. 12, December 1966 reprinted in the AISC Journal, July 1967.*)

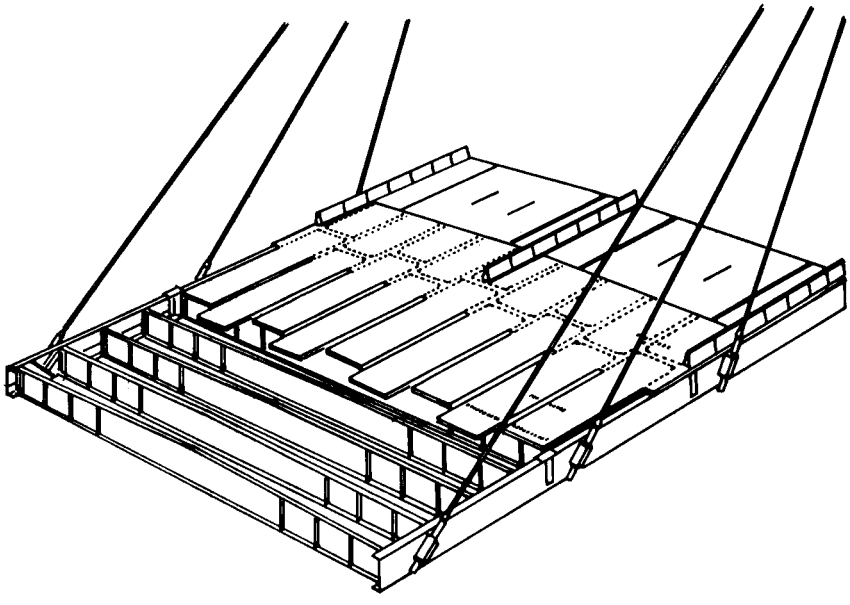

FIGURE 15.16 Composite steel-concrete superstructure girder of a cable-stayed bridge.

FIGURE 15.17 Ebro River Bridge, Navarra, Spain. (*Reprinted with permission from Stronghold International, Ltd.*)

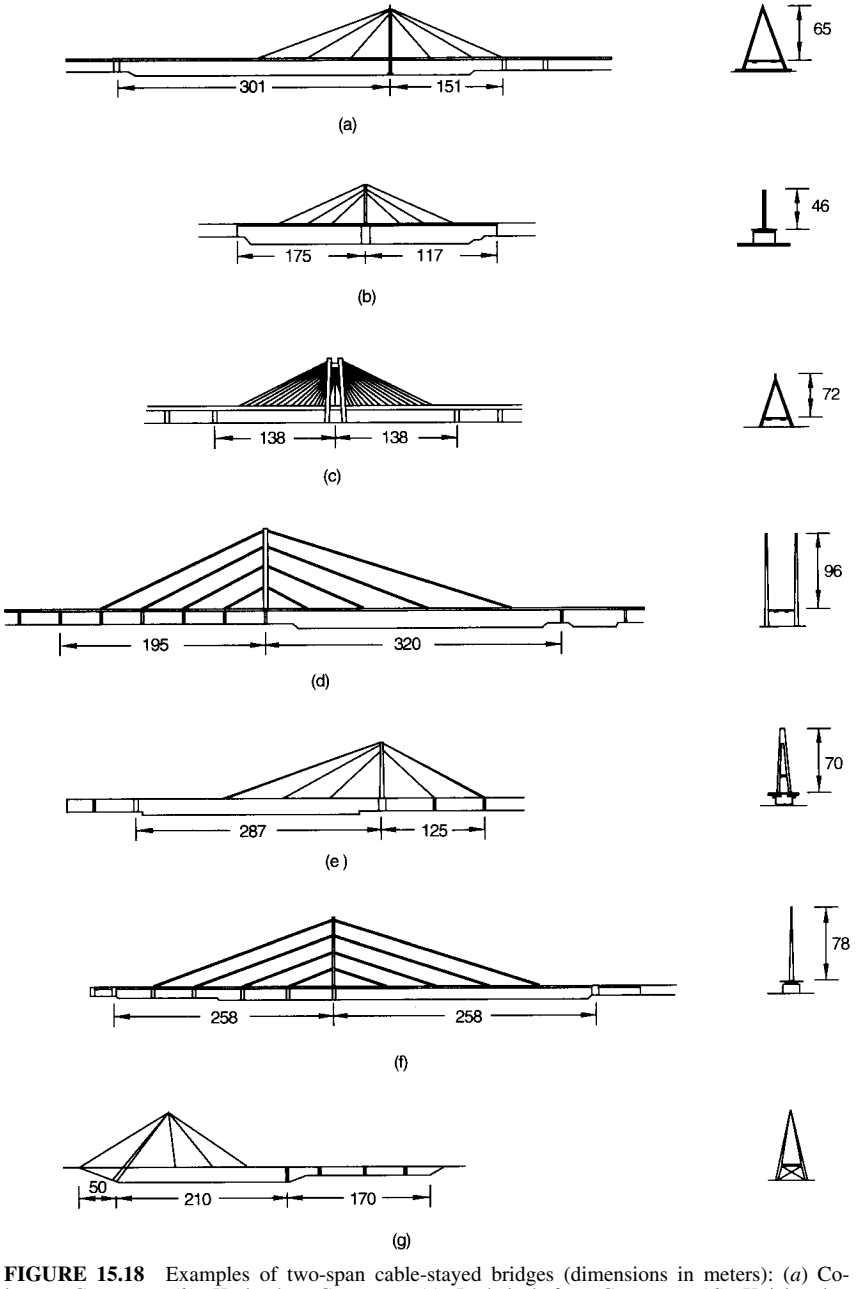

FIGURE 15.18 Examples of two-span cable-stayed bridges (dimensions in meters): (*a*) Cologne, Germany; (*b*) Karlsruhe, Germany; (*c*) Ludwigshafen, Germany; (*d*) Kniebrucke-Dusseldorf, Germany; (*e*) Manheim, Germany; (*f*) Dusseldorf-Oberkassel, Germany; (*g*) Batman, Australia; (*h*) Bratislava, Czechoslovakia.

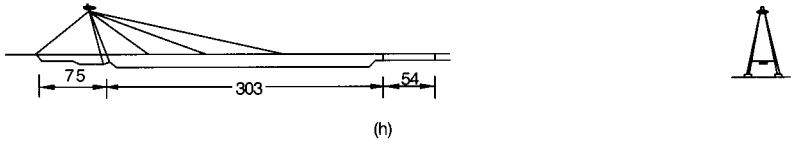

(h)

FIGURE 15.18 (*Continued*)

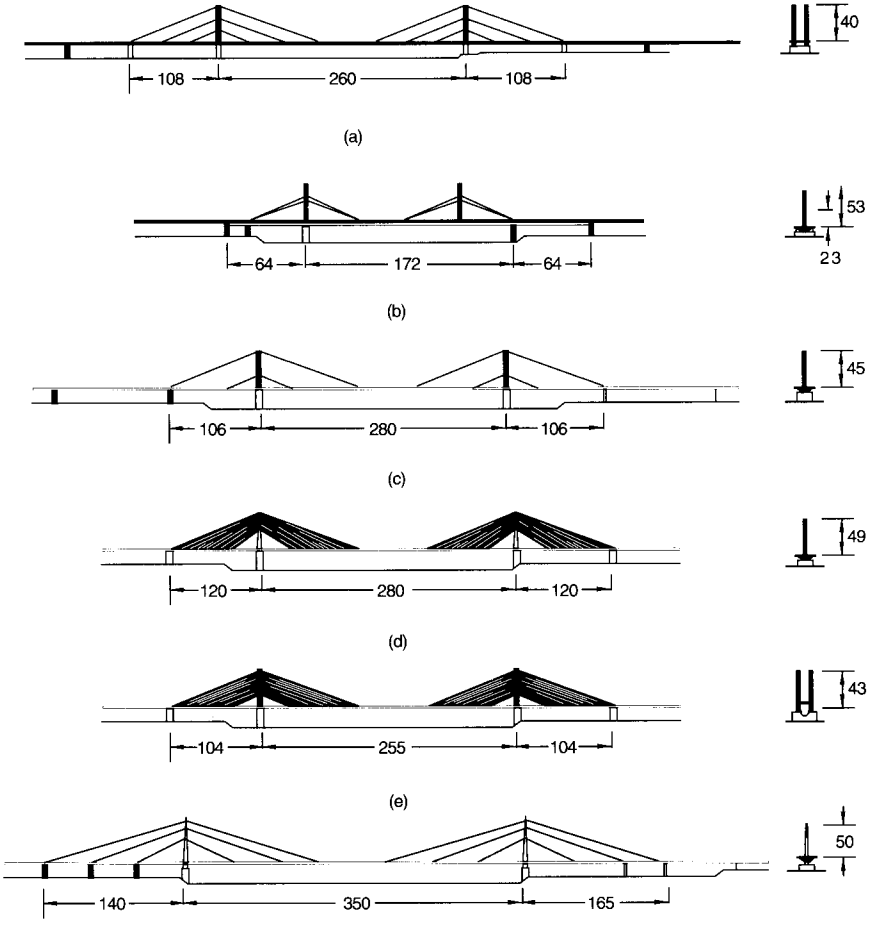

FIGURE 15.19 Examples of three-span cable-stayed bridges (dimensions in meters): (*a*) Dusseldorf-North, Germany; (*b*) Norderelbe, Germany; (*c*) Leverkusen, Germany; (*d*) Bonn, Germany; (*e*) Rees, Germany; (*f*) Duisburg, Germany; (*g*) Stromsund, Sweden; (*h*) Papineau, Canada; (*i*) Onomichi, Japan.

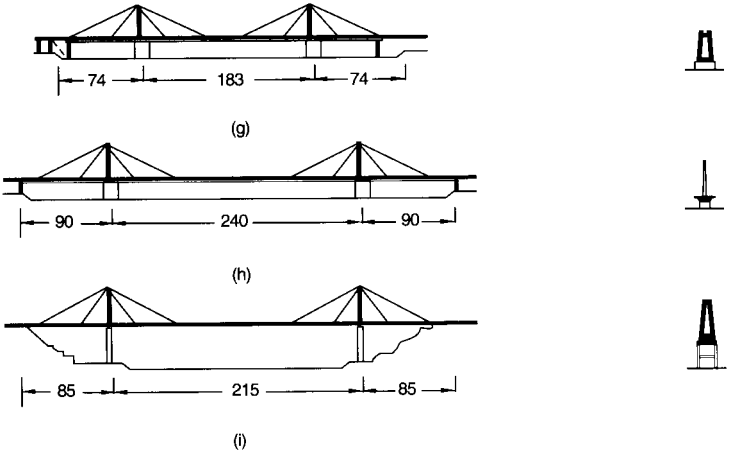

FIGURE 15.19 (*Continued*)

variety of transverse-stay geometry leads to numerous choices of pylon arrangements (Fig. 15.22).

There are four basic stay configurations in elevation (Fig. 15.23): radiating, harp, fan, and star. In the radiating system, all stays converge at the top of the pylon. In the harp system, the stays are parallel to each other and distributed over the height of the pylon. The fan configuration is a hybrid of the radiating and the harp system. The star system was used for the Norderelbe Bridge in Germany primarily for its esthetic appearance. The variety of configurations in elevation leads to a wide variation of geometric arrangements, as indicated by Fig. 15.23.

The number of stays used for support of the deck ranges from a single stay on each side of the pylon to a multistay arrangement, as illustrated in Figs. 15.18 to 15.20. Use of a few

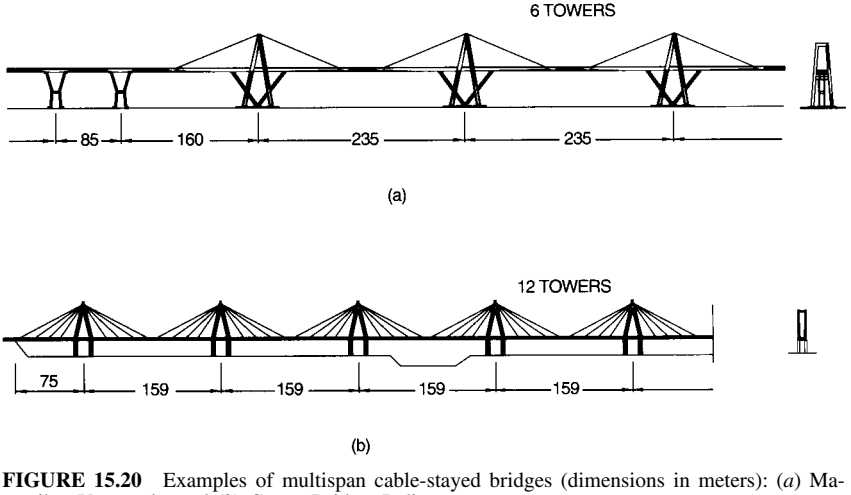

FIGURE 15.20 Examples of multispan cable-stayed bridges (dimensions in meters): (*a*) Maracaibo, Venezuela, and (*b*) Ganga Bridge, India.

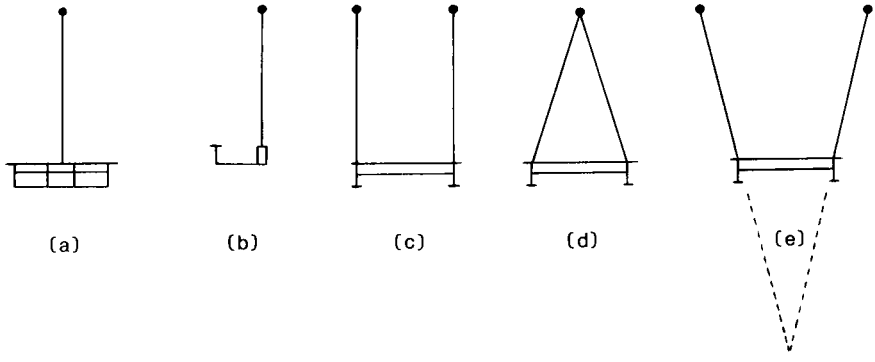

FIGURE 15.21 Cross sections of cable-stayed bridges showing variations in arrangements of cable stays. (*a*) Single-plane vertical. (*b*) Laterally displaced vertical. (*c*) Double-plane vertical. (*d*) Double-plane inclined. (*e*) Double-plane V-shaped. (*Reprinted with permission from W. Podolny, Jr., and J. B. Scalzi, "Construction and Design of Cable-Stayed Bridges," 2nd ed., John Wiley & Sons, Inc., New York.*)

stays leads to large spacing between attachment points along the girder. This necessitates a relatively deep stayed girder and large concentrations of stay force to the girder, with attendant complicated connection details. A large number of stays has the advantage of reduction in girder depth, smaller diameter stays, simpler connection details, and relative ease of erection by the cantilever method. However, the number of terminal stay anchorages is increased and there are more stays to install.

A list of major modern cable-stayed bridges is provided in Table 15.2.

15.5 CLASSIFICATION OF BRIDGES BY SPAN

Bridges have been categorized in many ways. They have been categorized by their principal use as highway, railroad, pedestrian, pipeline, etc.; by the material used in their construction as stone, timber, wrought iron, steel, concrete, and prestressed concrete; by their structural form as girder, box-girder, moveable, truss, arch, suspension, and cable-stayed; by structural

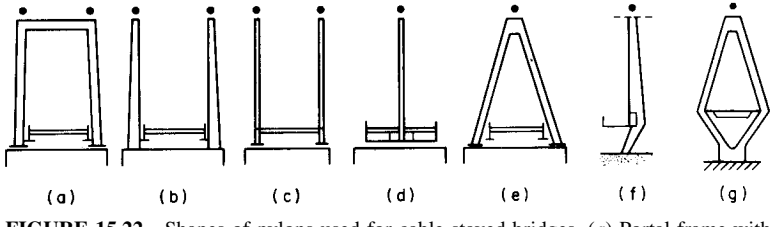

FIGURE 15.22 Shapes of pylons used for cable-stayed bridges. (*a*) Portal frame with top cross member. (*b*) Pylon fixed to pier and without top cross member. (*c*) Pylon fixed to girders and without top cross member. (*d*) Axial pylon fixed to superstructure. (*e*) A shaped pylon. (*f*) Laterally displaced pylon fixed to pier. (*g*) Diamond-shaped pylon. (*Reprinted with permission from A. Feige, "The Evolution of German Cable-Stayed Bridges—An Overall Survey," Acier-Stahl-Steel (English version), no 12, December 1966 (reprinted in the AISC Journal, July 1967.*)

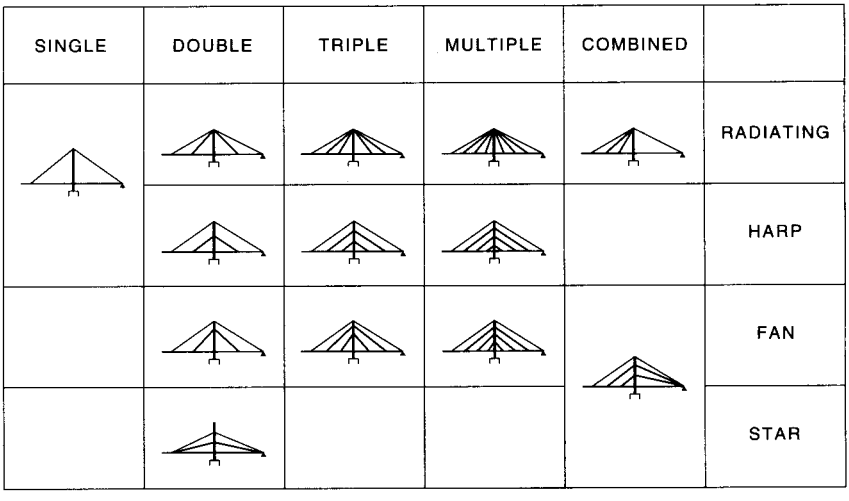

FIGURE 15.23 Stay configurations for cable-stayed bridges.

behavior as simple span, continuous, and cantilever; and by their span dimension as short, intermediate, and long-span. The last classification, specifically long-span, is the one of primary interest in this Section.

The span of a bridge is defined as the dimension (length), along the longitudinal axis of the bridge, between two supports. However, what defines a "long-span"? In other words, how long is long?

It should be understood that the word "long" is a relative term. Throughout the history of bridge construction and technology, as our methods of analysis improved and as we moved from one material to another more appropriate material, the span length has been constantly pushed forward to a new frontier. Therefore, what was considered a long-span in the eighteenth and nineteenth centuries may not be considered as such in the twentieth century. What is considered a long-span today may not be considered as such in the twenty-first century. It is conceptually simple to understand this concept of the relativity of span length, however, in of itself it does not define "long-span."

Perhaps the best definition of "long-span" is that presented by Silano as "if a bridge has a span too long to design from standard handbooks, you call it a long-span bridge." The current AASHTO Standard Specifications for Highway Bridges states that "They apply to ordinary highway bridges and supplemental specifications may be required for unusual types and for bridges with spans longer than 500 ft." Therefore, by the above criteria, the lower bound of long-span may be considered to be 500 ft, at least for highway bridges.

(Silano, L. G., "Design of Long-Span Bridges," reprinted from the Structural Group Lecture Series of the Boston Society of Civil Engineers/ASCE, April 1990, Parsons Brinckerhoff, New York.)

15.6 NEED FOR LONGER SPANS

Horizontal navigation clearances have increased in recent years to accommodate the increasing size and volume of marine traffic. The intense competition among port cities to attract ocean shipping has led to replacement of existing older bridges with those providing wider and taller navigation clearances. However, there are a number of other reasons for increased

TABLE 15.2 Major Cable-Stayed Bridges

Name	Location	Length of main or major span		Year completed
		ft.	m	
Tatara[1]	Ehime, Japan	2920	890	(1999)
Normandy	Le Havre, France	2808	856	1995
Nanjing Yangtze R.[1]	Nanjing, China	2060	618	(1999)
Wuhan Third Yangtze[1]	Wuhan, Hubei, China	2028	628	(1998)
Qingzhou Minjiang	Fuzhou, China	1985	605	1996
Yang Pu	Shanghai, China	1975	602	1993
Xupu	Shanghai, China	1936	590	1997
Meiko Chuo	Aichi, Japan	1936	590	1997
Patras Bridge	Greece	1837	560	
Skarnsundet Bridge	near Trondheim, Norway	1739	530	1991
Tsurumi Tsubasa	Kanagawa, Japan	1673	510	1994
Oresund[1]	Denmark/Sweden	1614	492	(2000)
Ikuchi	Hiroshima, Ehime, Japan	1608	490	1991
Higashi Kobe	Hyogo, Japan	1591	485	1993
Ting Kau[4]	Hong Kong	1558	475	1998
Seo Hae Grand[1]	Pyung Taek City/Dang Jin County, South Korea	1542	470	(1999)
Annacis (Alex Fraser)	Vancouver, B.C., Canada	1526	465	1986
Yokohama Bay	Kanagawa, Japan	1509	465	1989
Second Hooghly R.	Calcutta-Howrah, India	1499	457	1992
2nd Severn Crossing	Severn R., England/Wales	1496	456	1996
Queen Elizabeth II	Thems R., Dartford, England	1476	450	1991
Dao Kanong, ChaoPhraya R.	Bangkok, Thailand	1476	450	1987
Chongqing 2nd Br. over the Yangtze River	Chongqing, Sichuan Prov., China	1457	444	1991
Barrios De Luna	Cordillera, Spain	1444	440	1983
Tongling over Yangtze R.	Tongling, Anhui Prov., China	1417	432	1995
Kap Shui Mun[2,3]	Hong Kong	1411	430	1997
Helgeland	Sandnessjoen, Nordland, Norway	1394	425	1991
Quetzalapa Bridge	Quetzalapa, Mexico	1391	424	1993
Nan Pu	Shanghai, China	1388	423	1991
Vasco de Gaama	Lisbon, Portugal	1378	420	1998
Hitsuishijima[2]	Kagawa, Japan	1378	420	1988
Iwagurojima[2]	Kagawa, Japan	1378	420	1988
Yunyang over Hanjiang R.	Yunjang, Hubei Prov., China	1358	414	1994
Meiko Higashi	Aichi, Japan	1345	410	1997
Erasmus Bridge	Rotterdam, Netherlands	1345	410	1996
Volga R.	Ulyanovsk, Russia	1335	407	
Wadi Leban	Riyadh, Saudi Arabia	1329	405	1996
Meiko-Nishi	Nagoya, Aichi, Japan	1329	405	1985
Bridge over the Waal River	Ewijck, Netherlands	1325	404	1976
Saint Nazaire	Saint Nazaire, France	1325	404	1975
Elorn River	Brest/Quimper, France	1312	400	1994
Rande	Vigo, Spain	1313	400	1977
Wuhan Bridge over Yangtze	Wuhan, Hubei Prov., China	1312	400	1995
Dame Point	Jacksonville, FL, USA	1300	396	1988
Sidney Lanier Bridge[1]	Brunswick R., GA, USA	1250	381	(2000)

TABLE 15.2 Major Cable-Stayed Bridges (*Continued*)

Name	Location	Length of main or major span		Year completed
		ft.	m	
Houston Ship Channel	Baytown, Texas, USA	1250	381	1995
Hale Boggs Memorial	Luling, LA, USA	1222	372	1983
Dusseldorf—Flehe	Rhine River, Germany	1207	368	1979
Tjorn Bridge, Askerofjord	near Gothenberg, Sweden	1201	366	1982
William Natcher Bridge[1]	Ohio R., Ownesboro KY, USA	1200	366	(2001)
Sunshine Skyway	Tampa, FL, USA	1200	366	1987
Tampico	Panuco R., Mexico	1181	360	1988
Yamatogawa	Osaka, Japan	1165	355	1982
Novi Sad	Yugoslavia	1152	351	1981
Bill Emerson Memorial[1]	Rt. 74 over Miss. R., Cape Girardeau, MO, USA	1150	350.5	(2001)
My Thuan[1]	My Thuan, Vietnam	1148	350	(2000)
Batam—Tonton	Indonesia	1148	350	1998
Tempozan	Osaka, Japan	1148	350	1990
Ajigawa Br.	Osaka, Japan	1148	350	1987
Duisburg-Neuenkamp	Rhine R., Germany	1148	350	1970
Glebe Island Bridge	Sydney, Australia	1132	345	1994
Jindo Bridge	Uldolmok Straits, Korea	1129	344	1984
ALRT Fraser River Br.	Vancouver, B.C., Canada	1115	340	1988
Mesopotamia	Parana, Argentina	1115	340	1972
West Gate	Melbourne, Australia	1102	336	1978
Talmadge Memorial Bridge	Savannah, GA, USA	1100	335	1990
Hao Ping Hsi	Taiwan	1083	330	
Posadas Encarnacion	Argentina	1083	330	1986
Puente Brazo Largo[2]	Rio Parana, Argentina	1083	330	1976
Zarate[2]	Rio Parana, Argentina	1083	330	1975
Karnali River Bridge	Chisapani, Nepal	1066	325	1993
Kohlbrand	Hamburg, Germany	1066	325	1974
Int. Guadiana Bridge	Portugal/Spain	1063	324	1991
Maysville, over Ohio R.[1]	Maysville, KY, USA	1050	320	
Qi Ao, mouth of Pearl R.	Zhuhai and Hong Kong, China	1050	320	1998
Pont de Brotonne, Seine R.	Rouen, France	1050	320	1977
Kniebrücke	Rhine R., Dusseldorf, Germany	1050	320	1969
Wuhu over Yangtze R.[1]	Wuhu, China	1024	312	(1999)
Mezcala	Mexico City/Acapulco Highway	1024	312	1993
Daugava R.	Riga, Latvia	1024	312	1981
Emscher	Rhine R., Germany	1017	310	1990
Grenland Bridge	Frierfjord, Telemark, Norway	1001	305	1996
Dartford-Thurrock Bridge	Thames R., Great Britain	1001	305	1991
Erskine, River Clyde	Glasgow, Scotland	1000	305	1971
Ombla Bay	Dubrovnik, Yugoslavia	998	304	
Bratislava	Danube R., Czechoslovakia	994	303	1972
Severin	Cologne, Germany	990	302	1959
Mezcala	Mexico	984	300	1993
Moscovsky, Dnieper R.	Kiev, Ukraine	984	300	1976
Pasco-Kennewick	Washington, USA	981	299	1978
Neuwied	Rhine R., Germany	958	292	1977

TABLE 15.2 Major Cable-Stayed Bridges (*Continued*)

Name	Location	Length of main or major span		Year completed
		ft.	m	
Rama VIII[1]	Bangkok, Thailand	955	291	(1999)
Faro Bridge	Faro, Denmark	951	290	1985
Donaubrücke	Deggenau, Germany	951	290	1975
Coatzacoalcos R.	Mexico	945	288	1984
Dongying Br. over Yellow R.	Kenli, Shandong, China	945	288	1987
Kurt-Schumacher	Mannheim-Ludwigshafen, Germany	941	287	1971
Erasmus Bridge	Rotterdam, Netherlands	932	284	1996
Wadi Kuf	Sipac, Libya	925	282	1971
Wadi Dib	Algeria	919	280	1998
Dolsan	Yeosu, Korea	919	280	1984
Leverkusen	Germany	919	280	1964
Friedrich-Ebert (Bonn-Nord)	Bonn, Germany	919	280	1967
Rheinbrucke	Speyer, Germany	902	275	1974
East Huntington	East Huntington, WV, USA	900	274	1985
Bayview Bridge	Quincy, IL, USA	900	274	1987
South Bridge, Dnieper R.	Kiew, Ukraine	889	271	1993
Willems	Rotterdam, Netherlands	886	270	1981
Ewijk, Waal R.	nera Ewijk, Netherlands	886	270	1976
River Waal	Tiel, Netherlands	876	267	1975
Puente del Centenario	Spain	869	265	1992
Ikarajima	Japan	853	260	1996
Yonghe	Tianjin, China	853	260	1987
Theodor Heuss	Düsseldorf, Germany	853	260	1957
Burton	New Brunswick, Canada	850	259	1970
Oberkassel	Düsseldorf, Germany	846	258	1976
Waal R.	Zaltbommel, Netherlands	840	256	1994
Arade Bridge	Portimao, Portugal	840	256	1991
Rees	Rees-Kalkar, Germany	837	255	1967
Duisburg-Rheinhausen	Rhine R., Germany	837	255	1965
Save Rivert Railroad	Belgrade, Yugoslavia	833	254	1977
Tokachi	Japan	823	251	1995
Aswan	Egypt	820	250	1998
Raippaluto	Finland	820	250	1997
Weirton-Steubenville	West Virginia, USA	820	250	1990
Tokachi Chuo	Obihiro, Hokkaido, Japan	820	250	1989
Yobuko	Saga, Japan	820	250	1988
Suehiro	Tokushima, Japan	820	250	1975
Ishikari	Hokaido, Japan	820	250	1972
General Belgrano	Argentina	804	245	1998
Chaco/Corrientes	Parana River, Argentina	804	245	1973
Papineau-Leblanc	Montreal, Canada	790	241	1969
Karkistensalmi	Finland	787	240	1997
Aomori	Aomon, Japan	787	240	1992
Jianwei	Sichuan Prov., China	787	240	1990
Kessock	Inverness, Scotland	787	240	1982
Yasaka Bridge	Ohta, Yamaguchi, Japan	787	240	1987

TABLE 15.2 Major Cable-Stayed Bridges (*Continued*)

Name	Location	Length of main or major span		Year completed
		ft.	m	
Kamone	Osaka, Japan	787	240	1975
Sun Bridge	Japan	784	239	1993
Kemi[1]	Wakayama, Japan	784	239	
Sugawara-Shirokita	Osaka, Japan	780	238	1989
Cochrane	Mobile, AL, USA	780	238	1991
Lake Maracaibo	Venezuela	771	235	1962
Neuwied	Rhine R., Germany	770	235	1978
Wye River Bridge	England	770	235	1966
Albert Canal Bridge	Lanaye, Belgium	761	232	1985
Clark Bridge Replacement	Alton, IL, USA	756	230	1994
Shimen	Chongqing, Sichuan, China	755	230	1988
Chesapeake and Delaware Canal Bridge	Dover, Delaware, USA	750	229	1995
Donaubrucke	Hainburg, Austria	748	228	1972
Charles R. Bridge[1]	Boston, MA, USA	745	227	
Penang	Malaysia	738	225	1985
Fengtai	Anhui, China	735	224	1990
Bengbu over Huaihe R.	Bengbu, Anhui Prov., China	735	224	1989
Luangawa	Zambia	730	223	1968
Jinan Br. over Yellow R.	Jinan, Shandong Prov., China	722	220	1982
Katsushika	Katsushika, Tokyo, Japan	722	220	1987
Rokko	Hyogo, Japan	722	220	1976
Hawkshaw	New Brunswick, Canada	713	217	1967
Longs Creek	New Brunswick, Canada	713	217	1966
Toyosato	Osaka, Japan	709	216	1976
Evripos Bridge	Greece	707	215	1988
Onomichi	Hiroshima, Japan	705	215	1968
Donaubrucke	Linz, Austria	705	215	1972
Quetzalapa Bridge	Mexico	699	213	1993
Pereira-Dasquetradas	Colombia	692	211	1997
Chuo	Japan	692	211	1993
Mei Shywe	Taiwan	689	210	
Ohshiba[1]	Japan	689	210	(1998)
Xiangjiang North Br.	Changshu, Hunan Prov., China	689	210	1990
Chalkis	Greece	689	210	1989
Godsheide	Hasselet, Belgium	690	210	1978
Polcevera Viaduct	Genoa, Italy	682	208	1969
Arno	Florence, Italy	676	206	1977
Batman	Tasmania, Australia	675	206	1968
Burlington Bridge	Burlington, IA, USA	660	201	1993
Ayunose[1]	Japan	656	200	(1999)
Alamillo	Guadalquivir R., Seville, Spain	656	200	1992
Shin Inagawa[1]	Osaka, Japan	656	200	( )
Torikai-Niwaji (Yodogawa)	Settsu, Osaka, Japan	656	200	1987
Chung Yang	Taiwan	656	200	1984
Maogang	Shanghai, China	656	200	1982
Chichibu Park Bridge	Arakawa R., Saitama Pref., Japan	640	195	
Neches River	Texas, USA	640	195	1991

TABLE 15.2 Major Cable-Stayed Bridges (*Continued*)

Name	Location	Length of main or major span		Year completed
		ft.	m	
Dee Crossing	UK	635	194	1997
Ijssel Bridge	Kampen, Netherlands	635	194	1983
Tarascon Beaucaire	France	633	192.8	
James River Bridge	near Richmond, VA, USA	630	192	1989
Sakitama	Sakitama, Japan	623	190	1991
Ashigara	Kanagawa, Japan	607	185	1991
Bybrua	Norway	607	185	1978
Aratsu Bridge	Fukuoka, Japan	604	184	1988
Wandre	Belgium	600	183	1989
Strömsund	Sweden	600	183	1955

[1] Under Construction. [2] Railroad & Highway. [3] Double Deck. [4] 3 pylons, [4] 4 span continuous.

spans over that required for strictly navigation clearance requirements. One of the most obvious is the economic trade off of shorter spans requiring deep water foundations, as opposed to longer spans requiring shallow water foundations or foundations completely out of the water and on land.

Another reason is the concern for ship collision with piers. Besides the safety issue and potential loss of life resulting from a ship collision, there are a number of associated economic impacts: the closing or impairment of port and highway traffic resulting from a collapsed superstructure in the navigation channel, the repair or replacement of the bridge, the damage or loss of the vessel, and the potential for a hazardous materials spill from the damaged vessel. A risk analysis will generally reveal that consideration of a span longer than strictly required by navigation channel requirements is well warranted.

An emerging concern is where hazardous materials have settled to the bottom of the river or bay. Foundation excavation under this condition requires costly containment of this material and its relocation. This then requires minimization or elimination of piers in the waterway leading to longer spans. For the reasons given above, there appears to be a trend toward longer and longer spans.

15.7 POPULATION DEMOGRAPHICS OF SUSPENSION BRIDGES

A plot showing the number of bridges for each category of suspension bridge constructed for every year starting with the year 1990 is shown in Fig. 15.24. This plot clearly indicates that the classical catenary suspension bridge reached its zenith during the latter half of the 1920's. It also shows the impact that the introduction of stayed bridges, starting in 1955, has had on the catenary suspension bridge. The decreasing population of the catenary suspension bridge results from the limited number of sites requiring spans in excess of 2,000 ft.

The growth and popularity of the cable-stay bridge in the last half of the 20th century has been phenomenal. The cable-stay bridge has largely supplanted the classical catenary suspension bridge, for spans up to approximately 2,000 ft. The catenary suspension bridge is still dominant for spans exceeding the 2,000 ft limit, although the cable-stayed bridge is beginning to make inroads.

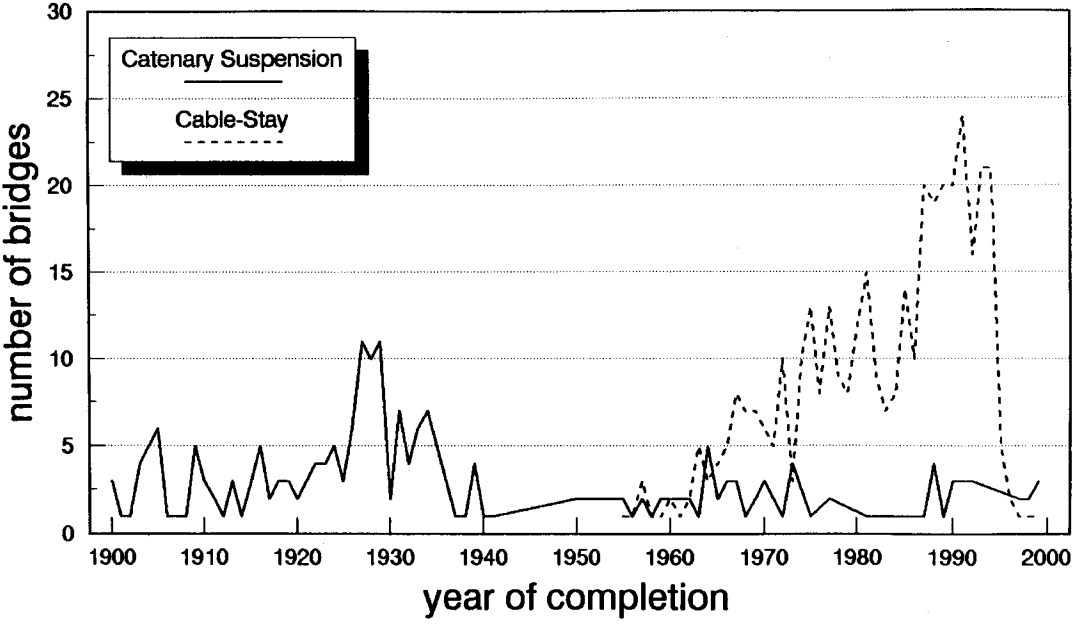

FIGURE 15.24 Suspension bridge population in the 20th century.

15.8 SPAN GROWTH OF SUSPENSION BRIDGES

Figure 15.25 shows the growth of maximum spans by year. It is obvious that in the 60-year period from the Golden Gate Bridge (1937) to the completion of the Storebelt Bridge in Denmark (1997), the rate of increase in maximum center span has been steady and gradual for catenary suspension bridges. The increase in span during this time frame is 27%. However, the Akashi Kaikyo Bridge completed in 1998 represents a 23% increase in span over the Storebelt Bridge, or a 55% increase over the Golden Gate Bridge. A similar change in cable-stay bridges occurred with the Normandy Bridge (1994) with a 42% increase in span over the Yang Pu Bridge (1993).

The Akashi Kaikyo Bridge, along with the contemplated Messina Straits and Gibraltar Straits Bridges, represent a dramatic change in span rate growth. It should be pointed out, however, that the schemes for the contemplated 5,000 m span Gibraltar Straits Bridge are a pure catenary suspension as well as several hybrid types, Fig. 15.26.

(Lin, T. Y. and Chow, P., "Gibraltar Straits Crossing—A Challenge to Bridge and Structural Engineers," Structural Engineering International, *Journal of the IABSE,* vol. 1, no. 2, May 1991.)

15.9 TECHNOLOGICAL LIMITATIONS TO FUTURE DEVELOPMENT

Cables are one of the main components to inhibit the extension of suspension bridge spans. As spans become progressively longer and dead load increases, the steel cables become longer and heavier. The relationship between center span length and dead load is shown in Fig. 15.27, for a three-span catenary suspension bridge with a stiffening truss girder. What

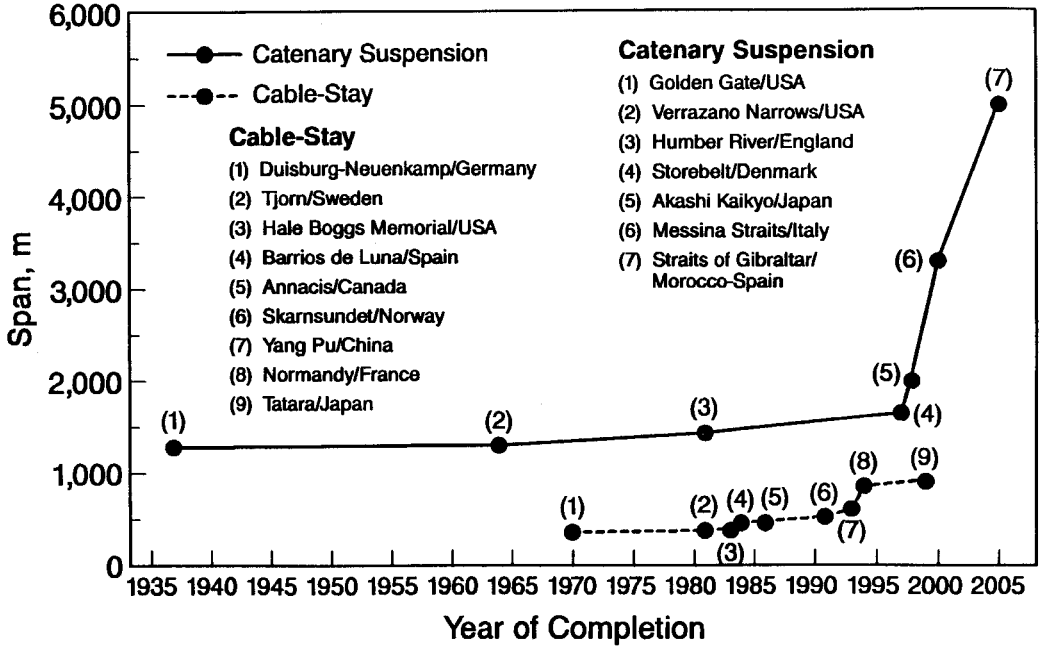

FIGURE 15.25 Suspension bridge span growth.

this indicates is that as the center span length increases, the cable weight increases at a faster rate than the dead weight of the suspended structure. Stated another way, as the span increases, there is a decreasing percentage capability of the cable to carry live load, Fig. 15.28. This results from the increase of the ratio of cable weight to weight supported with increasing span. By analogy, the same is true for the cable-stays of cable-stay bridges. This means cables for spans much larger than the Akashi Kaikyo and Tatare Bridges will become increasingly difficult to install and tension, become less efficient with respect to load carrying capacity, and become more costly to erect. Higher strength and lighter cables will be required for future spans exceeding today's technology.

(Yoshida, I. V., Fujiwara, M., and Yokoyama, K., "Future Projects for Highway Construction Across Straits in Japan, and Technical Considerations."

15.10 CABLE-SUSPENDED BRIDGES FOR RAIL LOADING

Because of flexibility and susceptibility to vibration under dynamic loads, pure suspension bridges are rarely constructed for railway spans. They are sometimes used, however, where dead load constitutes a relatively large proportion of the total load. Where provisions for both railway and highway traffic is necessary, as for the future extension of the Salazar Bridge (Fig. 15.7), the addition of inclined cable stays from the pylon to the stiffening girder is advantageous or a cable-stayed bridge may be used, for increased stiffness.

An important consideration in the design for rail loading (including rapid-transit trains) is the positioning of the tracks with respect to the transverse centerline of the deck structure. In the Williamsburg Bridge (Fig. 15.29*a*), the railway is positioned adjacent to the centerline, greatly minimizing torsional forces. In the Manhattan Bridge (Fig. 15.29*b*), the railway is

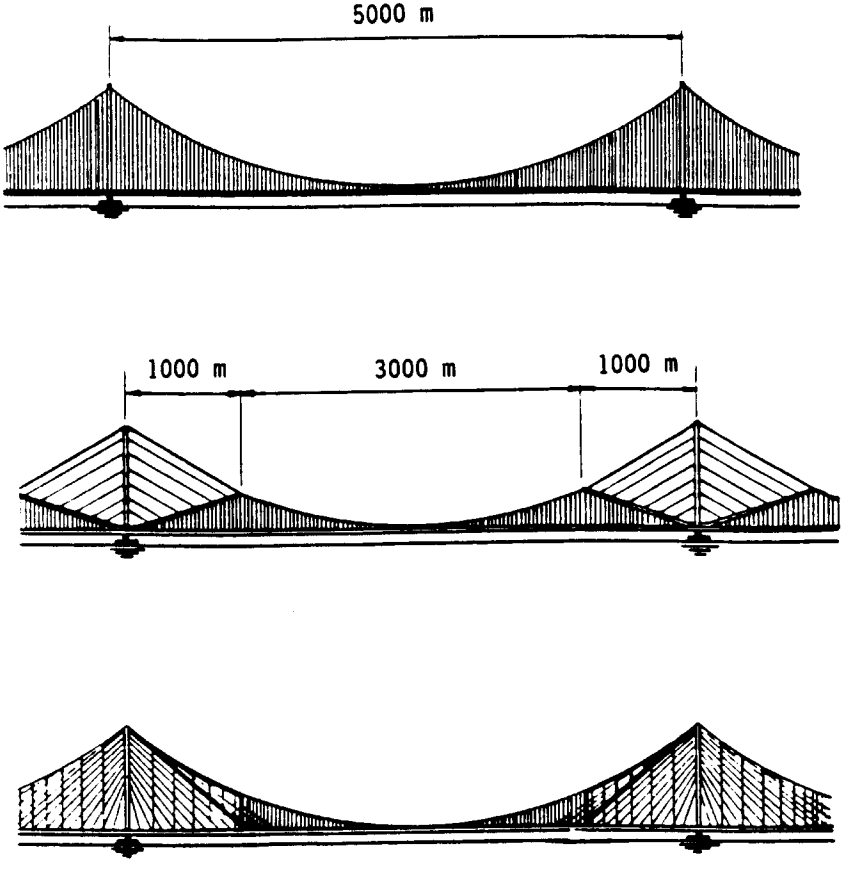

FIGURE 15.26 Hybrid bridge proposals for Gibraltar Straits Crossing.

positioned outboard of the centerline, resulting in large torsional forces. As a result of this positioning, the Manhattan Bridge, over the years, has suffered damage and had to be retrofitted with a torsion tube to increase its resistance to torsional forces.

The Zarate-Brazo Largo Bridges in Argentina (two identical structures) are unique cable-stayed bridges not only from the standpoint of supporting highway and railroad traffic, but also in that the rail line is on one side of the structures. This positioning necessitated an increased stiffness of the stays on the railroad side (see W. Podolny, Jr., and J. B. Scalzi, "Construction and Design of Cable-Stayed Bridges," 2d ed., John Wiley & Sons, Inc., New York.)

15.11 SPECIFICATIONS AND LOADINGS FOR CABLE-SUSPENDED BRIDGES

"Standard Specifications for Highway Bridges," American Association of State Highway and Transportation Engineers (AASHTO), covers ordinary steel bridges, generally with spans less than 500 ft. Specifications of the American Railway Engineering and Maintenance of

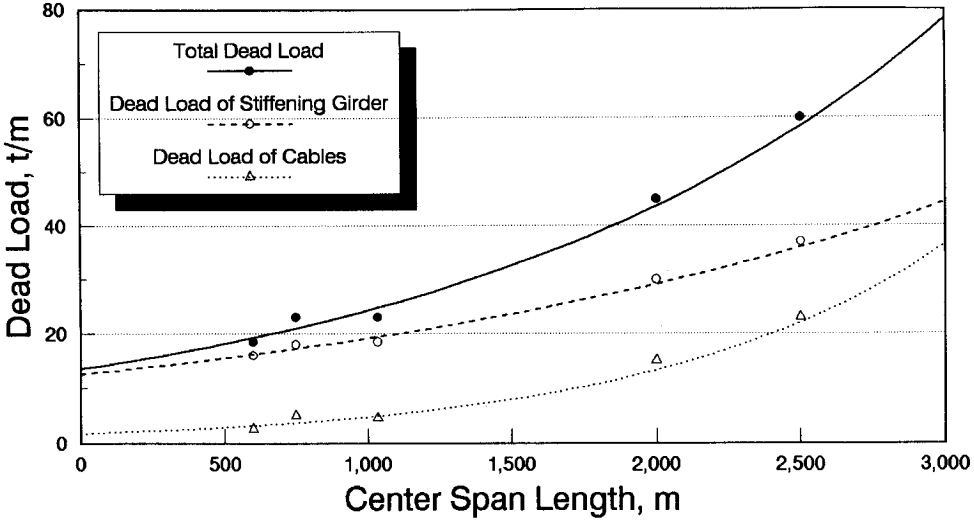

FIGURE 15.27 Relationship between center span length and dead load for a three-span suspension bridge with a stiffening truss girder.

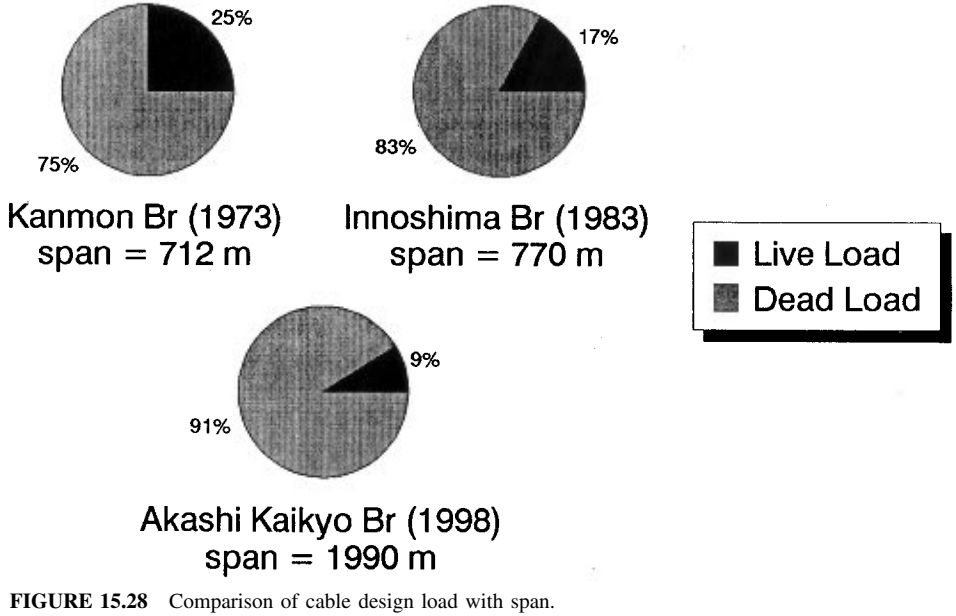

FIGURE 15.28 Comparison of cable design load with span.

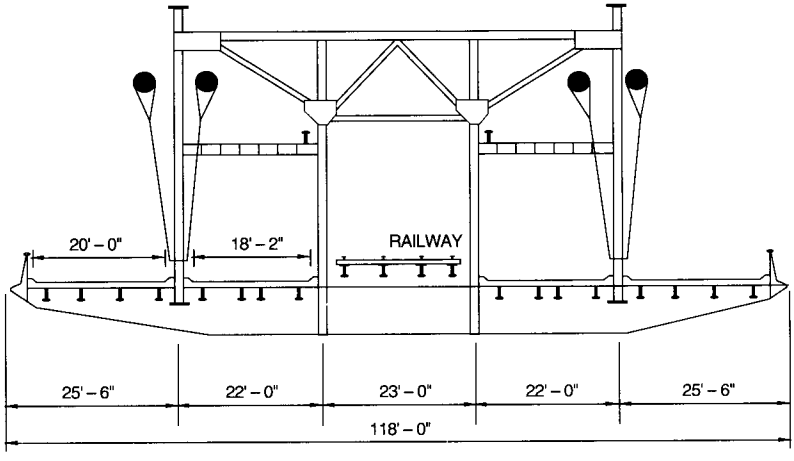

(a)

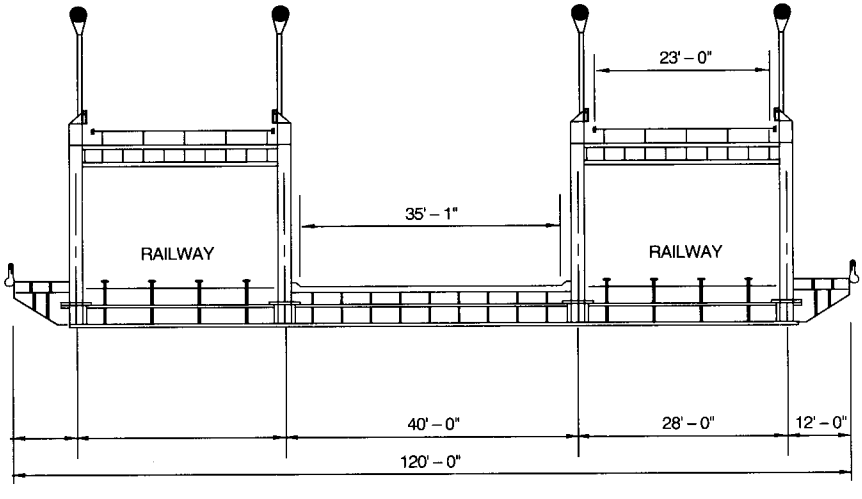

(b)

FIGURE 15.29 Position of rail loading on two suspension bridges: (*a*) Williamsburg Bridge and (*b*) Manhattan Bridge.

Way Association (AREMA) for steel railway bridges apply to spans not exceeding 400 ft. There are no standard American specifications for longer spans than these. AASHTO and AREMA specifications, however, are appropriate for design of local areas of a long-span structure, such as the floor system. A basically new set of specifications must be written for each long-span bridge to incorporate the special features brought about by site conditions, long spans, sometimes large traffic capacities, flexibility, aerodynamic and seismic conditions, special framing, and sophisticated materials and construction processes.

Structural analysis is usually applied to the following loading conditions: dead load, live load, impact, traction and braking, temperature changes, displacement of supports (including settlement), wind (both static and dynamic effects), seismic effects, and combinations of these. Guidelines for loadings on long-span bridges are given in P. G. Buckland, ''North American and British Long-Span Bridge Loads,'' *Journal of Structural Engineering,* vol. 117, no. 10, October 1991, American Society of Civil Engineers (ASCE). Recommendations for stay cables are presented in ''Recommendations for Stay-Cable Design, Testing and Installation,'' Committee on Cable-Stayed Bridges, Post-Tensioning Institute. See also ''Guide for the Design of Cable-Stayed Bridges,'' ASCE Committee on Cable-Stayed Bridges.

15.12 CABLES

The concept of bridging long spans with cables, flexible tension members, antecedes recorded history (Art. 15.1). Known ancient uses of metal cables include the following: A short length of copper cable discovered in the ruins of Ninevah, near Babylon, is estimated to have been made in about 685 B.C. in the Kingdom of Assyria. A piece of bronze rope was discovered in the ruins of Pompeii, which was destroyed by the eruption of Mt. Vesuvius in 79 A.D. The Romans made cables of wires and rope; on display in the Museo Barbonico at Naples, Italy, is a 1-in-dia., 15-in-long specimen of their lang-lay bronze rope, in which the direction of lay of both wires and strands is the same.

These early specimens of rope consisted of hand-made wires. In succeeding centuries, the craftsmanship reached such a state of the art that only a very close inspection reveals that wires were hand-made. Viking craftsmanship produced such uniform wire that some authorities believe that mechanical drawing was used.

Machine-drawn wire first appeared in Europe during the fourteenth century, but there is controversy as to whether the first wire rope resembling the current uniform, high-quality product was produced by a German, A. Albert (1834), or an Englishman named Wilson (1832). The first American machine-made wire rope was placed in service in 1846. Since then, with technological improvements, such as advances in manufacturing processes and introduction of high-strength steels, the quality of strand and rope has advanced to that currently available.

In structural applications, cable is generally used in a generic sense to indicate a flexible tension member. Several types of cables are available for use in cable-supported bridges. The form or configuration of a cable depends on its makeup; it can be composed of parallel bars, parallel wires, parallel strands or ropes, or locked-coil strands (Fig. 15.30). Parallel bars are not used for suspension bridges because of the curvature requirements at the pylon saddles. Nor are they used in cable-stayed bridges where a saddle is employed at the pylon, but they have been utilized in a stay where it terminates and is anchored at the pylon.

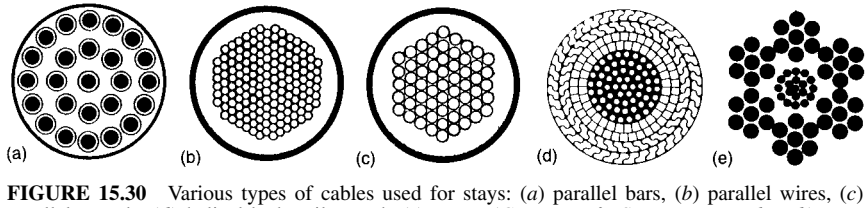

FIGURE 15.30 Various types of cables used for stays: (*a*) parallel bars, (*b*) parallel wires, (*c*) parallel strands. (*d*) helical lock-coil strands (*e*) ropes. (*Courtesy of VSL International, Ltd.*)

15.12.1 Definition of Terms

Cable. Any flexible tension member, consisting of one or more groups of wires, strands, ropes or bars.

Wire. A single, continuous length of metal drawn from a cold rod.

Prestressing wire. A type of wire usually used in posttensioned concrete applications. As normally used for cable stays, it consists of 0.25-in-dia. wire produced in the United States in accordance with ASTM A421 Type BA.

Structural strand (with the exception of parallel-wire strand). Wires helically coiled about a center wire to produce a symmetrical section (Fig. 15.31), produced in the United States in accordance with ASTM A586.

Lay. Pitch length of a wire helix.

Parallel-wire strand. Individual wires arranged in a parallel configuration without the helical twist (Fig. 15.31).

Locked-coil strand. An arrangement of wires resembling structural strands except that the wires in some layers are shaped to lock together when in place around the core (Fig. 15.31).

Structural rope. Several strands helically wound around a core that is composed of a strand or another rope (Fig. 15.32), produced in the United States in accordance with ASTM A603.

Prestressing strands. A 0.6-in-dia. seven-wire, low-relaxation strand generally used for prestressed concrete and produced in the United States in accordance with ASTM A416 (used for stay cables).

Bar. A solid, hot-rolled bar produced in the United States in accordance with ASTM A722 Type II (used for cable stays).

15.12.2 Structural Properties of Cables

A comparison of nominal ultimate and allowable tensile stress for various types of cables is presented in Table 15.3.

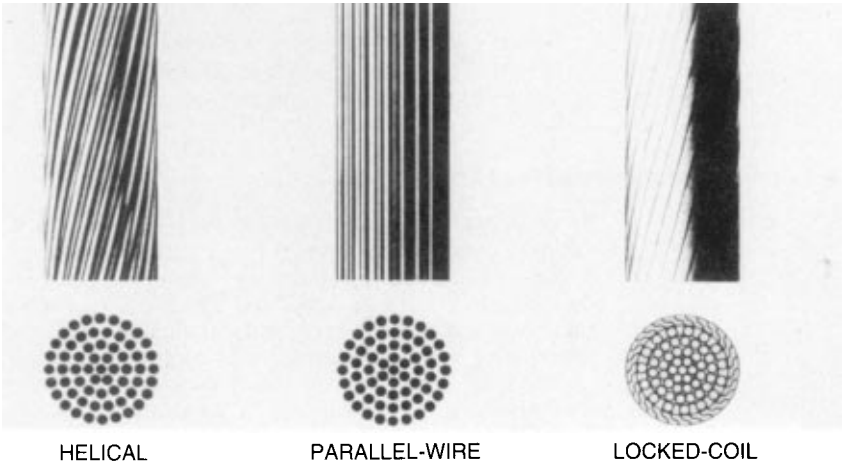

FIGURE 15.31 Types of strands. (*Courtesy of Bethlehem Steel Corporation.*)

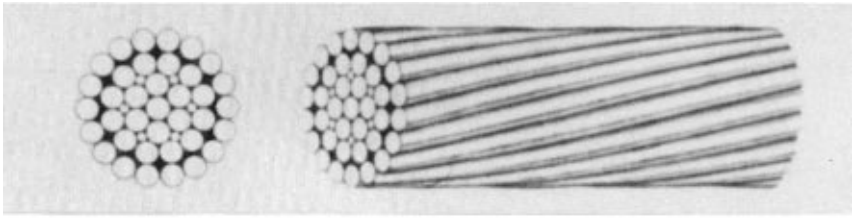

(a)

(b)

FIGURE 15.32 Configuration of (*a*) structural strand and (*b*) structural rope. (*Reprinted with permission from J. B. Scalzi et al., "Design Fundamentals of Cable Roof Structures," ADUSS 55-3580-01, U.S. Steel.*)

Structural strand has a higher modulus of elasticity, is less flexible, and is stronger than structural rope of equal size. The wires of structural strand are larger than those of structural rope of the same nominal diameter and, therefore, have a thicker zinc coating and better resistance to corrosion (Art. 15.14).

The total elongation or stretch of a structural strand is the result of several component deformations. One of these, termed constructional stretch, is caused by the lengthening of the strand lay due to subsequent adjustment of the strand wires into a denser cross section under load. Constructional stretch is permanent.

Structural strand and rope are usually prestretched by the manufacturer to approach a condition of true elasticity. Prestretching removes the constructional stretch inherent in the product as it comes from the stranding or closing machines. Prestretching also permits, under

TABLE 15.3 Comparison of Nominal Ultimate and Allowable Tensile Stress for Various Types of Cables, ksi

Type	Nominal tensile strength, F_{pu}	Allowable tensile strength, F_t
Bars, ASTM A722 Type II	150	$0.45F_{pu} = 67.5$
Locked-coil strand	210	$0.33F_{pu} = 70$
Structural strand, ASTM A586*	220	$0.33F_{pu} = 73.3$
Structural rope, ASTM A603*	220	$0.33F_{pu} = 73.3$
Parallel wire	225	$0.40F_{pu} = 90$
Parallel wire, ASTM A421	240	$0.45F_{pu} = 108$
Parallel strand, ASTM A416	270	$0.45F_{pu} = 121.5$

*Class A zinc coating (see Art. 15.14).

prescribed loads, the accurate measuring of lengths and marking of special points on the strand or rope to close tolerances. Prestretching is accomplished by the manufacturer by subjecting the strand to a predetermined load for a sufficient length of time to permit adjustment of the component parts to that load. The prestretch load does not normally exceed 55% of the nominal ultimate strength of the strand.

In bridge design, careful attention should be paid to correct determination of the cable modulus of elasticity, which varies with type of manufacture. The modulus of elasticity is determined from a gage length of at least 100 in and the gross metallic area of the strand or rope, including zinc coating, if present. The elongation readings used for computing the modulus of elasticity are taken when the strand or rope is stressed to at least 10% of the rated ultimate stress or more than 90% of the prestretching stress. The minimum modulus of elasticity of prestretched structural strand and rope are presented in Table 15.4. The values in the table are for normal prestretched, structural, helical-type strands and ropes; for parallel wire strands, the modulus of elasticity is in the range of 28,000 to 28,500 ksi.

For cable-stayed bridges, it is also necessary to use an equivalent reduced modulus of elasticity E_{eq} to account for the reduced stiffness of a long, taut cable due to sag under its own weight, especially during erection when there is less tension. The formula for this equivalent modulus was developed by J. H. Ernst:

$$E_{eq} = \frac{E}{1 + \dfrac{E(\gamma l)^2}{12\sigma_m^3}\left[\dfrac{(1+\mu)^4}{16\mu^2}\right]} \tag{15.1}$$

where E = modulus of elasticity of the steel from test
$\sigma_m = (\sigma_u + \sigma_o)/2 = \sigma_o(1 + \mu)/2$ = average stress
σ_u and σ_o = upper and lower stress limits, respectively
$\mu = \sigma_u/\sigma_o$
γ = weight of cable per unit of length per unit of cross-sectional area
l = horizontal projected length of cable

The bracketed term in the denominator becomes unity when $\sigma_o = \sigma_u$, that is, when the stress is constant. The reduction in modulus of elasticity of the cable due to sag is a major factor in limiting the maximum spans of cable-stayed bridges.

The effects of creep of cables of cable-supported bridges should be taken into account in design. Creep is the elongation of cables under large, constant stress, for instance, from dead loads, over a period of time. The effects can be evaluated by modification of the cable equation in the deflection theory. As an indication of potential magnitude, an investigation of the Cologne-Mulheim Suspension Bridge indicated that, in a 100-year period, the effects of cable creep would be the equivalent of about one-fourth the temperature drop for which the bridge was designed.

TABLE 15.4 Minimum Modulus of Elasticity of Prestretched Structural Strand and Rope*

Type	Diameter, in	Modulus of elasticity, ksi
Strand	½ to 2 9/16	24,000
	2⅝ and larger	23,000
Rope	⅜ to 4	20,000

*For Class B or Class C weight of zinc-coated outer wires, reduce modulus 1,000 ksi.

15.12.3 Erection of Cables

Until the 1960s, parallel-wire, suspension-bridge main cables were formed with a spinning wheel carrying one wire at a time (and more recently two or four wires) over the pylons from anchorage to anchorage (Fig. 15.33). Not only were the wires spun aerially individually, but each wire had to be removed from the spinning wheel at the anchorages, looped over a circular or semicircular strand shoe, then looped again over the spinning wheel for a return trip (Art. 15.23). Furthermore, wires had to be adjusted individually, then banded into strands and readjusted (Fig. 15.34*a*), and finally compacted into a circular cross section (Fig. 15.34*b*). This process is time-consuming, costly, and hazardous.

Prefabricated parallel-wire strands are an economical alternative. Large main cables of suspension bridges may be made up of many such strands, laid parallel to each other in a selected geometric pattern. In the commonly used hexagonal, there may be 19, 37, 61, 91, or 127 large strands. In a rectangular pattern, there may be 6 or more strands in each horizontal row and 6 or more vertical rows, with suitable spacers. The strands may have up to 233 wires each, all shop-fabricated, socketed, tested, and packaged on reels. Their use can yield a tremendous saving in erection time over the older process of aerial spinning of cables on the site.

For the Newport Bridge, which was completed in 1969, shop-fabricated, parallel-wire strands form the cables. Each cable is made up of 4,636 wires, each 0.202 in diameter, shop-fabricated into 76 parallel wire strands of 61 wires each. Thus, in place of thousands of spinning-wheel trips previously necessary, only 152 trips of a hauling rope were needed to form the two cables. Furthermore, thousands of sag adjustments of individual wires were eliminated from the field operation.

From a design point of view, parallel-wire cables are superior to cables made of helical-wire strands. Straight, parallel-laid wires deliver the full strength and modulus of elasticity of the steel, whereas strength and modulus of elasticity are both reduced (by about one-

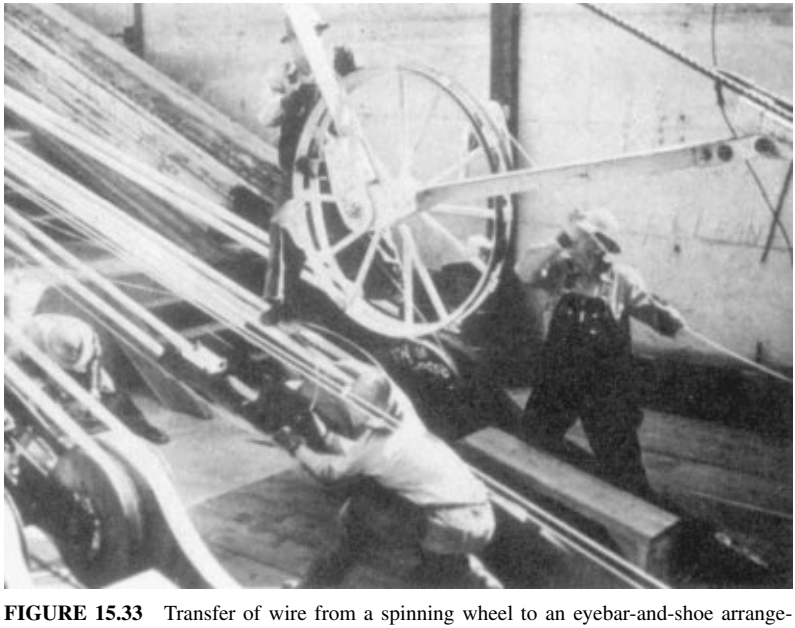

FIGURE 15.33 Transfer of wire from a spinning wheel to an eyebar-and-shoe arrangement at an anchorage.

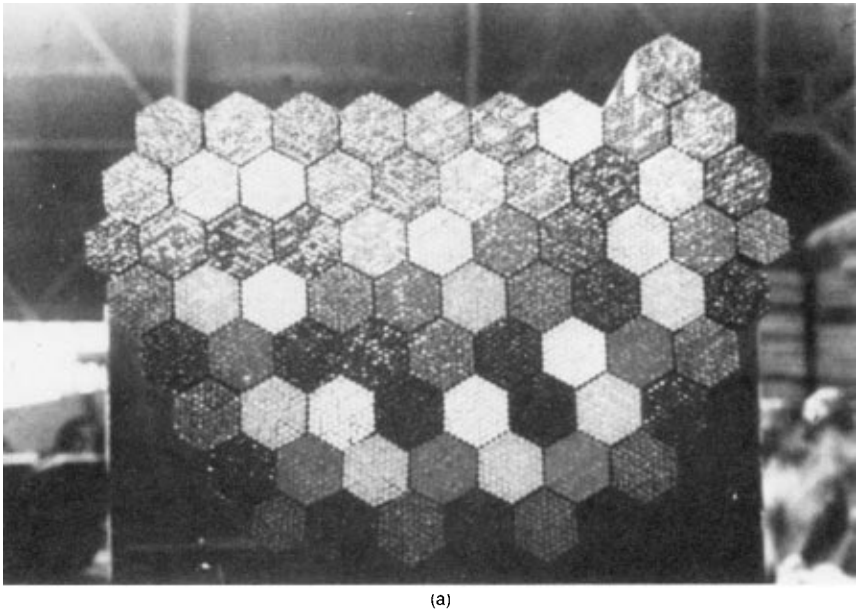

(a)

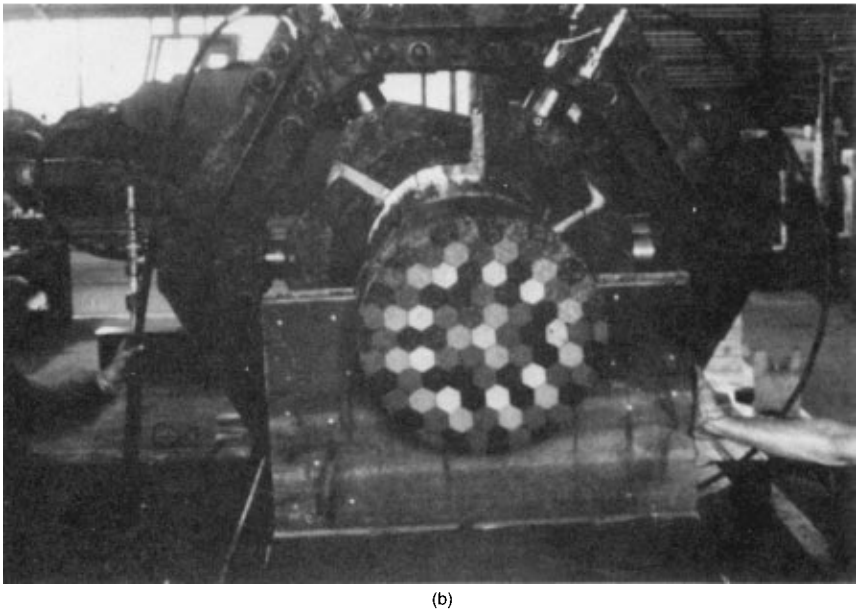

(b)

FIGURE 15.34 Parallel wire strand (*a*) before compaction from an hexagonal arrangement into a round cross section, and (*b*) after compaction.

eighth) with helical placement. On the other hand, from the bridge-erection standpoint, standard helical-strand-type cables are superior to field-assembled parallel-wire type. Strands are readily erected and adjusted, with a minimum of equipment and manpower. Therefore, they have been used on many small- to moderate-sized suspension bridges. Prefabricated parallel-wire strands, however, combine the erection advantages of strand-type cables with the superior in-place characteristics of parallel-wire cables.

For smaller cable bridges, cables with few strands may be arranged in an open form with strands separated. But for longer bridges, the strands are arranged in a closed form (Fig. 15.34*a*) in either a hexagonal or other geometrical pattern. They then may be compacted by machine (Fig. 15.34*b*) and wrapped for protection. Note that a group of helical-type strands cannot be compacted into as dense a mass as a group of parallel-wire strands.

Cable-stayed bridges formerly used traditional structural strands or locked-coil strands for the stays. Since then, stays composed of prestressing steels are generally used. Cable stays for cable-stayed bridges are similar to post-tensioning tendons in that they consist of the following primary elements:

- Prestressing steel (parallel wires, strands, or bars)
- Sheathing (duct), which encapsulates the prestressing steel and may be a steel pipe or a high-density polyethylene pipe (HDPE)
- A material that fills the void between the prestressing steel and the sheathing and may be a cementitious grout, petroleum wax, or other appropriate material
- Anchorages

There are two basic methods of manufacture and installation of stays: (1) assembly on site in final position and (2) prefabricated installation. Both methods have been successfully employed. Given various constraints for a specific project or site, it is generally a question of economics as to which method is employed. Prefabrication may be accomplished either at a factory remote from the construction site or, if feasible, at the project site (possibly on the bridge deck). Normally, factory-prefabricated stays are delivered to the site reeled on drums, complete with the bundle of wires or strands, the HDPE sheathing, and anchorages. (This method cannot be used with prestressing bars or steel pipe sheathing.) Usually, one or both anchorages are fitted to the stay.

At the site, prefabricated stays usually are erected into final inclined position either by crane or by a temporary guying system that is erected between anchorage points from which the stays are suspended. The stays are brought into final position by means of a winch or other suitable hydraulic equipment.

When a guying system is used, site assembly of stays in final position begins with installation of the guying system. The sheathing, either steel or HDPE, is then positioned in the final inclined position. Next, the strand or wire-bundle stays are pulled through the sheathing by winches. When strands are used, the push-through method may be employed. In that case, by use of specialized equipment, individual strands are pushed into the sheathing. Parallel prestressing bars are somewhat more difficult to install inasmuch as bar couplers must also be installed at intervals along the stay length.

15.13 CABLE SADDLES, ANCHORAGES, AND CONNECTIONS

Saddles atop towers of suspension bridges may be large steel castings in one piece (Fig. 15.35) or, to reduce weight, partly of weldment (Fig. 15.36). The size of the saddle may be determined by the permissible lateral pressures on the cables, which are a function of the radius of curvature of the saddle. Other saddles of special design may be required at side piers to deflect the anchor-span cables to the anchorages. Also, splay saddles may be needed at the anchorages.

FIGURE 15.35 Pylon saddle.

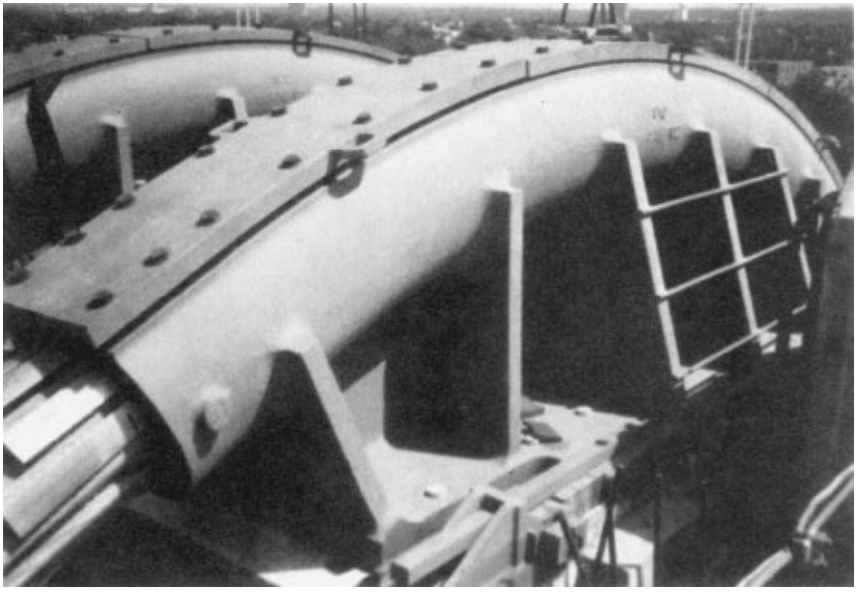

FIGURE 15.36 Pylon saddle used for the Hennepin Avenues Bridge.

In cable-stayed bridges, where the cable stays converge to the top of a pylon (radiating configuration) and are continuous over the pylon, massive saddles, similar to those for suspension-bridge towers, are used. For the types of cable-stay configurations where the stays are distributed along a cellular-type pylon, similar (but smaller) saddles may be used at the pylon. If the pylon is solid concrete, the saddles are generally steel pipe, bent to the appropriate degree of curvature and embedded in the concrete.

Suspension-bridge anchorages for the main cables are usually massive concrete blocks designed to resist, with mass and friction, the overturning and sliding effects of the main-cable pull. (Where local conditions permit, as with the Forth Road Bridge, the cables may be anchored in tunnels in rock.) The anchorages contain embedded steel eyebar chains to which the main wire cables are connected. A typical arrangement, as used for the Verrazano Narrows Bridge is shown in Fig. 15.37. A saddle is installed where the strands diverge to attach to the eyebars. Strand wires loop over a strand shoe and are attached to an eyebar (Fig. 15.33—see discussion of spinning in Art. 15.23).

A slightly different concept was used for the Newport Bridge (Fig. 15.38). In this case, the prefabricated strands of the main cable diverge and pass through 78 pipes held in position by a structural steel framework and transfer their loads to the anchorage through a bearing-type anchorage socket. The whole supporting framework is eventually encased in concrete. In this anchorage-block arrangement, the strand sockets bear on the back of the anchorage block instead of connecting with a tension linkage at the front of the block.

In suspension bridges, the suspender cables are attached to the main cables by cable bands. These are usually made of paired, semicylindrical steel castings with clamping bolts. There are basically two arrangements for attaching the suspenders. The first is typified by the detail used for the Forth Road Bridge (Fig. 15.39). In this arrangement, the cable band has grooves to accommodate looping of the structural rope over the main cable. Because of the bending of the suspender over the main cable, structural rope is used for the suspender, to take advantage of its flexibility. The second basic arrangement for attaching a suspender to a cable band was used for the Hennepin Avenue Bridge (Fig. 15.40). In this case, the

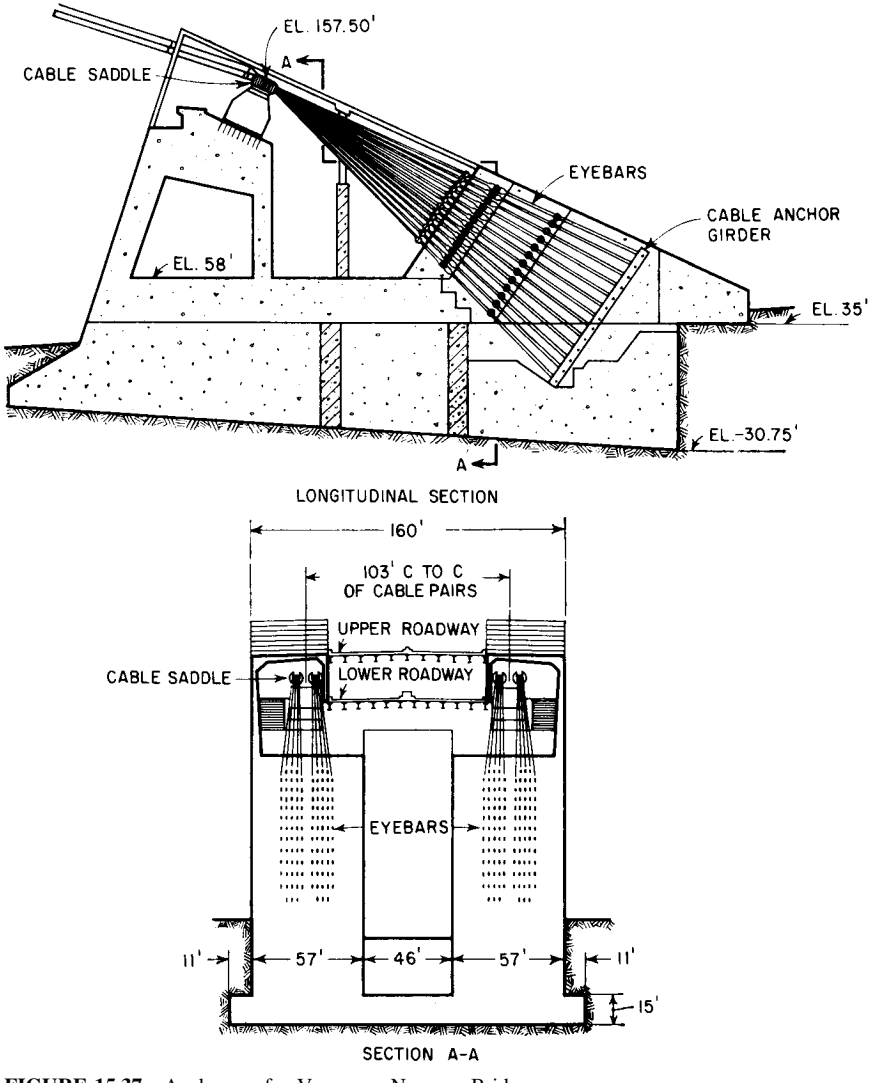

FIGURE 15.37 Anchorage for Verrazano Narrows Bridge.

suspender is attached to the cable band by standard zinc-poured sockets. Since bending of the suspender is not required, the suspender generally is a structural strand. Properly attached, zinc-poured sockets can develop 100% of the strength of strands and wire rope.

The end fittings or sockets of structural strand or rope are standardized by manufacturers and may be swaged or zinc-poured. These fittings include open or closed sockets of drop-forged or cast steel. Some are illustrated in Fig. 15.41. Fatigue must be considered in designing bridge cables that depend on zinc-poured socketing, particularly if they are subject to a wide range of stress.

The attachments of suspenders to girders depend on the type of girder detail. Generally, the end fitting of a suspender is a swaged or zinc-poured type. Where there are multiple strands or ropes in a suspender, the fitting may be specially made.

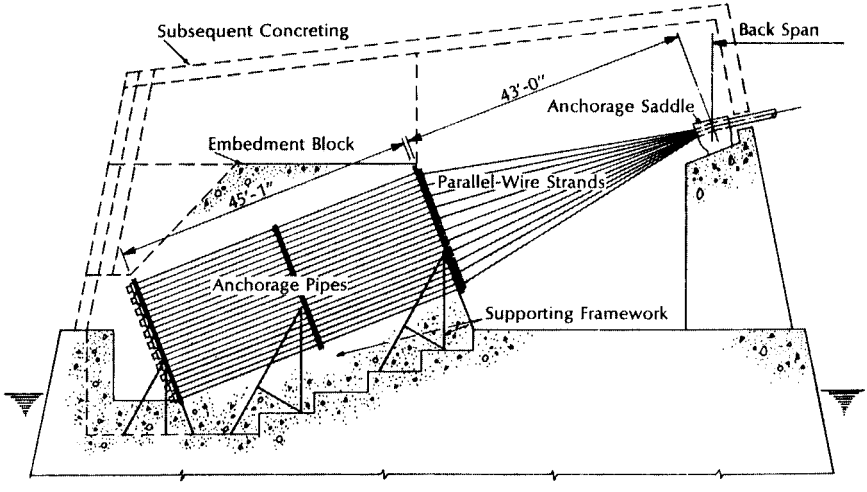

FIGURE 15.38 Anchorage for Newport Bridge.

Early cable-stayed bridges had stays consisting of parallel structural strands or locked-coil strands. These strands had conventional zinc-poured sockets. Because of concern with the low fatigue strength of structural strand with zinc-poured sockets, a new type of socket, called a HiAm (high amplitude) socket, was developed in 1968 by Prof. Fritz Leonhardt in conjunction with Bureau BBR Ltd., Zurich. It was intended for use with stays consisting of parallel ¼-in-dia. prestressing wires that terminate with button heads (ASTM A421 Type BA) in an anchor plate in the socket. The anchor socket is filled with steel balls and an epoxy-and-zinc dust binder. This type of anchorage increases the fatigue resistance to about twice that for zinc-poured sockets. The HiAm sockets were used in the United States for the Pasco-Kennewick, Luling, and East Huntington cable-stayed bridges. After those bridges were constructed, seven-wire prestressing strand came into general use, and several types of anchorages were developed to accommodate parallel prestressing strands in cable stays.

15.14 CORROSION PROTECTION OF CABLES

In the past, the method of protecting the main cables of suspension bridges against corrosion was by coating the steel with a red lead paste, wrapping the cables with galvanized, annealed wires, and applying a red lead paint. This method has met with a varying degree of success from excellent for the Brooklyn Bridge to poor for the General U. S. Grant Bridge at Portsmouth, Ohio. A potential defect in this system is that, as the cable stretches and shortens under live loads and temperature changes, some separation of adjacent turns of wire wrapping may occur. Depending on the degree of separation, the paint may crack and permit leakage of water and contaminants into the cable.

Alternative protection systems that have been used for some suspension bridges are as follows:

Bidwell Bar Bridge. This 1108 ft-span bridge has 11-in-dia., parallel, structural strand cables (Fig. 15.42). The protective system consists of the following components: plastic filler pieces, extruded from black polyethylene; a covering of nylon film; a "first pass" glass-reinforced acrylic-resin covering consisting of one layer of glass-fiber mat, two layers of glass cloth, and several coats of acrylic resin; a weather coat of acrylic resin;

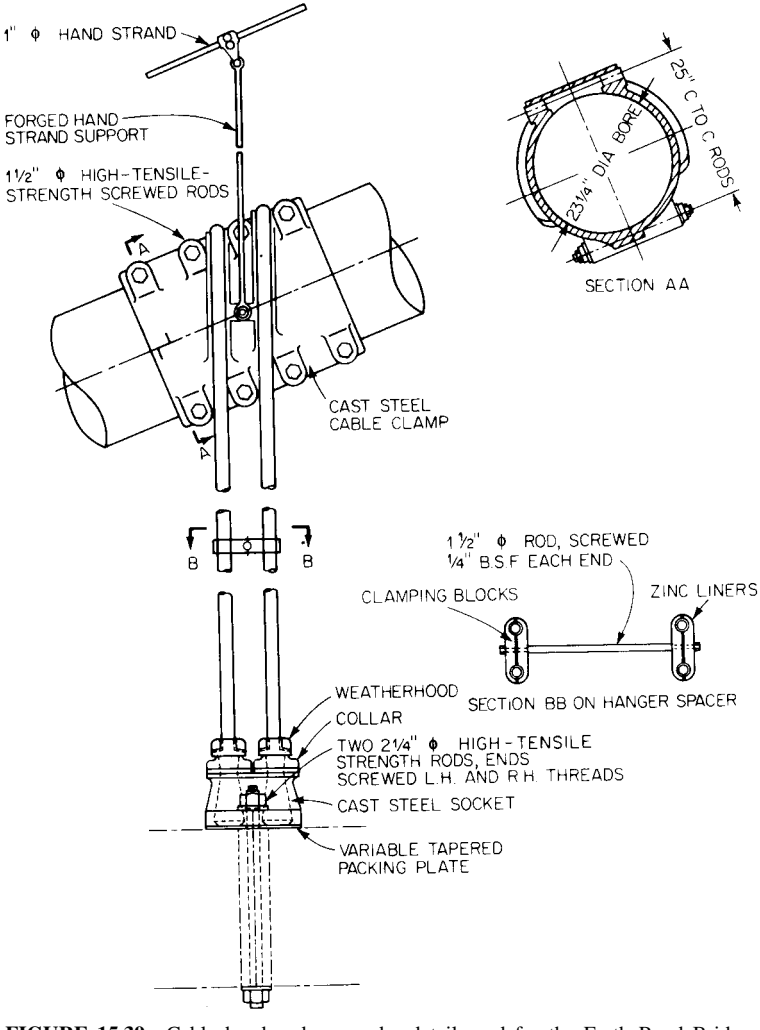

FIGURE 15.39 Cable band and suspender detail used for the Forth Road Bridge. (*Reprinted with permission from Sire Gilbert Roberts, "Forth Road Bridge," Institution of Civil Engineers, London.*)

and a finished coat of acrylic resin containing a sand additive to give the surface a rough texture. This type of covering was developed by Bethlehem Steel in conjunction with DuPont.

Newport, R.I., Bridge. The protective system for the cables of this bridge is the same as that described for the Bidwell Bar Bridge. However, since the cables consist of parallel wires, the black polyethylene filler pieces were not required.

General U. S. Grant Bridge, Ohio. The protective system comprises spiral-wrapped neoprene sheet and hypalon paint, a proprietary system developed by U. S. Steel.

Second Chesapeake Bay Bridge (William Preston Lane, Jr., Memorial). This has the same protective covering as applied to the General U. S. Grant Bridge.

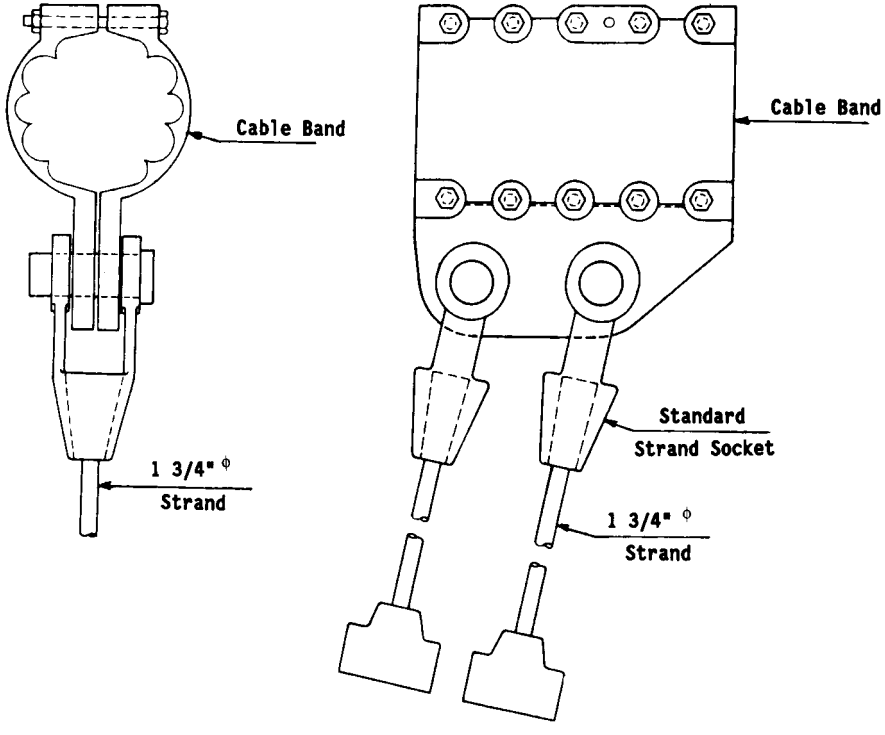

FIGURE 15.40 Cable band and suspender detail used for the Hennepin Avenus Bridge.

Hennepin Avenue Bridge. The protective system consists of a wrapped neoprene sheet and hypalon paint system.

The Bidwell Bar Bridge was constructed in 1964 for the California Department of Water Resources. The protective cable covering has been performing satisfactorily. In the early 1970s, some corrosion was discovered at the cable bands, presumably resulting from shrinkage of the covering. Bethlehem Steel corrected the condition by rewrapping a short portion at the cable bands and recalking. A 1991 inspection indicated no distress in the cable covering.

The similar system applied to the Newport Bridge (installed in 1969) is still performing satisfactorily. A 1980 inspection indicated that some crazing of the top surface had occurred in some areas, but these were superficial and did not extend through the thickness. These areas were patched. There also were some signs of distress at the cable bands, in the calking groove. As a result of thermal contraction of the covering, the calking had worked loose (presumably the same condition as that in the Bidwell Bar Bridge). Repairs were made with a more resilient type calk that accommodates thermal movement.

The system developed by U. S. Steel and applied to the Second Chesapeake Bay Bridge in 1973, the General U. S. Grant Bridge in 1980, and the Hennepin Avenue Bridge in 1990, has been performing satisfactorily. This type of system was also used for rewrapping the Brooklyn Bridge cables in 1986.

Table 15.5 presents a partial listing of suspension bridges with appropriate statistics and the corrosion protection used for the main cables.

An area where the main cable is particularly vulnerable extends from the splay saddle to the eyebars in the anchorage blocks. The only corrosion protection available is the zinc

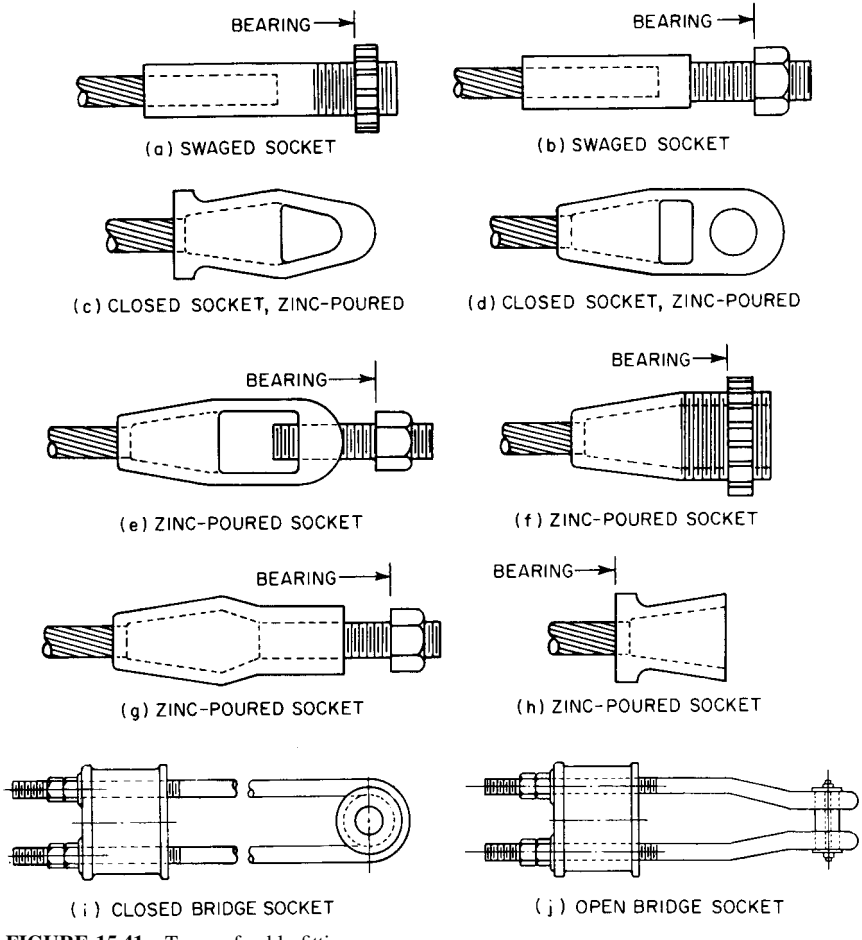

FIGURE 15.41 Types of cable fittings.

coating of the wires. Depending on environmental conditions in the anchorage blocks, the galvanizing may have a life expectancy on the order of 20 years. Serious corrosion in this area occurred in the Brooklyn, Williamsburg, and Manhattan Bridges, requiring corrective measures. In the rehabilitation of one anchorage of the Manhattan Bridge, dehumidification equipment was included to control humidity in the anchorage block.

Suspender Corrosion. Generally, corrosion of suspenders is likely to occur at the anchorage sockets at the stiffening trusses and at retainer castings on top of those trusses. This may be attributed to two possible sources: salt spray from roadway deicing salts, or moisture that enters the interstices of the strand or rope at an upper level and trickles down to the socket or casting.

A 1974 report on the condition of the suspenders of the Golden Gate Bridge revealed that there was considerable reduction in suspender area due to corrosion that occurred as high as 150 ft above the roadway. This could be attributed to saltwater mist or fog.

For corrosion protection, U. S. Steel developed a procedure for extruding high-density black polyethylene over strands and rope. In many applications, this jacket also reduces

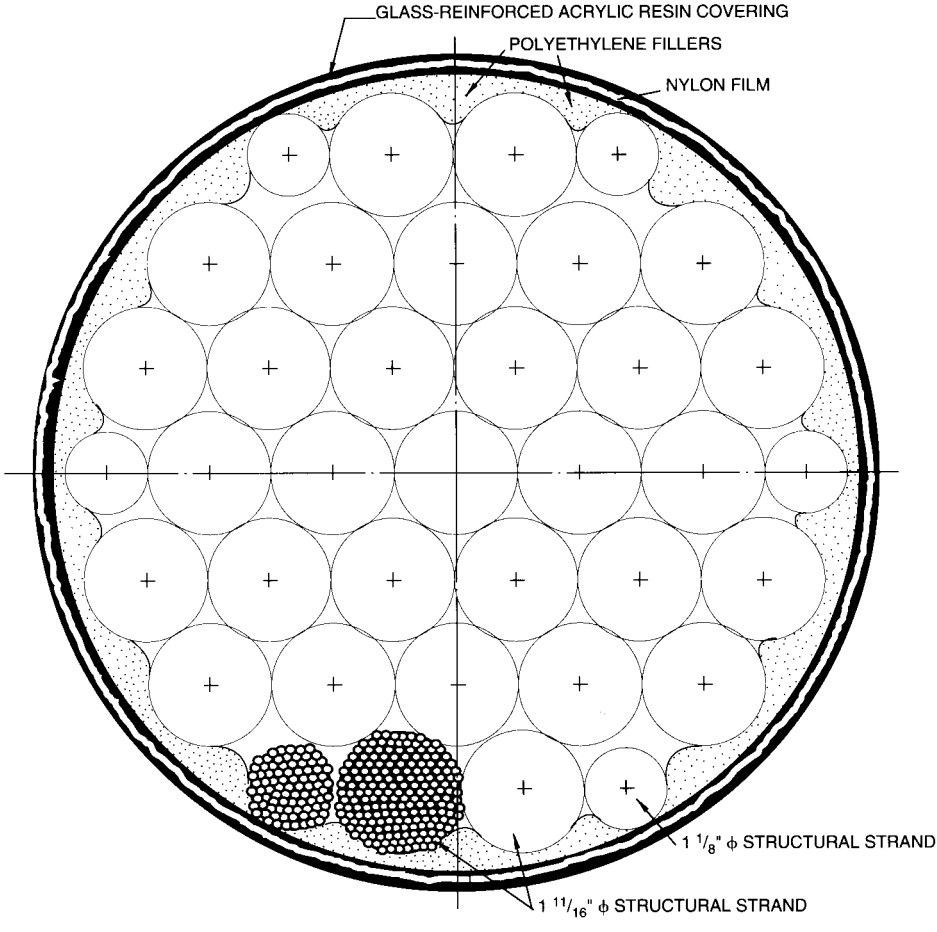

FIGURE 15.42 Cable corrosion protection system used for the Bidwell Bar Bridge. (*Reprinted with permission from J. L. Durkee and M. IABSE, "Advancements in Suspension Bridge Cable Construction," Paper No. 27, Symposium on Suspension Bridges, Lisbon, November 1966.*)

vibration fatigue. For this purpose, particular attention is given to sealing and ends and minimizing the bending of wires at the nose of the socket.

Galvanizing. Wires can be protected against corrosion by galvanizing, a sacrificial coating of zinc that prevents corrosion of the steel so long as the coating is unbroken. Corrosion protection of the individual wires in a structural strand or rope is provided by various thicknesses of zinc coating, depending on the location of the wire in the strand or rope and the degree of corrosive environment expected. The effectiveness of the zinc coating is proportional to its thickness, measured in ounces per square foot of surface area of the uncoated wire. Class A zinc coating varies from 0.40 to 1.00 oz/ft^2 depending on the nominal diameter of the coated wire. A Class B or C coating is, respectively, 2 or 3 times as heavy as the Class A coating.

Generally, there are three basic combinations of coating: Class A coating throughout all wires; Class A coating for the inner wires and Class B for the outer wires; and Class A

TABLE 15.5 Cable Construction and Corrosion Protection for Some Suspension Bridges

Name	Location	Year	No. of cables	Cable dia., in	No. of strands	No. of wires or strands	Wire dia., in	Cable construction[1]	Corrosion protection[2]
Brooklyn Bridge	Brooklyn, N.Y.	1883	4	15⅝	19	282	0.184[3]	AS	CWR
Williamsburg	New York, N.Y.	1904	4	18¾	37	208	0.192[4]	AS	Note[5]
Manhattan	New York, N.Y.	1910	4	20¾	37	256	0.195	AS	CWR
George Washington	New York, N.Y.	1931	4	26	61	434	0.196	AS	CWR
San Francisco-Oakland Bay	California	1936	2	28¾	37	472	0.195	AS	CWR
Bronx-Whitestone	New York, N.Y.	1939	2	21½	37	266		AS	CWR
Mackinac Straits	Michigan	1957	2	24¼	37	340	0.196	AS	CWR
Walt Whitman	Philadelphia, Pa.	1957	2	23⅛	37	308	0.196	AS	CWR
Throgs Neck	New York, N.Y.	1961	2	23	37	296	0.1875	AS	CWR
Bidwell Bar	State Rt. 62 Feather R., Calif.	1964	2	11	37[6]			PHSS	GRAR
Verrazano Narrows	New York, N.Y.	1964	4	35⅞	61	428		AS	CWR
Forth Road	Queensferry, Scotland	1964	2	24	37	314	0.196	AS	CWR
Tagus (Salazar)	Lisbon, Portugal	1966	2	23 1/16	37	304	0.196	AS	CWR
Severn River	Beachley, England	1966	2	20	19	440	0.196	AS	CWR
Newport	Newport, R.I.	1969	2	15¼	76	61	0.202	FPWS	GRAR
Bosporus	Istanbul, Turkey	1973	2	23	19	548	0.2	AS	CWR
Humber	England	1980	2	27½	37	404	0.2	AS	CWR
Gen U. S. Grant	Portsmouth, Ohio	1927	2	7⅛	3	486	0.162[4]	SFPW	CWR
		1940	2	7 13/16	19[7]			PHSS	CWR
		1980	2		[8]			PHSS	NSHP
Hennepin Ave.	Minneapolis, Minn.	1990	4	15⅜	19[9]			PHSS	NSHP

[1] Cable construction: AS = aerial spinning, PHSS = parallel helical structural strand, SFPW = site fabricated parallel wire strand, FPWS = factory fabricated prefabricated parallel wire strand.

[2] Corrosion protection: CWR = conventional wire wrapping and red lead, GRAR = glass reinforced acrylic resin, NSHP = neoprene sheet and hypalon paint.

[3] Deduced average diameter of the galvanized wire, average bare-wire diameter 0.181 in.

[4] Ungalvanized wires.

[5] Between 1916 and 1922, the original canvas wrapping and steel sheet protection of the cables was removed and replaced by glavanized wrapping wire.

[6] 31 helical structure strands, 1 11/16-in dia., and 6 helical strands, 1 ⅛-in dia.

[7] 13 helical structural strands, 1 ¾-in dia., and 6 helical strands, 1 ¼-in dia., Class A coating.

[8] Same configuration as under note 7; i.e., same basic steel area, but changed coating from Class A to Class C.

[9] 13 helical structural strands, 3 ⅜-in dia., and 6 helical strands, 2 ⅝-in dia.

coating for the inner wires and Class C for the outer wires, depending on the degree of protection desired. Other coating thicknesses and arrangements are possible.

The heavier zinc coatings displace more of the steel area. This necessitates a reduction in rated breaking strength of strand or rope. ASTM A586 and A603 specify minimum breaking strengths required for various sizes of strand or rope in accordance with the three combinations of coating previously described. For other combinations of coating, the manufacturer should be consulted as to minimum breaking strength and modulus of elasticity.

Galvanizing has some disadvantages. Depending on environmental conditions, for example, galvanizing may be expected to last only about 20 years. Also, the possibility that hot-dip galvanizing may cause hydrogen embrittlement is of concern. (There is some indication, however, that, with current technology, the hot-dip galvanizing method is not as likely to cause hydrogen embrittlement as previously.) In addition, it may be difficult to meet specifications for a Class C coating with the hot-dip method. Furthermore, wire with hot-dip galvanizing may not have the fatigue resistance that wire coated by electrolytic galvanizing has.

Protection of Stays. In early cable-stayed bridges, stays, consisting of locked-coil or structural strands, were protected against corrosion by galvanizing and paint. Nevertheless, extensive corrosion occurred (S. C. Watson and D. G. Strafford, ''Cables in Trouble,'' *Civil Engineering,* vol 58, no. 4, April 1988, American Society of Civil Engineers). Contemporary stays, in contrast, are similar to external tendons generally used for posttensioned concrete. They consist of prestressing steel, sheathing, corrosion-protection materials, and anchorages.

The Schillerstrasse footbridge in Stuttgart, Germany, completed in 1961, was the first cable-stayed bridge to employ a sheathed and cement-grout-injected stay system. The stays consist of a bundle of parallel prestressing wire encapsulated in a polyethylene (PE) pipe and injected with cement grout. The purpose of the PE sheathing is twofold: to provide a form for the cement grout and to serve as a corrosion barrier. The stays have been inspected on numerous occasions and have shown no signs of corrosion. The first use of this system in the United States was for the Pasco-Kennewick Bridge, completed in 1978. The stays of the bridge were inspected in 1990. After 12 years in service, the exposed wire was as bright and as good as the day it was installed, indicating that with proper care and procedures for installation, cementitious grout can be an effective corrosion inhibitor.

A sheathing of high-density polyethylene (HDPE) pipe is airtight. A ¼-in thickness provides the same vapor barrier as a 35-ft-thick concrete wall. However, the HDPE pipe must be handled with care. If abused, as in the case of the Luling Bridge (related to excessive grout pressure), the pipe may, in time, develop longitudinal cracks. In addition, the cement-grout column may develop transverse cracks from cyclic tension in the stays, among other reasons. Thus, there is need to prevent direct access to the bare prestressing steel by corrosive agents.

Alternative materials to cement grout or means of providing additional corrosion barriers have been sought to increase corrosion protection of steel stays. Such materials as grease, wax, polymer-cement grout, and polybutadiene polyurethane have been tried with varying degrees of success.

Corrosion protection systems may be either two-phase or single-phase. In the two-phase method, the permanent corrosion protection is applied as the last operation of construction of the structure. This means that a temporary corrosion protection is required during a construction period that may be two to four years or longer in duration. The effectiveness of most temporary corrosion protection methods is short lived. If replenishment is overlooked or not accomplished, for whatever reason, there is a distinct risk of corrosion occurring before the permanent corrosion protection can be applied and the risk of having to replace the cable. There is currently a trend to a single-phase corrosion protection system that provides both the temporary and permanent system simultaneously, i.e., a system that provides protection from the manufacture of the cable throughout its service life.

The use of alternative materials for cementitious grout attempts to overcome the problem of grout cracking, and thus obviate the potential of a direct path for the corrosive agents to

the steel, in the event the outside sheathing is compromised. However, the use of alternative materials for cementitious grout does not overcome the problem related to temporary corrosion protection of the steel strands.

To overcome the potential problems of a sheathed and grouted system, multiple barrier systems have been developed. The concept simply provides multiple corrosion barriers such that one or more materials take over the protective function for a material that has failed, or stated another way, provides increased redundancy in the corrosion protection system.

Generally, these additional barriers are provided by one of the following two methods:

- Individual greased and sheathed strands (the so-called monostrand method). It should be noted that the word grease as used in this context is generic, the material may be grease, wax, epoxy-tar or some other appropriate material.
- A coating applied directly to the strand such as galvanizing or epoxy.

Both of the above systems are installed or applied prior to shipment, thus, they are not only incorporated into the final total corrosion protection system, but they also provide the temporary corrosion protection during shipping, storage, after installation until the final grouting operation, and during service life.

In the search for corrosion protection methods and materials, consideration has been given to coatings applied directly to the prestressing steel. Galvanized prestressing wire has been used in some multibarrier systems. Galvanized prestressing steel should never be used where it is in direct contact with cementitious grout and the designer must be cognizant of the effects of galvanizing, if any, on the material properties of the steel.

A relatively recent development is an epoxy coated and filled strand whereby the interstices between the wires are filled with epoxy. This eliminates the concern for corrosive agents gaining access to the interior of the strand. Epoxy coating and filling of the individual strands provides both temporary and permanent corrosion protection to the strand, and eliminates the concern for aggressive corrosion agents reaching the prestressing steel as a result of cracked cement grout and potential cracks in the outside sheathing. So as not to compromise the effectiveness of the system, attention must be paid to the anchorage details. Special wedges are required that bite through the epoxy thickness and grip the prestressing strand. The epoxy should not be stripped from the strand.

The so-called monostrand system as used for cable stays is an adaptation or transfer of technology of the post-tensioning monostrands that are used for parking garage or flat slab construction. The stay consists of a parallel bundle of 0.6 in diameter unbonded prestressing strands that are individually greased and sheathed, and enclosed in a HDPE external pipe and grouted. The corrosion protection of unbonded prestressing strand relies to a large extent on the prevention of moisture and corrosive materials from reaching the steel. Therefore, the sheathing on the individual strands must be completely watertight throughout its length, up to and including the anchorages.

15.15 STATICS OF CABLES

The following summary of elementary statics of cables applies to completely flexible and inextensible cables but includes correction for elastic stretch. The formulas derive from the fundamental differential equation of a cable shape

$$y'' = -\frac{w}{H} \tag{15.2}$$

where y'' = second derivative of the cable ordinate with respect to x
x = distance, measured normal to the cable ordinate, from origin of coordinates to point where y'' is taken

H = horizontal component of cable tension produced by w
w = distributed load, which may vary with x

Two cases are treated: catenary, the shape taken by a cable when the load is uniformly distributed over its length, and parabola, the shape taken by a cable when the load is uniformly distributed over the projection of the span normal to the load.

Table 15.6 lists equations for symmetrical cable. These equations, however, may be extended to asymmetrical cables, as noted later.

The derivation of the equations considered the cable as inextensible. Actually, the tension in the cable stretches it. The stretch, in, of half the cable length may be estimated from

$$\Delta s = \frac{(T + H)s}{2AE} \tag{15.3}$$

where s = half the length of cable, in
T = cable tension, kips, at point of attachment
H = horizontal component of cable tension, kips
A = cross-sectional area of cable, in^2
E = modulus of elasticity of cable steel, ksi

Properties of asymmetrical cables may be obtained by determining first the properties of their component symmetrical elements.

For a parabolic cable (Fig. 15.43), determine point C on the cable, which lies on a horizontal line through a point of attachment. The horizontal distance of C from the support at the cable high point may be computed from $2l_1 - l$, where the cable span $l = l_1 + l_2$, after l_1 has been found from

$$l_1 = \frac{f_1 l}{c}\left(1 \pm \sqrt{1 - \frac{c}{f_1}}\right) \tag{15.4}$$

where l_1, l_2 = horizontal distances from M, the cable low point, to the high and low supports A and B, respectively
f_1 = cable sag measured from high point
c = vertical distance between points of support

The portion of the cable between C and the lower support is symmetrical. Its ordinates, slope, length, and cable tension may be computed from the equations in Table 15.6.

For a catenary cable (Fig. 15.44), point C on a horizontal line through the lower support may be located by stepwise solution of the equation $y = h \cos x/h$ for a symmetrical catenary. An initial solution may be obtained by use of a parabola. Substitution in the exact equation then yields more accurate values. When distances l_1 and l_2 of C from the supports have been determined, the ordinates, slope, length, and cable tension of the symmetrical portion of the cable may be computed.

The portion of the cable from C to the high point is an oblique cable (Fig. 15.45), a special case of the asymmetrical cable. Its properties can be obtained with the equations in Table 15.6 and Eq. (15.4) by treating the oblique cable as part of a symmetrical one.

(See also Art. 4.8.)

15.16 SUSPENSION-BRIDGE ANALYSIS

Structural analysis of a suspension bridge is that step in the design process whereby, for given structural geometry, materials, and sizes, the moments and shears in stiffening trusses, axial loads in cables and suspenders, and deflections of all elements are determined for given

TABLE 15.6 Equations for Catenary and Parabolic Cables*

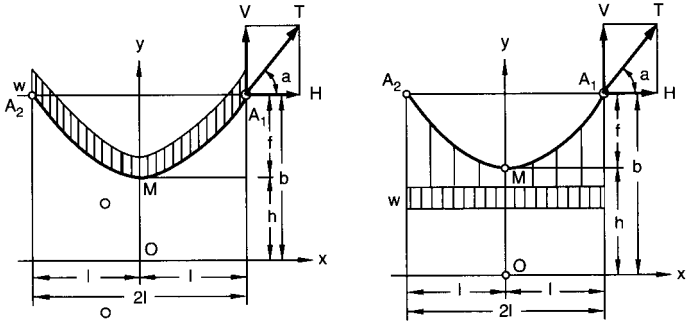

	Catenary	Parabola
Cable ordinate y†	$y = (e^{x/h} + e^{-x/h})h/2$ $= h \cosh x/h$	$y = h + x^2/2h$
Coordinate b of attachment points A_1 and A_2	$b = f + h$ $= h \cosh l/h$	$b = f + h$ $= h + l^2/2h$ $= (l^2 + 4f^2)/2f$
Sag-span ratio a	$a = f/2l$	$a = f/2l$
Slope y' of cable	$y' = \sinh x/h$	$y' = x/h$
Ordinate h of cable low point	$h = H/w$	$h = H/w$ $= l^2/2f$ $= l/4a$ $= f/8a^2$
Sag f	$f = h(\cosh l/h - 1)$	$f = l^2/2h$
Half length s of cable	$s = \sqrt{b^2 - h^2}$ $= \sqrt{f^2 + 2hf}$ $= \sqrt{2fb - f^2}$	$s = \frac{l}{2h}\sqrt{h^2 + l^2} + \frac{h}{2} \times [\log_e (l + \sqrt{h^2 + l^2}) - \log_e h]$ $= \frac{l}{2h}\sqrt{h^2 + l^2} + \frac{h}{2}\sinh^{-1}\frac{l}{h}$ $\approx l\left(1 + \frac{8}{3}a^2 - \frac{32}{5}\alpha^4 + \frac{256}{7}a^6 - \cdots\right)$
Angle α of cable at A_1 and A_2	$\tan \alpha = \sin l/h$ $= \frac{1}{h}\sqrt{f^2 + 2fh}$ $= \frac{1}{b - f}\sqrt{2fb - f^2}$ $= s/h$ $= \frac{1}{h}\sqrt{b^2 - h^2}$ $\cos \alpha = h/b$ $= h/(h + f)$ $= (b - f)/b$ $\sin \alpha = \frac{1}{b}\sqrt{2fb - f^2}$ $= s/b$ $= \frac{1}{b}\sqrt{b^2 - h^2}$ $= \frac{1}{h + f}\sqrt{f^2 + 2fh}$	$\tan \alpha = l/h$ $= \sqrt{2f/h}$ $= \sqrt{2f/(b - f)}$ $= 2f/l$ $= 4a$ $= 1/\sqrt{1 + 16a^2}$ $\cos \alpha = h/\sqrt{h^2 + l^2}$ $= h/\sqrt{h^2 + 2fh}$ $= (b - f)/\sqrt{b^2 - f^2}$ $= l/\sqrt{l^2 + 4f^2}$ $\sin \alpha = \sqrt{2f/(b + f)}$ $= l/\sqrt{h^2 + l^2}$ $= \sqrt{2f/(h + 2f)}$ $= 2f/\sqrt{l^2 + 4f^2}$ $= 4a/\sqrt{1 + 16a^2}$

TABLE 15.6 Equations for Catenary and Parabolic Cables* (*Continued*)

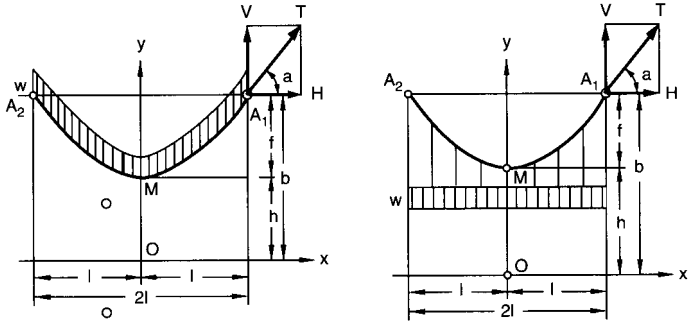

	Catenary	Parabola
Vertical component V of cable tension	$V = w\sqrt{b^2 - h^2}$ $= w\sqrt{f^2 + 2fh}$ $= w\sqrt{2fb - f^2}$ $= ws$	$V = w\sqrt{2fh}$ $= wl$ $= 4wah$
Horizontal component H of cable tension	$H = wh$ $= w(b - f)$	$H = wh$ $= wl^2/2f$ $= wl/4a$ $= wf/8a^2$
Cable tension T	$T = wb$	$T = w\sqrt{h^2 + l^2}$ $= w\sqrt{2fh + h^2}$ $= wh\sqrt{1 + 16a^2}$

*Adapted from H. Odenhausen, "Statical Principles of the Application of Steel Wire Ropes in Structural Engineering," *Acier-Stahl-Steel,* no. 2, pp. 51–65, 1965.

† Since

$$\cosh \frac{x}{h} = 1 + \frac{(x/h)^2}{2!} + \frac{(x/h)^4}{4!} + \frac{(x/h)^6}{6!} + \cdots$$

the parabolic profile (obtained by dropping the third and subsequent terms) is an approximation for the catenary. The accuracy of this approximation improves as sag f becomes smaller.

loads and temperature changes. The stress analysis usually is carried out in two broad categories: static and dynamic.

15.16.1 Static Analysis—Elastic Theory

Before the Manhattan Bridge was designed about 1907, suspension bridges were analyzed by the classical theory of structures, the so-called elastic, or first-order, theory of indeterminate analysis. This neglects the deformations of the structural geometry under load in formulation of the equations of equilibrium. The earliest theory was developed by Rankine, who assumed that a stiffening truss distributes the loads uniformly to the cable from which it is suspended. The elastic theory is advantageous because the resulting equations are linear in the loads and internal forces, and linear superposition applies for internal forces caused by different loads. Distortions of the structural geometry under live load, however, can cause a gross overstatement of moments, shears, and deflections calculated by the elastic theory.

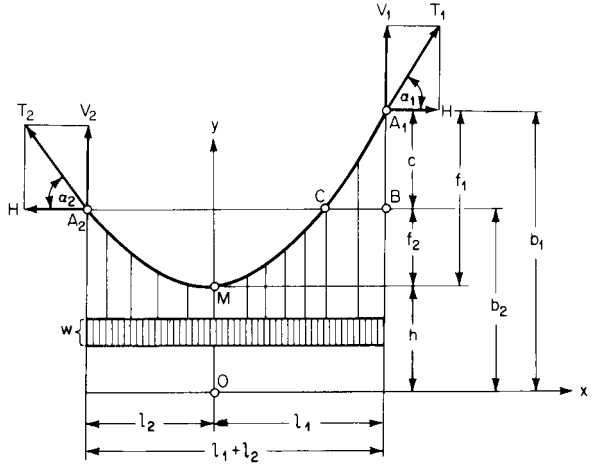

FIGURE 15.43 Cable assumes parabolic shape when subjected to a uniform load acting over its horizontal projection.

This theory, therefore, is seldom used, except as a basis for preliminary design or for design of bridges with short spans or rigid stiffening trusses for which large distortions are not possible. (See also Art. 15.16.2.)

The elastic-theory equations following apply to the structure in Fig. 15.46 with unloaded side spans and pin-ended, main-span stiffening truss. This structure has one redundant, the horizontal component H of cable reaction. An equation for determining H is obtained by making the structure statically determinate by cutting the cable at its low point and applying H there. The gap that is opened at the cut by loads on the stiffening truss must equal the oppositely directed movement at that point produced by H. These deflections can be cal-

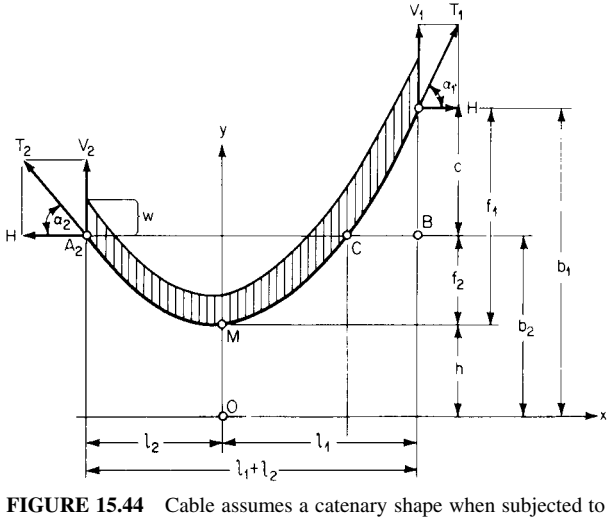

FIGURE 15.44 Cable assumes a catenary shape when subjected to a uniform load acting over its length.

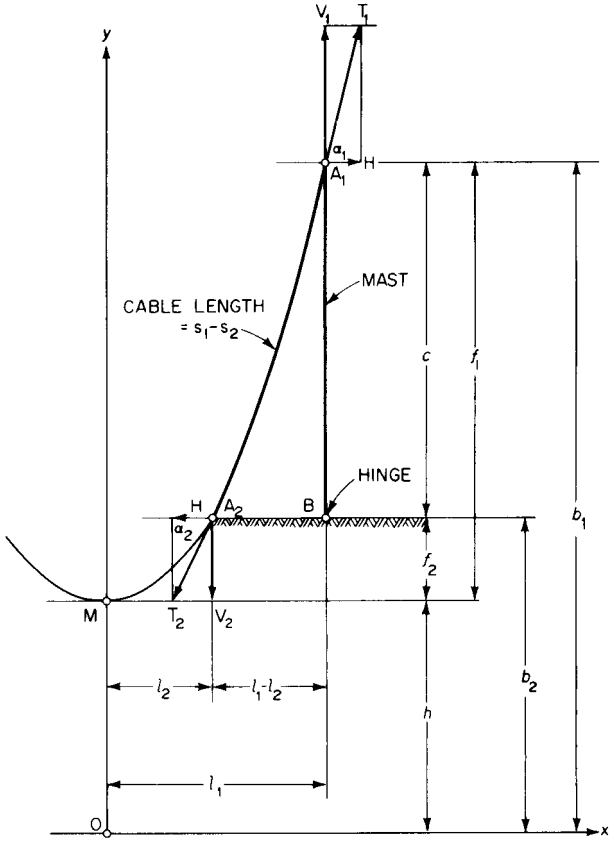

FIGURE 15.45 Part of catenary between low point and a support.

culated by the virtual work or dummy-unit-load method, and the equation can readily be solved for H.

For loads,

$$H = \frac{\delta_{ao}}{\delta_{aa}} \tag{15.5}$$

where $\delta_{aa} = \int \frac{M_a^2\, ds}{EI} + \int \frac{N_a^2\, ds}{AE}$

$\delta_{ao} = \int \frac{M_a M_o\, ds}{EI} + \int \frac{N_a N_o\, ds}{AE}$

M_a = statically determinate moment due to unit horizontal force applied at cut end of cable

M_o = statically determinate moment due to loads

N_a = statically determinate axial forces due to unit horizontal force applied at cut end of cable

N_o = statically determinate axial forces due to loads

E = modulus of elasticity of stiffening-truss steel

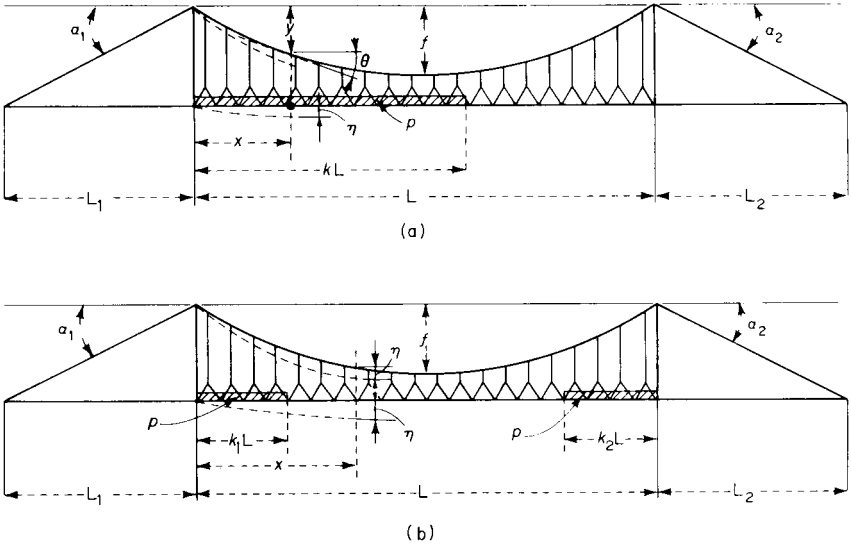

FIGURE 15.46 Suspension bridge with unloaded side spans and pin-ended main-span truss. (*a*) Single uniform load extending from a pylon into the main span. (*b*) Uniform load extending from both pylons into the main span.

I = moment of inertia of stiffening truss
A = cross-sectional area of member subjected to axial force

For temperature change,

$$H_t = -\frac{\delta_{at}}{\delta_{aa}} \tag{15.6}$$

where $\delta_{at} = \int \frac{\epsilon_t t \sec \theta}{A_c E_c}\, ds = \int \frac{ds}{dx} \frac{\epsilon_t t}{A_c E_c}\, ds$

ϵ_t = coefficient of thermal expansion
t = temperature change
A_c = cross-sectional area of cable
E_c = modulus of elasticity of cable steel

Assumptions. To evaluate Eqs. (15.5) and (15.6), the following conditions are assumed for the structure in Fig. 15.46:

1. The cable takes the shape of a parabola under dead load w.
2. Elongation of suspenders and shortening of pylons are so small that they can be neglected.
3. Spacing of suspenders is so small relative to span that the suspenders can be considered a continuous sheet.
4. The horizontal component of cable tension in side spans equals the horizontal component of cable tension in main span. This holds if the cable is fixed to the top of flexible pylons or to a movable saddle atop the pylons.
5. The stiffening truss acts as a beam of constant moment of inertia simply supported at the ends. Under dead load, it is straight and horizontal. Usually erected so that it carries none

of the dead load, the stiffening truss therefore is stressed only by live load and temperature changes.

Thus, the horizontal component of cable tension due to temperature rise t may be computed from

$$H_t = -\frac{3EI\epsilon_t t L_t}{f^2 NL} \tag{15.7}$$

where f = cable sag
L = length of main span
$L_t = \int_0^S (ds/dx)\, ds + L_1 \sec^2 \alpha_1 + L_2 \sec^2 \alpha_2$
$\approx L + {}^{16}\!/_{3} a^2 L + L_1 \sec^2 \alpha_1 + L_2 \sec^2 \alpha_2$
$a = f/L$
S = length of main-span cable
$N = \frac{8}{5} + \frac{3EI}{A_c E_c f^2}(1 + 8a^2) + \frac{3EIL_t}{A_c E_c L f^2} \sec^3 \alpha_1 + \frac{3EIL_2}{A_c E_c L f^2} \sec^3 \alpha_2$
L_1, L_2 = lengths of side spans
α_1, α_2 = angle with respect to horizontal of side-span cables

The horizontal component of cable tension due to a uniform live load p extending a distance kL from either end of the main span may be computed from

$$H_p = \frac{pL}{5Na}\left(\frac{5}{2}k^2 - \frac{5}{2}k^4 + k^5\right) \tag{15.8}$$

For maximum cable stress ($k = 1$), the horizontal component due to dead load is

$$H_w = \frac{wL}{8a} \tag{15.9}$$

For live load over the whole span,

$$H_p = \frac{pL}{5Na} \tag{15.10}$$

The sum yields the maximum horizontal component of cable tension:

$$H_{\max} = \frac{L}{a}\left(\frac{w}{8} + \frac{p}{5N}\right) \tag{15.11}$$

For maximum moment at distance x *from pylon:*

A. When $0 \leqq x \leqq NL/4$, solve for k (Fig. 15.46*a*):

$$k + k^2 - k^3 = \frac{NL}{4(L - x)} \tag{15.12}$$

Maximum positive moment with loaded length kL then may be obtained from

$$M_{\max} = \frac{px}{2}(L - x)\left\{1 - \frac{8}{5N}[1 - {}^{1}\!/_{2}(1 - k)^4(2 + 3k)]\right\} \tag{15.13a}$$

Maximum negative moment with loaded length $L - kL$ may be computed from

$$M'_{\max} = -\frac{2}{5}\frac{px(L-x)}{N}(1-k)^4(2+3k) \tag{15.13b}$$

B. When $NL/4 \leqq x \leqq L/2$, solve for k_1 and k_2 (Fig. 15.46*b*):

$$1 - 2k_1^2 + k_1^3 = \frac{NL}{4x} \tag{15.14}$$

$$1 - 2k_2^2 + k_2^3 = \frac{NL}{4(L-x)} \tag{15.15}$$

Maximum negative moment with loaded lengths k_1L and k_2L may be obtained from

$$M = -\frac{2}{5}\frac{px(L-x)}{N}[k_1^4(5-3k_1) + k_2^4(5-3k_2)] \tag{15.16}$$

Maximum positive moment with loaded length $L - L(k_1 + k_2)$ may be calculated from

$$M_{\max} = \frac{1}{2}px(L-x)\left\{1 - \frac{4}{5N}[2 - k_1^4(5-3k_1) - k_2^4(5-3k_2)]\right\} \tag{15.17}$$

For maximum shear at distance x *from pylon:*

A. When $0 \leqq x \leqq (1 - N/4)L/2$, solve for k_o:

$$k_o + k_o^2 - k_o^3 = \frac{NL}{4(L-2x)} \tag{15.18}$$

Maximum positive shear with load between distances x and k_oL from a pylon may be obtained from

$$V_{\max} = V_1 - V_2 \tag{15.19}$$

$$V_1 = \frac{pL}{2}\left(1 - \frac{x}{L}\right)^2\left[1 - \frac{8}{5N}\left(\frac{1}{2} - \frac{x}{L}\right)\left(2 + \frac{4x}{L} + \frac{x^2}{L^2} - 2\frac{x^3}{L^3}\right)\right] \tag{15.20a}$$

$$V_2 = \frac{pL}{2}(1-k_o)^2\left[1 - \frac{8}{5N}\left(\frac{1}{2} - \frac{x}{L}\right)(2 + 4k_o + k_o^2 - 2k_o^3)\right] \tag{15.20b}$$

B. When $(1 - N/4)L/2 \leqq x \leqq L/2$,

$$V = \frac{pL}{2}\left(1 - \frac{x}{L}\right)^2\left[1 - \frac{8}{5N}\left(\frac{1}{2} - \frac{x}{L}\right)\left(2 + \frac{4x}{L} + \frac{x^2}{L^2} - 2\frac{x^3}{L^3}\right)\right] \tag{15.21}$$

(S. P. Timoshenko and D. H. Young, "Theory of Structures," 2d ed., McGraw-Hill Book Co., Inc., New York; A. G. Pugsley, "Theory of Suspension Bridges," Edward Arnold, Ltd., London.)

15.16.2 Static Analysis—Deflection Theory

Distortions of structural geometry of long suspension spans under live load may be very large. As a consequence, the elastic theory (Art. 15.16.1) gives unduly conservative moments, shears, and deflections. For economy, therefore, a deflection theory, also referred to as an exact or second-order theory, that accounts for effects of deformations should be used.

With the notation and assumptions given for the elastic theory in Art. 15.16.1, a differential equation can be written for the structure in Fig. 15.46 to include the vertical defection η of the cable (and stiffening truss) at any point x. This equation expresses the flexural relationship between the horizontal component of cable tension H under dead and live loads and the stiffening-truss deflection under uniform live load p:

$$EI\eta'''' = p + H_p y'' + H\eta'' \tag{15.22}$$

where each prime represents a differentiation with respect to x.

Equation (15.22) by itself is not sufficient for solution for the two unknowns, η and the horizontal component of cable tension H_p due to live load. (*Note:* H can be expressed in terms of H_p.) Therefore, an additional compatibility equation is necessary. It expresses the cable condition that the total horizontal projection of cable length between anchorages remains unchanged.

The differential equations are not linear, and linear superposition is technically not applicable. This would imply that the use of influence lines for handling moving live loads is not permissible.

In the conventional deflection theory, however, the differential equations are linearized over a small range by assuming that the exponential terms containing H in the solution of the equations are constant during integration (even though that assumption is not valid for a particular loading case). This assumption may be made because, for example, the loading length for maximum moment at a point is not greatly affected by the magnitude of H. With this quasi-linear theory, an average value of H, or two values, $H_{\min}$ and $H_{\max}$, may be used as a basis for drawing linearized influence lines as in first-order theory. With two influence lines (maximum and minimum) thus available, the results can be interpolated for more accurate values of H.

H. Bleich and S. P. Timoshenko suggested that the zero points of the influence lines be determined in this quasi-linear theory to establish the most unfavorable live-loading position. Then, the final results may be calculated by the classical theory with the live load in this position.

Besides the preceding classical differential-equation approach, a trigonometric-series method also is useful. Other advantageous procedures include successive approximation by relaxation theory, simultaneous-linear-equation approach of the flexibility-coefficient methods, elastic-foundation analogy, and analogy of an axially loaded beam.

Much of the literature on classical suspension-bridge theory deals with the effects of minor terms neglected in the assumptions of the deflection theory. S. P. Timoshenko gave an excellent account of the effect of horizontal displacements of the cable, elongation of suspenders, shear deflections, and temperature changes in the cable. (S. P. Timoshenko and D. H. Young, ''Theory of Structures,'' 2d ed., McGraw-Hill, Inc., New York.) Other investigators have extended the theory to stiffening trusses that are continuous (such as in the Salazar Bridge) or have variable moments of inertia, widely spaced or inclined suspenders, or multiple main spans.

In general, inclined suspenders can have an important effect on results. Continuous spans are of advantage primarily in short bridges, but the advantage diminishes with long spans. Simple supports are preferred because they avoid settlement problems.

The following treatment of the classical approach is based on A. A. Jakkula's generalization of the work of many investigators. It is restricted here to the case of a suspension bridge with unloaded backstays and a two-hinged stiffening truss (Figs. 15.46 and 15.47). This presentation is useful because it has been extended to configurations with loaded backstays, or other variations of the suspension system, and has been programmed for computers.

Advances in computational methods have prompted several new approaches to analysis of suspension-bridges that differ from the classical deflection theory in that they adapt discrete mathematical models to computer programming. For example, if the suspenders are treated as finitely spaced elements (instead of an assumed continuous sheet as in classical

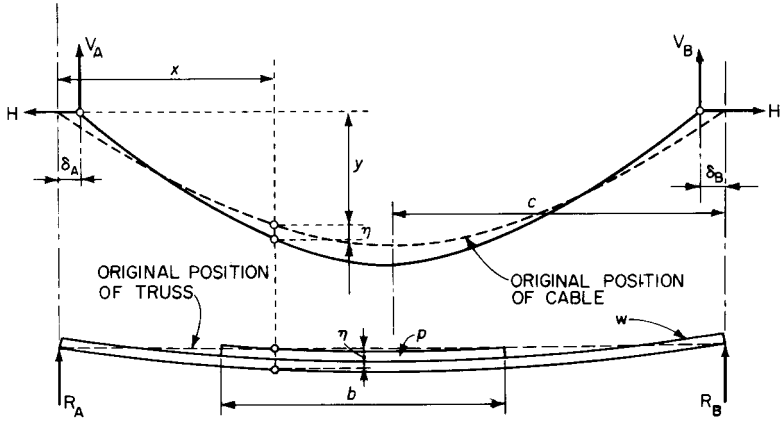

FIGURE 15.47 Original and deflected positions of the main-span cable and stiffening truss for the bridge in Fig. 15.46. Cable and truss have equal deflections at distance x from a pylon.

methods), the analysis becomes that of an open-panel truss. Solution is required of a set of simultaneous transcendental equations, which are nonlinear because of the effects of distortion. Such solutions involve iterative techniques, the use of the Newton-Raphson method, and other sophisticated mathematical operations. An analogous continuous formulation adapted to computer use has also been proposed.

The solution of the fundamental differential equation [Eq. (15.22)] can be expressed in terms of hyperbolic functions or exponential functions. In the latter form, the solution is

$$\eta = C_1 e^{ax} + C_2 e^{-ax} + \frac{1}{H_w + H_s}\left(M_1 - \frac{p}{a^2}\right) - \frac{H_s}{H_w + H_s}\left(y - \frac{8f}{a^2 L^2}\right) \qquad (15.23)$$

where x = horizontal distance from cable support to point where deflection η is measured
y = vertical distance from cable support to cable at point where deflection η is measured
e = 2.71828
a = sag-span ratio f/L
f = cable sag
L = length of main span
H_w = horizontal component of cable tension produced by uniform dead load w
H_s = horizontal component of cable tension produced by all causes other than dead load
M_1 = bending moment in stiffening truss calculated as if the truss were a simple beam independent of the cable
p = total uniform live load per cable

Constants C_1 and C_2 are integration constants to be evaluated, for each load position, from the end conditions and conditions of continuity.

Another method for finding the equation of the deflected truss is to represent deflection by a trigonometric series. If the stiffening truss is considered a free body, it will be in equilibrium under the force system indicated in Fig. 15.48. The truss is acted on by dead load w over the entire span, live load p over any length of span $k_2L - k_1L$, and suspender pull $w + q$, where q is the portion of the uniform live load carried by the cable.

The deflection of the truss can be given by the trigonometric series:

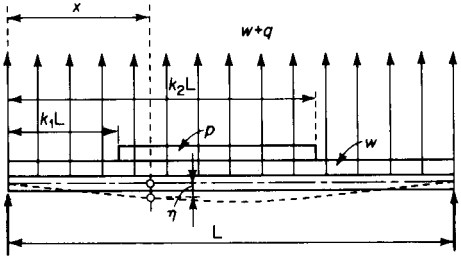

FIGURE 15.48 Forces acting on the truss of Fig. 15.46.

$$\eta = \sum_{n=1}^{\infty} a_n \sin \frac{n\pi x}{L} = a_1 \sin \frac{\pi x}{L} + a_2 \sin \frac{2\pi x}{L} + a_3 \sin \frac{3\pi x}{L} + \cdots \tag{15.24}$$

The Fourier coefficients a_n are determined by energy methods.

$$a_n = \frac{(\cos n\pi k_1 - \cos n\pi k_2)qL/n\pi - (1 - \cos n\pi)wL\beta/n\pi}{n^4 EI\pi^4/2L^3 + (1 + \beta)H_w\pi^2 n^2/2L} \tag{15.25}$$

where $\beta = H_s/H_w$
E = modulus of elasticity of stiffening-truss steel
I = moment of inertia of stiffening truss

In the following development of the deflection theory, the trigonometric-series solution is used. It converges rapidly and avoids difficulties with the integration constants C_1 and C_2, which hold only for values of x for which M_1 has the same algebraic form. (Thus, the loading in Fig. 15.48 requires evaluation of six constants of integration.)

Equations (15.23) to (15.25) contain the unknown H_s. It must be determined before deflections can be numerically evaluated for any particular case. The energy method may be used for this purpose: the work done by the suspender forces moving through the deflection undergone by the cable is equated to the internal work done by the internal stress in the cable moving through the deformation suffered by the cable.

The force system acting on the cable treated as a free body is shown in Fig. 15.49. Application of the energy equation yields the so-called cable condition:

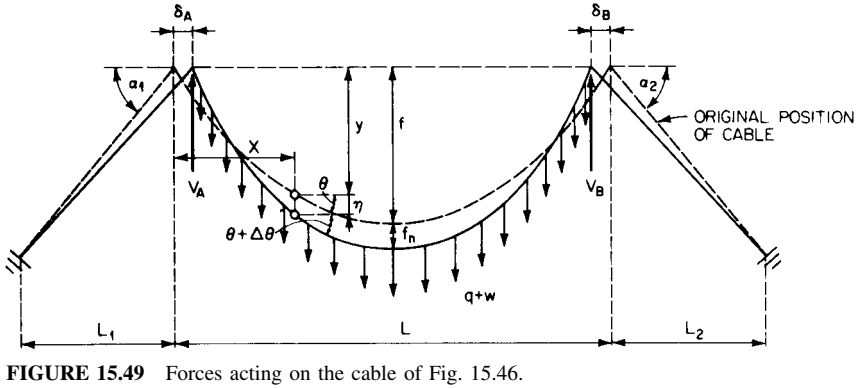

FIGURE 15.49 Forces acting on the cable of Fig. 15.46.

$$\frac{H_s L_c}{A_c E_c} + \epsilon_t L_t = \frac{8f}{L^2} \int_0^L \eta \, dx - \frac{1 + \beta}{2 + \beta} \int_0^L \eta'' \eta \, dx \tag{15.26}$$

where ϵ_t = coefficient of thermal expansion
t = temperature change
$\beta = H_s / H_w$
A_c = cross-section area of cable
E_c = modulus of elasticity of cable steel
$L_t = \int_0^S (ds/dx)\, ds + L_1 \sec^2 \alpha_1 + L_2 \sec^2 \alpha_2$
$\approx L + 16/3 \alpha^2 L + L_1 \sec^2 \alpha_1 + L_2 \sec^2 \alpha_2$
L_1, L_2 = lengths of side spans
α_1, α_2 = angle with respect to horizontal of side-span cables
$L_c = \int_0^S (ds/dx)^2\, ds + L_1 \sec^3 \alpha_1 + L_2 \sec^3 \alpha_2$
$\approx L + 8a^2 L + L_1 \sec^3 \alpha_1 + L_2 \sec^3 \alpha_2$
S = length of main-span cable
$a = f/L$

Substitution of Eq. (15.24) in Eq. (15.26) yields the Timoshenko "exact" form of the equation for H_s.

$$\frac{H_s L_c}{A_c E_c} \pm \epsilon_t t L_t - \frac{16f}{L\pi} \left(a_1 + \frac{a_3}{3} + \frac{a_5}{5} + \cdots \right) - \frac{1 + \beta}{2 + \beta} \left(\frac{\pi^2}{2L} \right) [a_1^2 + (2a_2)^2 + (3a_3)^2 + \cdots] = 0 \tag{15.27}$$

The last term on the left side of the equation accounts for the actual distribution of live load to the cable. If this term is neglected, the simpler Timoshenko approximate solution is obtained. Direct solution of Eq. (15.27) is possible only by successive approximations.

Successive differentiation of Eq. (15.27) with respect to x yields:

Stiffening-truss angular deflection

$$\phi_x = \eta' = \frac{\pi}{L} \sum_{n=1}^{\infty} n a_n \cos \frac{n\pi x}{L} \tag{15.28}$$

Moment

$$M_x = -EI\eta'' = \frac{EI\pi^2}{L^2} \sum_{n=1}^{\infty} n^2 a_n \sin \frac{n\pi x}{L} \tag{15.29}$$

Shear

$$V_x = -EI\eta''' = \frac{EI\pi^3}{L^3} \sum_{n=1}^{\infty} n^3 a_n \cos \frac{n\pi x}{L} \tag{15.30}$$

An alternative form of the equation for H_s, known as the Melan equation, derived from Eqs. (15.23) and (15.26).

$$H_s^2 \frac{L_c}{A_c E_c} + H_s \left(\frac{H_w L_c}{A_c E_c} \pm \epsilon_t t L_t + \frac{16 f^2}{3L} - \frac{64 f^2 K_2}{L^2} \right) + \left(\frac{pfLK_1}{3} \pm \epsilon_t t L_t + H_w + \frac{8fpK_3}{L^2} \right) = 0 \quad (15.31)$$

where $K_1 = k_2^2(4k_2 - 6) - k_1^2(4k_1 - 6)$

$$K_2 = \frac{4 + aL(e^{aL} - e^{-aL}) - 2(e^{aL} - e^{-aL})}{a^3(e^{aL} - e^{-aL})}$$

$$K_3 = \frac{(e^{aL} - 1)(e^{-ak_2L} - e^{-ak_1L}) + (e^{-aL} - 1)(e^{ak_2L} - e^{ak_1L})}{a^3(e^{aL} - e^{-aL})} + \frac{(e^{aL} - e^{-aL})(ak_2L - ak_1L)}{a^3(e^{aL} - e^{-aL})}$$

This form of the equation frequently is useful for determining H_p or H_s directly. Once either has been evaluated, however, the deflections are more readily determined by the series method. Moments are then calculated from

$$M = M_1 - (H_w + H_s)\eta - H_{sy} \quad (15.32)$$

Example. The Ambassador Bridge (Table 15.1), with unloaded backstays and a two-hinged stiffening truss, has the following properties:

$f = 205.6$ ft $\quad A_c = 240.89$ in^2

$L = 1850$ ft $\quad E_c = 27{,}000$ ksi

$L_1 = 984.2$ ft $\quad E = 30{,}000$ ksi

$L_2 = 833.9$ ft $\quad I = 113.71$ ft^4

$\alpha_1 = 20°32'$ $\quad \alpha_2 = 24°$

From the bridge data:

$w = 6.2$ kips per ft for the east cable

$H_w = 12{,}920$ kips for the east cable

The structure is analyzed for live loads of 0.2 to 2.0 kips per ft in increments of 0.2. These live loads are placed in various positions: over the entire span, the end half, the center half, the end quarter, the quarter nearest the center, and the center quarter. Analysis is made by both the Timoshenko approximate and exact forms of Eq. (15.27).

Approximate Method. Equation (15.27) becomes, when the proper values of the given data are used:

$$H_p = 848.60269a_1 + 282.86755a_3 + 169.72053a_5 \quad (15.33)$$

The coefficients a_1, a_3, and a_5 contain $\beta = H_p/H_w$. So a method of successive approximations must be used. First, a value of H_p or β is assumed. Then, this value is used in Eq. (15.25) to get values of a_1, a_3, and a_5. These, in turn, are substituted in Eq. (15.33) to obtain H_p. This computed value of H_p will not agree with the assumed value unless by accident the correct value of H_p had been guessed.

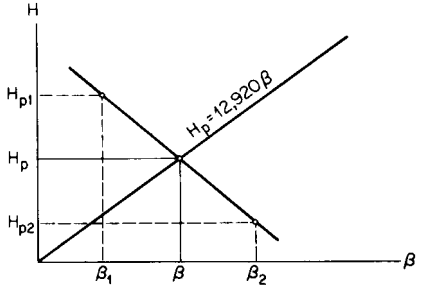

FIGURE 15.50 Chart for linear interpolation of horizontal component H_p of the cable tension.

This procedure is repeated again. Thus, for two assumed values of β, β_1, and β_2, two calculated values of H_p, H_{p1}, and H_{p2} are obtained. On a graph, the straight line $H_p = \beta H_w = 12{,}920\beta$ is drawn (Fig. 15.50), and the points β_1, H_{p1} and β_2, H_{p2} plotted. A straight line between these points intersects the line $H_p = 12{,}920\beta$ at the correct value of H and β. (As many as six points were plotted, and always the calculated value of H_p lay on a straight line.)

The preceding procedure was used in calculating 60 values of H_p. Each was checked by finding correct values of a_1, a_3, and a_5 with Eq. (15.31). Values of H_p yielded by both methods are given in Table 15.7. The values of H_p from Fig. 15.50 are the values most nearly correct, since the check values of H_p often changed several kips when H_p from Fig. 15.50 was changed a few tenths of a kip.

In calculating the deflections, it was found necessary, especially for unsymmetrical loading, to use five terms of Eq. (15.24). Table 15.8 gives deflections, ft. for a typical point.

Timoshenko Exact Method. For the full Eq. (15.27), Table 15.9 gives the values of H_p, kips, for two of the load distributions. The results show that the actual distribution of live load did not increase the value of H_p more than 1%.

(S. O. Asplund, "Structural Mechanics: Classical and Matrix Methods," Prentice-Hall, Inc., Englewood Cliffs, N.J.

E. Egervary, "Bases of a General Theory of Suspension Bridges Using a Matrical Method of Calculation," *International Association of Bridge and Structural Engineers* (*IABSE*) *Publication,* vol. 16, pp. 149–184, 1956.

TABLE 15.7 Cable Tension Component H_p, kps

H_p = values from Fig. 15.50, H'_p = check value from Eq. (15.31)

Live load, kips per ft	$k_1 = 0$, $k_2 = 1$		$k_1 = 0$, $k_2 = 0.5$		$k_1 = 0.25$, $k_2 = 0.75$		$k_1 = 0$, $k_2 = 0.25$		$k_1 = 0.25$, $k_2 = 0.50$		$k_1 = 0.375$, $k_2 = 0.625$	
	H_p	H'_p	H_p	H'_p	H_p	H'_p	H_p	H'_p	H_p	H'_p	H_p	H'_p
0.2	385	386	193	193	269	268	59	59	134	135	144	146*
0.4	770	765	385	383	536	538	117	117	269	268	289	287
0.6	1151	1160*	578	575	803	811*	176	174*	403	403	432	433
0.8	1534	1524	769	770	1069	1079	234	236	537	534	576	576
1.0	1912	1915	961	956	1336	1331	292	293	671	666*	719	720
1.2	2291	2281	1152	1149	1600	1601	351	352	804	804	863	857
1.4	2668	2658	1343	1341	1863	1879	409	413	937	938	1005	1006
1.6	3041	3054	1534	1524*	2127	2139	468	465	1070	1070	1148	1145
1.8	3416	3419	1723	1722	2391	2383	526	526	1203	1203	1291	1286
2.0	3789	3786	1913	1906	2651	2661	584	587	1335	1337	1433	1422
		0.78*		0.65*		1.00*		1.15*		0.75*		1.39*

*Maximum difference, % of H_p.

TABLE 15.8 Deflections, ft, at $x = 0.2L$

Live load, kips per ft	$k_1 = 0$ $k_2 = 1$	$k_1 = 0$ $k_2 = 0.5$	$k_1 = 0.25$ $k_2 = 0.75$	$k_1 = 0$ $k_2 = 0.25$	$k_1 = 0.25$ $k_2 = 0.50$	$k_1 = 0.375$ $k_2 = 0.625$
0.2	0.2744	0.6962	0.0594	0.4122	0.2879	−0.0214
0.4	0.5440	1.3267	0.1229	0.7951	0.5445	−0.0448
0.6	0.8249	2.0758	0.1908	1.1888	0.8622	−0.0646
0.8	1.0842	2.7167	0.2582	1.5838	1.1277	−0.0829
1.0	1.3448	3.2418	0.3170	2.0394	1.3385	−0.1000
1.2	1.6241	3.8637	0.3906	2.3625	1.6768	−0.1211
1.4	1.8926	4.4757	0.4723	2.7514	1.8599	−0.1322
1.6	2.1746	5.0835	0.5435	3.1326	2.1137	−0.1499
1.8	2.4355	5.6719	0.6056	3.5173	2.3668	−0.1634
2.0	2.6870	6.2535	0.6937	4.0276	2.7363	−0.1801

M. Esslinger, "Suspension Bridge Design Calculations by Electronic Computer," *Acier-Stahl-Steel,* no. 5, pp. 223–230, 1962.

A. A. Jakkula, "Theory of the Suspension Bridge," *IABSE Publication,* vol. 4, pp. 333–358, 1936.

C. P. Kuntz, J. P. Avery, and J. L. Durkee, "Suspension-bridge Truss Analysis by Electronic Computer," *ASCE Conference on Electronic Computation,* Nov. 20–21, 1958.

D. J. Peery, "An Influence-line Analysis for Suspension Bridges," *ASCE Transactions,* vol. 121, pp. 463–510, 1956.

T. J. Poskitt, "Structural Analysis of Suspension Bridges," *ASCE Proceedings,* ST1, February, 1966, pp. 49–73.

G. C. Priester, "Application of Trigonometric Series to Cable Stress Analysis in Suspension Bridges," *Engineering Research Bulletin* 12, University of Michigan, 1929.

TABLE 15.9 H_p, kips, Obtained by Exact Method [Eq. (15.27)]

Live load, kips per ft	$k_1 = 0$ $k_2 = 0.5$	$k_1 = 0$ $k_2 = 0.25$
0.2	193	59
0.4	386	117
0.6	579	176
0.8	773	235
1.0	966	294
1.2	1,159	353
1.4	1,352	412
1.6	1,545	472
1.8	1,738	531
2.0	1,931	591

A. G. Pugsley, "Theory of Suspension Bridges," Edward Arnold (Publishers), Ltd., London.

A. G. Pugsley, "A Flexibility Coefficient Approach to Suspension Bridge Theory," *Institute of Civil Engineering Proceedings,* vol. 32, 1949.

S. A. Saafan, "Theoretical Analysis of Suspension Bridges," *ASCE Proceedings,* ST4, August, 1966, pp. 1–12.

S. P. Timoshenko, "The Stiffness of Suspension Bridges," *ASCE Transactions,* vol. 94, pp. 377–405, 1930.

S. P. Timoshenko and D. H. Young, "Theory of Structures," 2d ed., McGraw-Hill Book Company, New York.)

15.17 PRELIMINARY SUSPENSION-BRIDGE DESIGN

Since suspension bridges are major structures, it is desirable even in preliminary design to proceed into rather detailed refinement of the involved mathematical computations. Often, complete deflection-theory analysis is advisable at that stage. Such refinement is economically feasible with computers. Two procedures for preliminary design are described in the following.

Preliminary design may be started by examining pertinent site factors (clearance requirements, roadway width, foundation materials, etc.) and studying the details of existing structures of similar proportions and conditions. Table 15.10 gives typical data. Such data should be used with discretion, however, because of major differences in codes with regard to live loads, safety factors, allowable working stresses, and deflections. There also may be significant differences in details, such as roadway structure, which has a major effect on dead loads; as well as different underclearances, lengths of side spans, wind conditions, and other site conditions that influence the weight of steel required. Many published weights per unit area may be misleading because of inclusion of sidewalks, bicycle paths, and other elements in the widths of continental bridges.

Span Ratios. With straight backstays, the ratio of side to main spans may be about 1:4 for economy. For suspended side spans, this ratio may be about 1:2. Physical conditions at the site may, however, dictate the selected span proportions.

Sag. The sag-span ratio is important. It determines the horizontal component of cable force. Also, this ratio affects height of towers, pull on anchorages, and total stiffness of the bridge. For minimum stresses, the ratio should be as large as possible for economy, say 1:8 with suspended side spans, or 1:9 with straight backstays. But the towers may then become high. Several comparative trials should be made. For the Forth Road Bridge, the correct sag-span ratio of 1:11 was thus determined. The general range of this ratio in practice is 1:8 to 1:12, with an average around 1:10.

Truss Depth. Stiffening-truss depths vary from $\frac{1}{60}$ to $\frac{1}{170}$ the span. Aerodynamic conditions, however, play a major role in shaping the preliminary design, and some of the criteria given in Art. 15.21 should be studied at this stage.

Other Criteria. Allowable stresses in main cables may vary from 80 to 86 ksi. Permissible live-load deflections in practice are seldom specified but usually do not exceed $\frac{1}{300}$ the span. In Europe, greater reliance is placed on limiting the radius of curvature of the roadway (thus, to 600 or 1,000 meters); or to limiting the cross slope of the roadway under eccentric load (thus, to about 1%); or to limiting the vertical acceleration under live load (thus, to 0.31 meter per sec^2).

TABLE 15.10 Details of Major Suspension Bridges*

Item	Verrazano Narrows Bridge	Golden Gate Bridge	Mackinac Bridge	George Washington Bridge	Salazar Bridge (Portugal)	Forth Bridge (Scotland)	Severn Bridge (England-Wales)	Tacoma Narrows Bridge II	San Francisco-Oakland Bay Bridge†	Bronx-Whitestone Bridge	Delaware Memorial Bridge I	Walt Whitman Bridge
Length of main span, ft	4,260	4,200	3,800	3,500	3,323	3,300	3,240	2,800	2,310	2,300	2,150	2,000
Length of each side span, ft	1,215	1,125	1,800	610,650	1,586	1,340	1,000	1,100	1,160	735	750	770
Length of suspended structure, ft	6,690	6,450	7,4000	4,760	6,495	5,980	5,240	5,000	10,450	3,770	3,650	3,540
Length including approach structure, ft	13,700	8,981	19,205	5,800	10,575	8,244	7,640	5,979	43,500	7,995	10,750	11,687
Width of bridge (c to c cables), ft	103	90	68	106	77	78	75	60	66	74	57	79
Number of traffic lanes	12	6	4	14‡	4	4	4	4	9	6	4	7
Height of towers above MHW, ft	690	746	552	595	625	512	470	500	447	377	440	378
Clearance at center above MHW, ft	228	215	148	220‡	246	150	120	187	203	150	175	150
Deepest foundation below MHW, ft	170	115	210	75	260	106	75	224	235	165	115	107
Diameter of cable, in	35⅞	36	24½	36	23 1/16	24	29	20¼	28¾	22	19¾	23⅛
length of one cable, ft	7,205	7,650	8,683	5,235	7,899	7,000	5,600	5,500	5,080	4,166	4,015	3,845
Number of wires per cable	26,108	27,572	12,580	26,474	11,248	11,618	8,300	8,702	17,464	9,842	8,284	11,396
Total length of wire used, miles	142,500	80,000	41,000	105,000	33,600	30,800	18,000	20,000	70,800	14,800	12,600	16,600
Year of completion	1964	1937	1957	1931	1966	1964	1966	1950	1936	1939	1951	1957

*Courtesy of *Engineering News-Record.*
†Twin spans.
‡With new lower deck.

15.17.1 Preliminary Design by Steinman-Baker Procedure

Analysis by elastic theory is sufficiently accurate for short spans and designs with deep, rigid stiffening systems that limit deflections to small amounts. The simple calculations of elastic theory are also useful, however, for preliminary designs and estimates if tubular percentage corrections are applied, based on experience with the deflection theory.

The corrections depend principally on the magnitude of the dead load and on the flexibility of the structure. The magnitude of the corrections increase with the deflection η and with the horizontal component of cable tension H_w under dead load. They therefore increase with span L and dead load w, while decreasing with truss stiffness EI and cable sag f. D. B. Steinman expressed this in a simple parameter S, the stiffness factor, such that

$$S = \frac{1}{L}\sqrt{\frac{EI}{H_w}} = \frac{1}{L^2}\sqrt{\frac{8fEI}{w}} \tag{15.34}$$

This value is used in the Steinman-Baker charts, Fig. 15.51, to obtain the percentage C to be applied to elastic-theory shears and moments to get deflection-theory shears and moments.

Roughly, the percentage reductions from the approximate theory are proportional to $1/S$, which might be called a flexibility factor; that is, the magnitude of the reduction increases considerably with long spans and heavy dead load, and diminishes with stiffness and sag.

The Steinman-Baker charts are based on the following proportions: side span, one-half the main span; sag-span ratio, 0.1; moment of inertia I, constant; cable design stress, 80 ksi; modulus of elasticity E, 29,000 ksi; ratio of dead to live load, 3. Further refinement of C for other proportions is suggested as follows:

For unloaded side spans, increase C by 2½% of its value.

For sag-span ratio = 0.12 (or 0.08) instead of 0.10, decrease (or increase) C by 2% of its value.

For cable stress = 120 (or 40) instead of 80 ksi, increase (or decrease) C by ½% of its value.

For $I/I_1 = 0.75$ instead of 1.00, increase C by 1½% of its value.

For $L_1/L = 0.25$ instead of 0.50, increase C by 2% of its value.

For load ratio $w/p = 5$ instead of 3, add 1% to C; for $w/p = 2$, subtract 1% from C; for $w/p = 1½$, subtract 2% from C.

In elastic-theory analysis for preliminary design of a bridge with two cable planes, the bridge may be treated as plane frameworks loaded in each plane; that is, the action as a space structure may be disregarded. The alleviating effects of torsion of the stiffening girders, of the unloading action of the cross frames or diaphragms between the girders, and of the participation of the connection of the pylons may all be left for more refined later analysis.

15.17.2 Preliminary Design by Hardesty-Wessman Procedure

Hardesty and Wessman presented an approximate, partly empirical, preliminary design method based on the distortion of an unstiffened cable. The maximum moments at the quarter point and at the center of the main span at constant mean temperature are computed in two major steps:

1. The deflections η' of an unstiffened cable under partial live load, for various ratios of live to dead load p/w, are obtained from Fig. 15.52. These charts were developed with average live-load lengths from a study of bridges in service and also based on the assumptions that the cable length is unchanged and the pylon tops do not move.

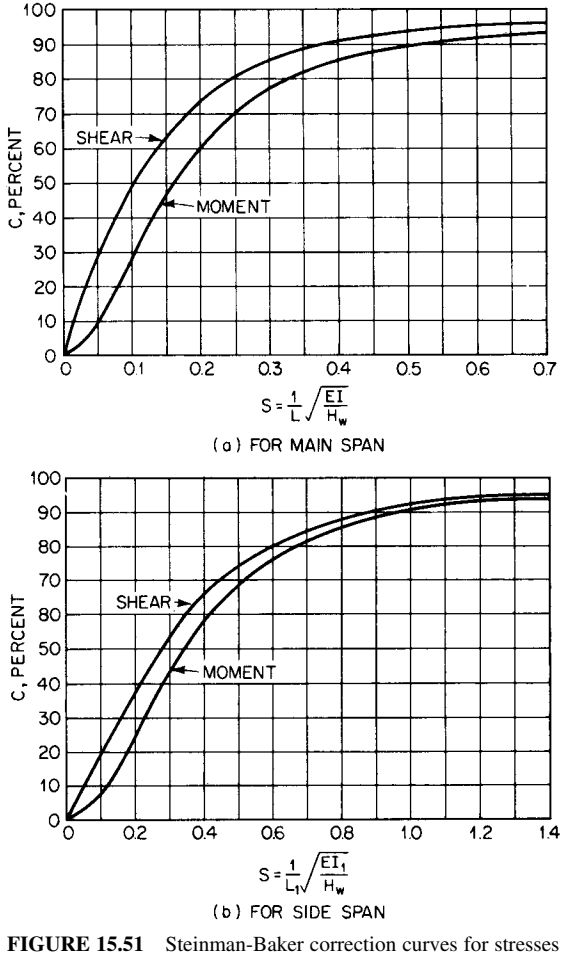

FIGURE 15.51 Steinman-Baker correction curves for stresses obtained by elastic theory for suspension bridges. (*Reprinted with permission form D. B. Steinman, "A Practical Treatise on Suspension Bridges," 2d ed., John Wiley & Sons, Inc., New York.*)

2. Corrections then are made for the effect of adding the stiffening truss (which reduces deflection η'). A trial moment of inertia is used and corrected later if necessary. Equations (15.35) are used for a first estimate of the maximum horizontal components of cable tension $H_w + H_p$. Then, Eqs. (15.36) are used to determine the bending moment M_t induced in the stiffening truss when it is bent to the deflections η' of the unstiffened cable.

Maximum positive moment at a quarter point, with live load at the same end over a length of $0.4L$, where L = main span, ft, is

$$H_w + H_p = \frac{1}{f + n_c'}(0.125wL^2 + 0.040pL^2) \qquad (15.35a)$$

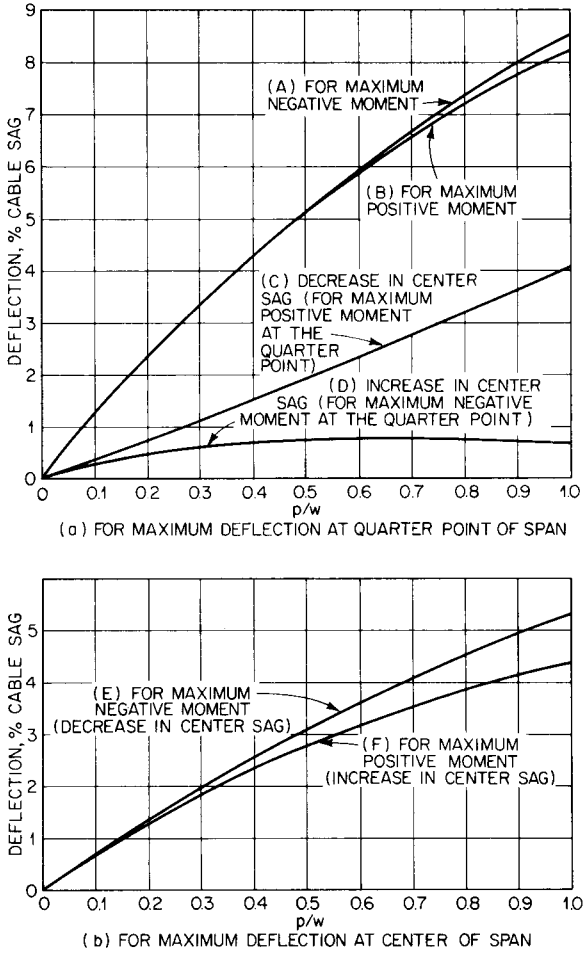

FIGURE 15.52 Chart gives deflections of unstiffened cables under partial load. (*Reprinted with permission from S. Hardesty and H. E Wessman, "Preliminary Design of Suspension Bridges," ASCE Transactions, vol. 104, 1939.*)

where f = cable sag, ft
η_c' = deflection at center of unstiffened cable, ft
w = uniform dead load
p = uniform live load

Maximum negative moment at a quarter point, with live load at the opposite end over a length of $0.6L$, is

$$H_w + H_p = \frac{1}{f + \eta_c'}(0.125wL^2 + 0.085pL^2) \tag{15.35b}$$

Maximum positive moment at the center, with live load at the center over a length of $0.3L$, is

$$H_w + H_p = \frac{1}{f + \eta_c'}(0.125wL^2 + 0.0638pL^2) \tag{15.35c}$$

Maximum negative moment at the center, with live load over a length of $0.35L$ at each end, is

$$H_w + H_p = \frac{1}{f + \eta_c'}(0.125wL^2 + 0.0613pL^2) \tag{15.35d}$$

In each of the preceding equations, the quantity within the parentheses is the bending moment at the center of a simple span due to dead load over the entire span and live load over a part of the span. The deflection η_c' is positive when downward and negative when upward.

Since $H_w = wL^2/8f$ is known, Eqs. (15.35) yield a trial value of H_p, with which the following bending moments in the truss can be computed:

Maximum positive moment at quarter points:

$$M_t = 47.0\frac{EI\eta'}{L^2} \tag{15.36a}$$

where I = moment of inertia of stiffening truss and E = modulus of elasticity of truss steel.

Maximum negative moment at quarter points:

$$M_t = 43.0\frac{EI\eta'}{L^2} \tag{15.36b}$$

Maximum positive moment at center:

$$M_t = 65.8\frac{EI\eta'}{L^2} \tag{15.36c}$$

Maximum negative moment at center:

$$M_t = 59.2\frac{EI\eta'}{L^2} \tag{15.36d}$$

Since the truss is neither infinitely flexible nor infinitely stiff, the cable will be forced back only a part of the distance η'. The moment in the truss is reduced from M_t to

$$M = M_t\frac{(H_w + H_p)\eta'}{M_t + (H_w + H_p)\eta'} \tag{15.37}$$

And the deflection is reduced to

$$\eta = \eta'\frac{(H_w + H_p)\eta'}{M_t + (H_w + H_p)\eta'} \tag{15.38}$$

Finally, changes in length of cable due to live load or temperature, and the sag changes caused by movement of pylon tops, cable stress, and temperature, are combined in one change in the center sag. These effects are

Change in length of cable due to stress:

Main span:
$$\Delta L_s = \frac{H_p L}{A_c E_c}(1 + {}^{16}\!/_{3}a^2) \tag{15.39}$$

where $a = f/L$
A_c = cross-sectional area of cable
E_c = modulus of elasticity of cable steel

Unloaded side span:
$$\Delta L_{1s} = \frac{H_p L_1}{A_c E_c} \sec^2 \alpha_1 \tag{15.40}$$

where α_1 = angle side-span cable makes with horizontal.

Change in length of cable due to temperature:

Main span:
$$\Delta L_t = \epsilon_t \, \Delta t L (1 + {}^8\!/_3 a^2) \tag{15.41}$$

where ϵ = coefficient of expansion and Δt = temperature change.

Unloaded side span:
$$\Delta L_{1t} = \epsilon_t \, \Delta t L_1 \sec \alpha_1 \tag{15.42}$$

Change in sag in main span due to temperature:

$$\Delta f = \frac{15}{16a(5 - 24a^2)} \Delta L \tag{15.43}$$

Change in sag due to movement of pylon top:

$$\Delta f = \frac{15 - 40a^2 + 288a^4}{16a(5 - 24a^2)} (2\Delta L_1 \sec \alpha_1) \tag{15.44}$$

Moment caused by change in sag:

Main span at center:
$$M = 9.4 \frac{EI}{L^2} \Delta f \tag{15.45}$$

Main span at quarter-point:
$$M = 7.6 \frac{EI}{L^2} \Delta f \tag{15.46}$$

The corrected value of the sag allows a second trial value of H_p to be obtained. Then, the process is repeated.

In applying this method to preliminary design, an arbitrary moment of inertia is selected, based on a tentative chord section and truss depth. The procedure is repeated with other values of I, say one-half and double those in the first analysis. Final selection may be based on limiting values of desired deflection and grade change due to load.

(D. B. Steinman, "A Practical Treatise on Suspension Bridges," 2d ed., John Wiley & Sons, Inc., New York; S. Hardesty and H. E. Wessman, "Preliminary Design of Suspension Bridges," *Transactions of the American Society of Civil Engineers,* vol. 104, 1939.)

15.18 SELF-ANCHORED SUSPENSION BRIDGES

Self-anchored suspension bridges differ from the type discussed in Arts. 15.16 and 15.17 only in that external anchorages are dispensed with (see Art. 15.3). Unlike the externally anchored type, self-anchored suspension bridges may properly be analyzed by the elastic theory, since the effect of distortions of the structural geometry under live load is practically eliminated. The structure is also not stressed by uniform temperature change of cables and stiffening girders. The analysis is thus simpler. But the favorable reductions of bending

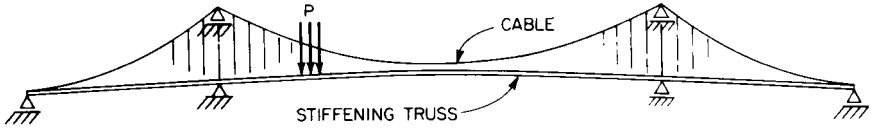

FIGURE 15.53 Self-anchored suspension bridge.

moments that occur with externally anchored suspension bridges are lost. Furthermore, the effect of axial load in the stiffening girder must be considered, as well as the effect of girder camber.

For a symmetrical three-span structure with continuous stiffening girders (Fig. 15.53), a plane system (cable, suspenders, and girder) has three redundants. C. H. Gronquist derived in simple form the elastic-theory equations for determining the redundants for a continuous stiffening-truss system. He took into account camber and its action in reducing cable and truss stress by archlike action. He also demonstrated that the equations for the horizontal component of cable tension H_p under live load for the self-anchored bridge, with girder camber and shortening eliminated, are the same as the elastic-theory equations for an externally anchored suspension bridge.

(C. H. Gronquist, "Simplified Theory of the Self-Anchored Suspension Bridge," *Transactions of the American Society of Civil Engineers,* vol. 107, 1942.)

15.19 CABLE-STAYED BRIDGE ANALYSIS

The static behavior of a cable-stayed girder can best be gaged from the simple, two-span example of Fig. 15.54. The girder is supported by one stay cable in each span, at *E* and *F*, and the pylon is fixed to the girder at the center support *B*. The static system has two internal cable redundants and one external support redundant.

If the cable and pylon were infinitely rigid, the structure would behave as a continuous four-span beam *AC* on five rigid supports *A, E, B, F,* and *C*. The cables are elastic, however, and correspond to springs. The pylon also is elastic, but much stiffer because of its large cross section. If cable stiffness is reduced to zero, the girder assumes the shape of a deflected two-span beam *ABC*.

Cable-stayed bridges of the nineteenth century differed from those of the 1960s in that their stays constituted relatively soft spring supports. Heavy and long, the stays could not be highly stressed. Usually, the cables were installed with significant slack, or sag. Consequently, large deflections occurred under live load as the sag decreased. In contrast, modern cables are made of high-strength steel, are relatively short and taut, and have low weight. Their elastic action may therefore be considered linear, and an equivalent modulus of elas-

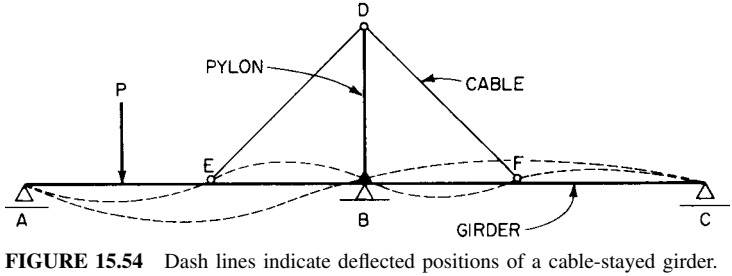

FIGURE 15.54 Dash lines indicate deflected positions of a cable-stayed girder.

ticity may be used [Eq. (15.1)]. The action of such cables then produces something more nearly like a four-span beam for a structure such as the one in Fig. 15.54.

If the pylon were hinged at its base connection with a stayed girder at *B*, rather than fixed, the pylon would act as a pendulum column. This would have an important effect on the stiffness of the system, for the spring support at *E* would become more flexible. The resulting girder deflection might exceed that due to the elastic stretch of the cables. In contrast, the elastic shortening of the pylon has no appreciable effect.

Relative girder stiffness plays a dominant role in the structural action. The stayed girder tends to approach a beam on rigid supports *A, E, B, F, C* as girder stiffness decreases toward zero. With increasing girder stiffness, however, the support of the cables diminishes, and the bridge approaches a girder supported on its piers and abutments *A, B, C.*

In a three-span bridge, a side-span cable connected to the abutment furnishes more rigid support to the main span than does a cable attached to some point in the side span. In Fig. 15.54, for example, the support of the load *P* in the position shown would be improved if the cable attachment at *F* were shifted to *C*. This explains why cables from the pylon top to the abutment are structurally more efficient, though not as esthetically pleasing as other arrangements.

The stiffness of the system also depends on whether the cables are fixed at the towers (at *D*, for example, in Fig. 15.54) or whether they run continuously over (or through) the pylons. Some early designs with more than one cable to a pylon from the main span required one of the cables to be fixed to the pylon and the others to be on movable saddle supports. Most contemporary designs fix all the stays to the pylon.

The curves of maximum-minimum girder moments for all load variations usually show a large range of stress. Designs providing for the corresponding normal forces in the girder may require large variations in cross sections. By prestressing the cables or by raising or lowering the support points, it is possible to achieve a more uniform and economical moment capacity. The amount of prestressing to use for this purpose may be calculated by successively applying a unit force in each of the cables and drawing the respective moment diagrams. Then, by trial, the proper multiples of each force are determined so that, when their moments are superimposed on the maximum-minimum moment diagrams, an optimum balance results.

(''Guidelines for the Design of Cable-Stayed Bridges,'' Committee on Cable-Stayed Bridges, American Society of Civil Engineers.)

15.19.1 Static Analysis—Elastic Theory

Cable-stayed bridges may be analyzed by the general method of indeterminate analysis with the equations of virtual work.

The degree of internal redundancy of the system depends on the number of cables, types of connections (fixed or movable) of cables with the pylons, and the nature of the pylon connection at its base with the stayed girder or pier. The girder is usually made continuous over three spans. Figure 15.55 shows the order of redundancy for various single-plane systems of cables.

If the bridge has two planes of cables, two stayed girders, and double pylons, it usually also must be provided with a number of intermediate cross diaphragms in the floor system, each of which is capable of transmitting moment and shear. The bridge may also have cross girders across the top of the pylons. Each of these cross members adds two redundants, to which must be added twice the internal redundancy of the single-plane structure, and any additional reactions in excess of those needed for external equilibrium as a space structure. The redundancy of the space structure is very high, usually of the order of 40 to 60. Therefore, the methods of plane statics are normally used, except for large structures.

For a cable-stayed structure such as that illustrated in Fig. 15.56*a*, it is convenient to select as redundants the bending moments in the stayed girder at those points where the

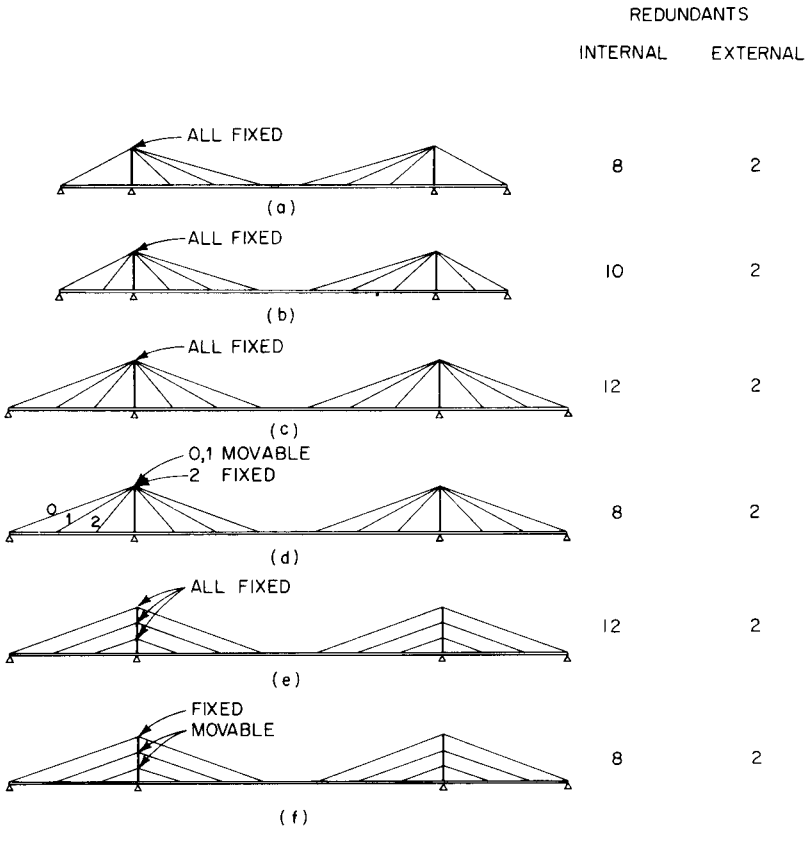

FIGURE 15.55 Number of internal and external redundants for various types of cable-stayed bridges.

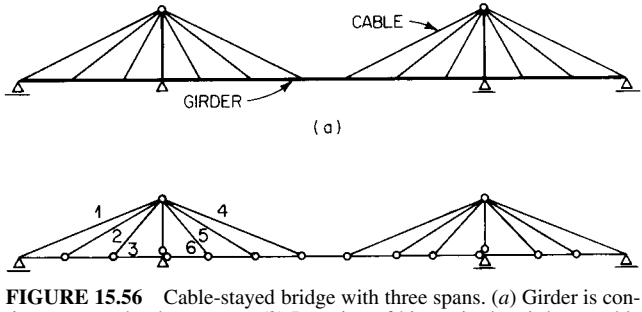

FIGURE 15.56 Cable-stayed bridge with three spans. (*a*) Girder is continuous over the three spans. (*b*) Insertion of hinges in the girder at cable attachments makes system statically determinate.

cables and pylons support the girder. When these redundants are set equal to zero, an articulated, statically determinate base system is obtained, Fig. 15.56*b*. When the loads are applied to this choice of base system, the stresses in the cables do not differ greatly from their final values; so the cables may be dimensioned in a preliminary way.

Other approaches are also possible. One is to use the continuous girder itself as a statically indeterminate base system, with the cable forces as redundants. But computation is generally increased.

A third method involves imposition of hinges, for example at *a* and *b* (Fig. 15.57), so placed as to form two coupled symmetrical base systems, each statically indeterminate to the fourth degree. The influence lines for the four indeterminate cable forces of each partial base system are at the same time also the influence lines of the cable forces in the real system. The two redundant moments X_a and X_b are treated as symmetrical and antisymmetrical group loads, $Y = X_a + X_b$ and $Z = X_a - X_b$, to calculate influence lines for the 10-degree indeterminate structure shown. Kern moments are plotted to determine maximum effects of combined bending and axial forces.

A similar concept is illustrated in Fig. 15.58, which shows the application of independent symmetric and antisymmetric group stress relationships to simplify calculations for an 8-degree indeterminate system. Thus, the first redundant group X_1 is the self-stressing of the lowest cables in tension to produce $M_1 = +1$ at supports.

The above procedures also apply to influence-line determinations. Typical influence lines for two bridge types are shown in Fig. 15.59. These demonstrate that the fixed cables have a favorable effect on the girders but induce sizable bending moments in the pylons, as well as differential forces on the saddle bearings.

Note also that the radiating system in Fig. 15.55*c* and *d* generally has more favorable bending moments for long spans than does the harp system of Fig. 15.59. Cable stresses also are somewhat lower for the radiating system, because the steeper cables are more effective. But the concentration of cable forces at the top of the pylon introduces detailing and construction difficulties. When viewed at an angle, the radiating system presents esthetic problems, because of the different intersection angles when the cables are in two planes. Furthermore, fixity of the cables at pylons with the radiating system in Fig. 15.55*c* and *d* produces a wider range of stress than does a movable arrangement. This can adversely influence design for fatigue.

A typical maximum-minimum moment and axial-force diagram for a harp bridge is shown in Fig. 15.60.

The secondary effect of creep of cables (Art. 15.12) can be incorporated into the analysis. The analogy of a beam on elastic supports is changed thereby to that of a beam on linear viscoelastic supports. Better stiffness against creep for cable-stayed bridges than for comparable suspension bridges has been reported. (K. Moser, "Time-Dependent Response of the Suspension and Cable-Stayed Bridges," International Association of Bridge and Structural Engineers, 8th Congress Final Report, 1968, pp. 119–129.)

(W. Podolny, Jr., and J. B. Scalzi, "Construction and Design of Cable-Stayed Bridges," 2d ed., John Wiley & Sons, Inc., New York.)

15.19.2 Static Analysis—Deflection Theory

Distortion of the structural geometry of a cable-stayed bridge under action of loads is considerably less than in comparable suspension bridges. The influence on stresses of distortion

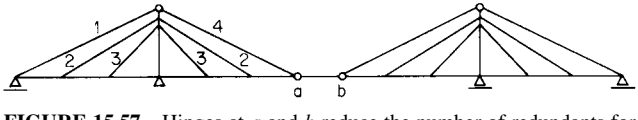

FIGURE 15.57 Hinges at *a* and *b* reduce the number of redundants for a cable-stayed girder continuous over three spans.

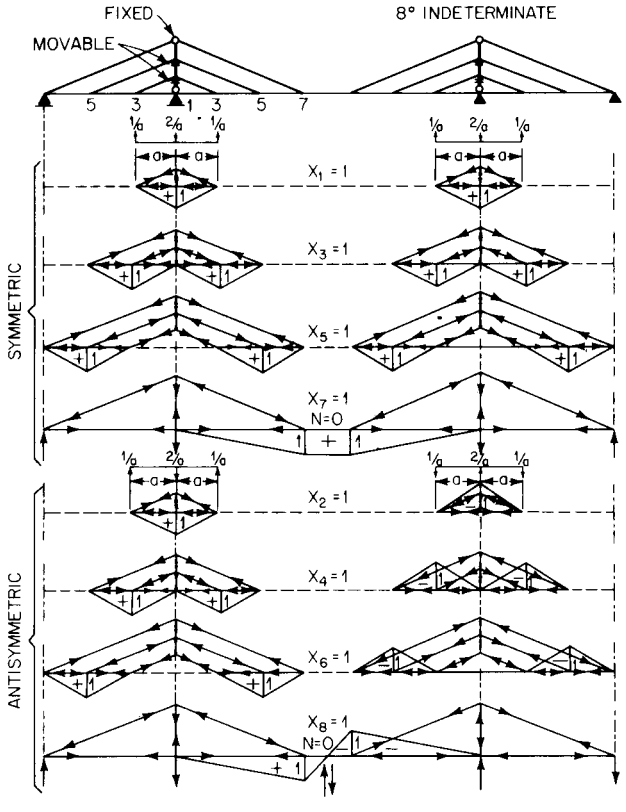

FIGURE 15.58 Forces induced in a cable-stayed bridge by independent symmetric and antisymmetric group loadings. (*Reprinted with permission from O. Braun, "Neues zur Berchnung Statisch Unbestimmter Tragwerke, "Stahlbau, vol. 25, 1956.*)

of stayed girders is relatively small. In any case, the effect of distortion is to increase stresses, as in arches, rather than the reverse, as in suspension bridges. This effect for the Severn Bridge is 6% for the stayed girder and less than 1% for the cables. Similarly, for the Düsseldorf North Bridge, stress increase due to distortion amounts to 12% for the girders.

The calculations, therefore, most expeditiously take the form of a series of successive corrections to results from first-order theory (Art. 15.19.1). The magnitude of vertical and horizontal displacements of the girder and pylons can be calculated from the first-order theory results. If the cable stress is assumed constant, the vertical and horizontal cable components V and H change by magnitudes ΔV and ΔH by virtue of the new deformed geometry. The first approximate correction determines the effects of these ΔV and ΔH forces on the deformed system, as well as the effects of V and H due to the changed geometry. This process is repeated until convergence, which is fairly rapid.

15.20 PRELIMINARY DESIGN OF CABLE-STAYED BRIDGES

In general, the height of a pylon in a cable-stayed bridge is about 1/6 to 1/8 the main span. Depth of stayed girder ranges from 1/60 to 1/80 the main span and is usually 8 to 14 ft, averaging 11 ft. Live-load deflections usually range from 1/400 to 1/500 the span.

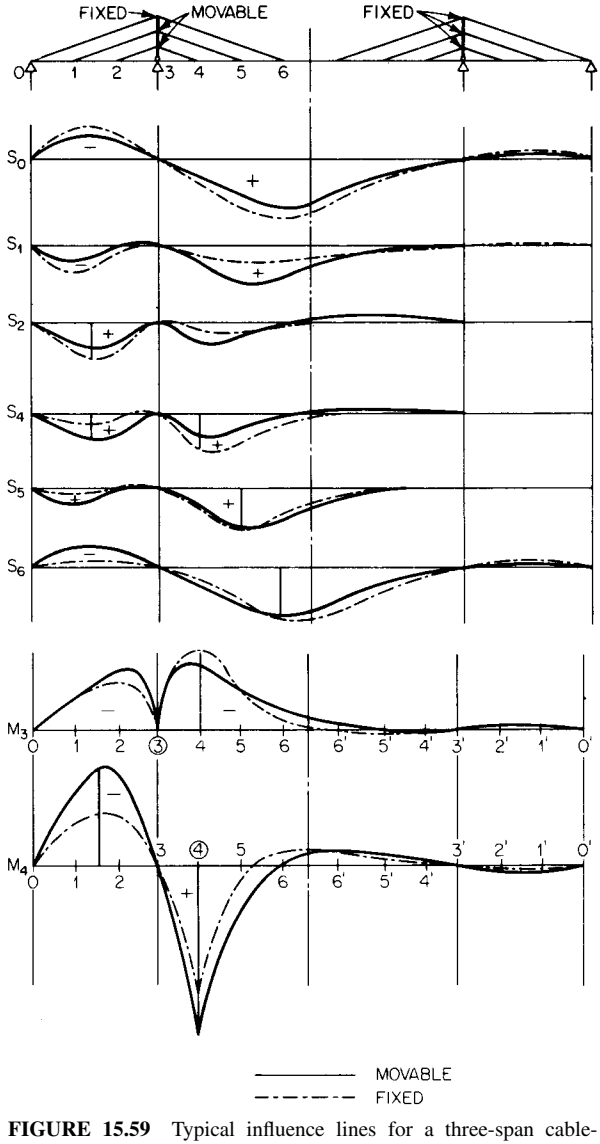

FIGURE 15.59 Typical influence lines for a three-span cable-stayed bridge showing the effects of fixity of cables at the pylons. (*Reprinted with permission from H. Homberg, "Einflusslinien von Schrägseilbruchen," Stahlbau, vol. 24, no. 2, 1955.*)

To achieve symmetry of cables at pylons, the ratio of side to main spans should be about 3:7 where three cables are used on each side of the pylons, and about 2:5 where two cables are used. A proper balance of side-span length to main-span length must be established if uplift at the abutments is to be avoided. Otherwise, movable (pendulum-type) tiedowns must be provided at the abutments.

Wide box girders are mandatory as stayed girders for single-plane systems, to resist the torsion of eccentric loads. Box girders, even narrow ones, are also desirable for double-plane

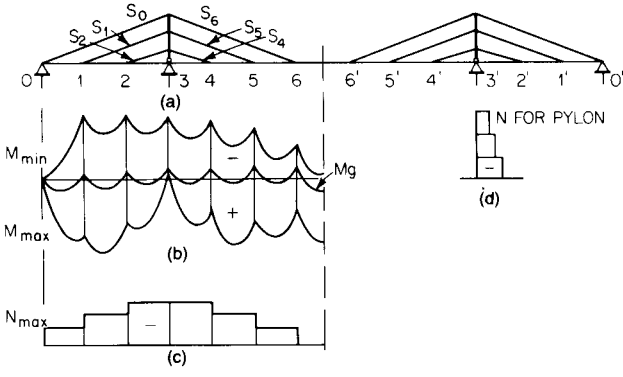

FIGURE 15.60 Typical moment and force diagrams for a cable-stayed bridge. (*a*) Girder is continuous over three spans. (*b*) Maximum and minimum bending moments in the girder. (*c*) Compressive axial forces in the girder. (*d*) Compressive axial forces in a pylon.

systems to enable cable connections to be made without eccentricity. Single-web girders, however, if properly braced, may be used.

Since elastic-theory calculations are relatively simple to program for a computer, a formal set may be made for preliminary design after the general structure and components have been sized.

Manual Preliminary Calculations for Cable Stays. Following is a description of a method of manual calculation of reasonable initial values for use as input data for design of a cable-stayed bridge by computer. The manual procedure is not precise but does provide first-trial cable-stay areas. With the analogy of a continuous, elastically supported beam, influence lines for stay forces and bending moments in the stayed girder can be readily determined. From the results, stress variations in the stays and the girder resulting from concentrated loads can be estimated.

If the dead-load cable forces reduce deformations in the girder and pylon at supports to zero, the girder acts as a beam continuous over rigid supports, and the reactions can be computed for the continuous beam. Inasmuch as the reactions at those supports equal the vertical components of the stays, the dead-load forces in the stays can be readily calculated. If, in a first-trial approximation, live load is applied to the same system, the forces in the stays (Fig. 15.61) under the total load can be computed from

$$P_i = \frac{R_i}{\sin \alpha_i} \tag{15.47}$$

where R_i = sum of dead-load and live-load reactions at i and α_i = angle between girder and stay i. Since stay cables usually are designed for service loads, the cross-sectional area of stay i may be determined from

$$A_i = \frac{R_i}{\sigma_a \sin \alpha_i} \tag{15.48}$$

where σ_a = allowable unit stress for the cable steel.

The allowable unit stress for service loads equals $0.45 f_{pu}$, where f_{pu} = the specified minimum tensile strength, ksi, of the steel. For 0.6-in-dia., seven-wire prestressing strand (ASTM A416), f_{pu} = 270 ksi and for ¼-in-dia. ASTM A421 wire, f_{pu} = 240 ksi. Therefore, the allowable stress is 121.5 ksi for strand and 108 ksi for wire.

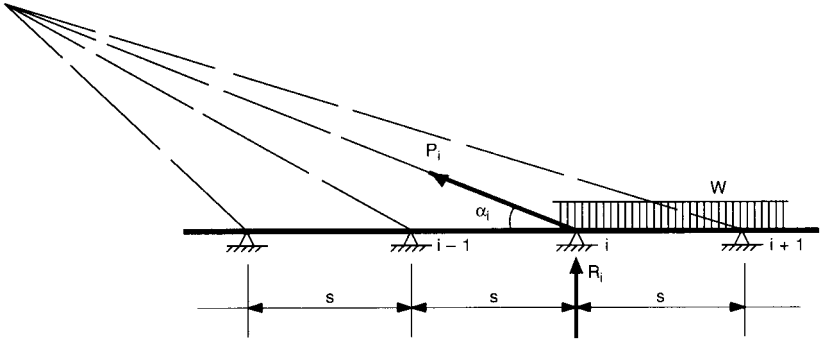

FIGURE 15.61 Cable-stayed girder is supported by cable force P_i at ith point of cable attachment. R_i is the vertical component of P_i.

The reactions may be taken as $R_i = ws$, where w is the uniform load, kips per ft, and s, the distance between stays. At the ends of the girder, however, R_i may have to be determined by other means.

Determination of the force P_o acting on the back-stay cable connected to the abutment (Fig. 15.62) requires that the horizontal force F_h at the top of the pylon be computed first. Maximum force on that cable occurs with dead plus live loads on the center span and dead load only on the side span. If the pylon top is assumed immovable, F_h can be determined from the sum of the forces from all the stays, except the back stay:

$$F_h = \sum \frac{R_i}{\tan \alpha_i} - \sum \frac{R_i'}{\tan \alpha_i'} \tag{15.49}$$

where R_i, R_i' = vertical component of force in the ith stay in the main span and side span, respectively
α_i, α_i' = angle between girder and the ith stay in the main span and side span, respectively

Figure 15.63 shows only the pylon and back-stay cable to the abutment. If, in Fig. 15.63, the change in the angle α_o is assumed to be negligible as F_h deflects the pylon top, the load in the back stay can be determined from

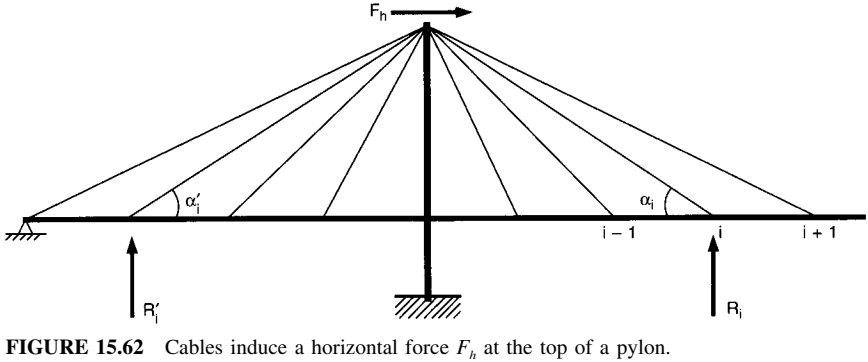

FIGURE 15.62 Cables induce a horizontal force F_h at the top of a pylon.

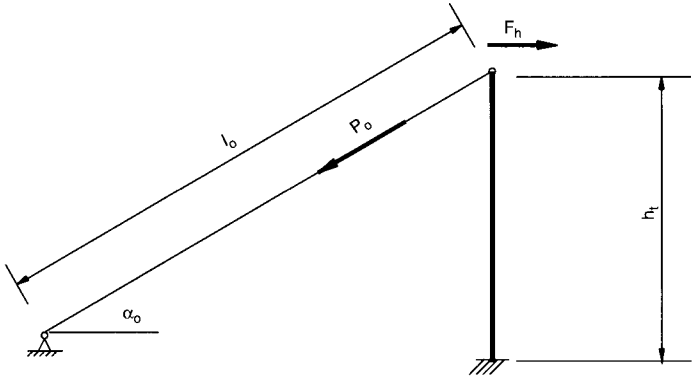

FIGURE 15.63 Cable force P_o in backstay to anchorage and bending stresses in the pylon resist horizontal force F_h at the top of the pylon.

$$P_o = \frac{F_h h_t^3 \cos \alpha_o}{3l_o(E_c I/E_s A_s) + h_t^3 \cos^2 \alpha_o} \tag{15.50}$$

If the bending stiffness $E_c I$ of the pylon is neglected, then the back-stay force is given by

$$P_o = F_h / \cos \alpha_o \tag{15.51}$$

where h_t = height of pylon
l_o = length of back stay
E_c = modulus of elasticity of pylon material
I = moment of inertia of pylon cross section
E_s = modulus of elasticity of cable steel
A_s = cross-sectional area of back-stay cable

For the structure illustrated in Fig. 15.64, values were computed for a few stays from Eqs. (15.47), (15.48), (15.49), and (15.51) and tabulated in Table 15.11*a*. Values for the final design, obtained by computer, are tabulated in Table 15.11*b*.

Inasmuch as cable stays 1, 2, and 3 in Fig. 15.64 are anchored at either side of the anchor pier, they are combined into a single back-stay for purposes of manual calculations. The edge girders of the deck at the anchor pier were deepened in the actual design, but this increase in dead weight was ignored in the manual solution. Further, the simplified manual solution does not take into account other load cases, such as temperature, shrinkage, and creep.

Influence lines for stay forces and girder moments are determined by treating the girder as a continuous, elastically supported beam. From Fig. 15.65, the following relationships are obtained for a unit force at the connection of girder and stay:

$$P_i = \frac{1}{\sin \alpha_i} \qquad \Delta l_{si} = \frac{P_i l_{si}}{A_{si} E_s} = \delta_i \sin \alpha_i$$

which lead to

$$\delta_i = \frac{l_{si}}{A_{si} E_s \sin^2 \alpha_i}$$

With Eq. (15.48) and $l_{si} = h_t \sin \alpha_i$, the deflection at point i is given by

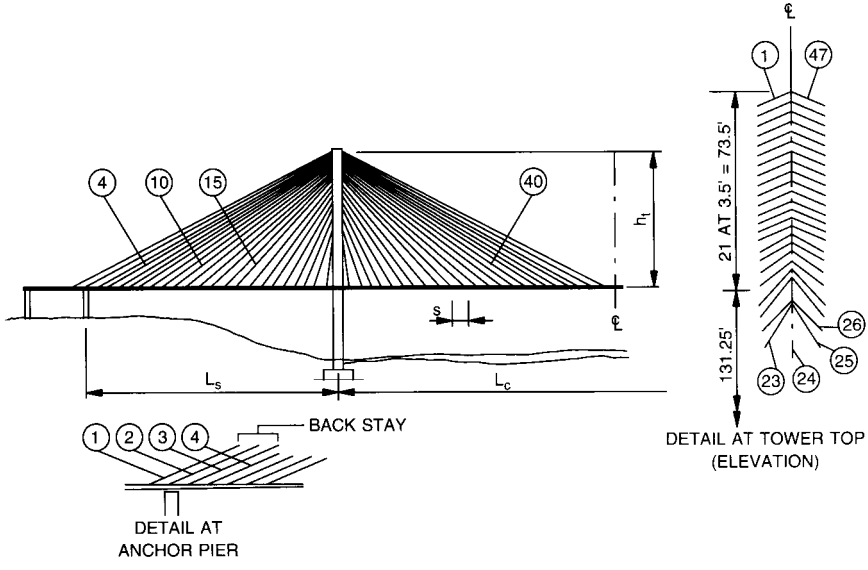

FIGURE 15.64 Half of a three-span cable-stayed bridge. Properties of components are as follows:

Girder		Tower	
Main span L_c	940 ft	Height h_d	204.75 ft
Side span L_b	440 ft	Area A	120 ft^2
Stay spacing s	20 ft	Moment of inertia I	3620 ft^4
Area A	101.4 ft	Elastic modulus E_t	45,000 ksi
Moment of inertia I	48.3 ft^4		
Elastic modulus E_g	47,000 ksi	Stays	
		Elastic modulus E_s	28,000 ksi

(*Reprinted with permission from W. Podolny, Jr., and J. B. Scalzi, "Construction and Design of Cable-Stayed Bridges," 2d ed., John Wiley & Sons, Inc. New York.*)

$$\delta_i = \frac{h_t \sigma_a}{R_i E_s \sin^2 \alpha_i} \tag{15.52}$$

With R_i taken as $s(w_{DL} + w_{LL})$, the product of the uniform dead and live loads and the stay spacing s, the spring stiffness of cable stay i is obtained as

$$k_i = \frac{1}{\delta_i s} = \frac{(w_{\mathrm{DL}} + w_{\mathrm{LL}}) E_s \sin^2 \alpha_i}{h_t \sigma_a} \tag{15.53}$$

For a vertical unit force applied on the girder at a distance x from the girder-stay connection, the equation for the cable force P_i becomes

$$P_i = \frac{\xi W s}{2 \sin \alpha_i} \eta_p \tag{15.54}$$

where $\eta_p = e^{-\xi x}(\cos \xi x + \sin \xi x)$

TABLE 15.11 Comparison of Manual and Computer Solution for the Stays in Fig. 15.64*

Stay number	(*a*) According to Eqs. (14.47), (14.48), (14.49), and (14.51)					(*b*) Computer solution			
	R_{DL}, kips	P_{DL}, kips	R_{DL+LL}, kips	P_{DL+LL}, kips	A, in^2	P_{DL}, kips	P_{DL+LL}, kips‡	Number of 0.6-in strands§	Strand area, in^2 §
Back stay‡	—	2596	—	3969	32.667	2775	3579	136	29.512
4	360	824	400	916	7.539	851	1049	40	8.680
10	360	684	400	760	6.255	695	797	31	6.727
15	360	550	400	611	5.029	558	654	25	5.425
40	360	734	400	815	6.708	756	878	34	7.378

*Reprinted with permission from W. Podolny, Jr., and J. B. Scalzi, "Construction and Design of Cable-Stayed Bridges," 2d ed., John Wiley & Sons, Inc., New York.
† Stays No. 1, 2, and 3 combined into one back stay.
‡ Maximum live load.
§ Per plane of a two-plane structure.

$$\xi = \sqrt[4]{\frac{k_i}{4E_c I}} \tag{15.55}$$

The bending moment M_i at point i may be computed from

$$M_i = \frac{W}{4\xi} e^{-\xi x}(\cos \xi x - \sin \xi x) = \frac{W}{4\xi} \eta_m \tag{15.56}$$

where $\eta_m = e^{-\xi x}(\cos \xi x - \sin \xi x)$.

(W. Podolny, Jr., and J. B. Scalzi, "Construction and Design of Cable-Stayed Bridges," 2d ed., John Wiley & Sons, Inc., New York.)

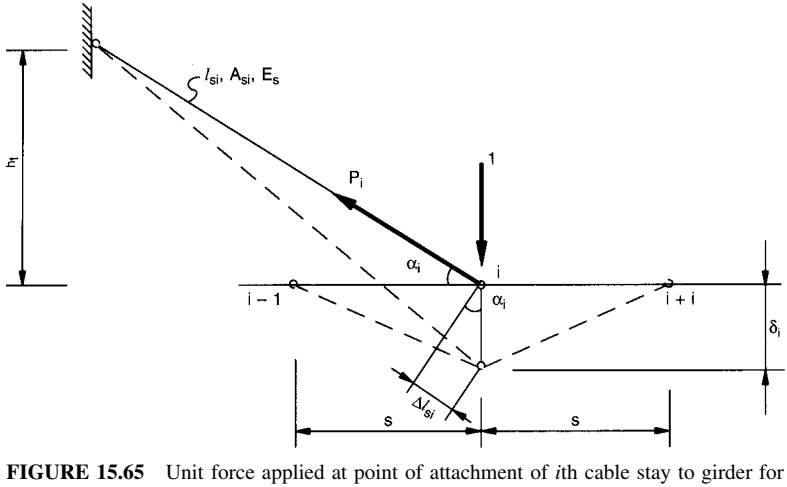

FIGURE 15.65 Unit force applied at point of attachment of *i*th cable stay to girder for determination of spring stiffness.

15.21 AERODYNAMIC ANALYSIS OF CABLE-SUSPENDED BRIDGES

The wind-induced failure on November 7, 1940, of the Tacoma Narrows Bridge in the state of Washington shocked the engineering profession. Many were surprised to learn that failure of bridges as a result of wind action was not unprecedented. During the slightly more than 12 decades prior to the Tacoma Narrows failure, 10 other bridges were severely damaged or destroyed by wind action (Table 15.12). As can be seen from Table 12*a*, wind-induced failures have occurred in bridges with spans as short as 245 ft up to 2800 ft. Other ''modern'' cable-suspended bridges have been observed to have undesirable oscillations due to wind (Table 15.12*b*).

15.21.1 Required Information on Wind at Bridge Site

Prior to undertaking any studies of wind instability for a bridge, engineers should investigate the wind environment at the site of the structure. Required information includes the character of strong wind activity at the site over a period of years. Data are generally obtainable from local weather records and from meteorological records of the U.S. Weather Bureau. However,

TABLE 15.12 Long-Span Bridges Adversely Affected by Wind*

(*a*) Severely damaged or destroyed

Bridge	Location	Designer	Span, ft	Failure date
Dryburgh Abbey	Scotland	John and William Smith	260	1818
Union	England	Sir Samuel Brown	449	1821
Nassau	Germany	Lossen and Wolf	245	1834
Brighton Chain Pier	England	Sir Samuel Brown	255	1836
Montrose	Scotland	Sir Samuel Brown	432	1838
Menai Straits	Wales	Thomas Telford	580	1839
Roche-Bernard	France	Le Blanc	641	1852
Wheeling	U.S.A.	Charles Ellet	1010	1854
Niagara-Lewiston	U.S.A.	Edward Serrell	1041	1864
Niagara-Clifton	U.S.A.	Samuuel Keefer	1260	1889
Tacoma Narrows I	U.S.A.	Leon Moisseiff	2800	1940

(*b*) Oscillated violently in wind

Bridge	Location	Year built	Span, ft	Type of stiffening
Fyksesund	Norway	1937	750	Rolled I beam
Golden Gate	U.S.A.	1937	4200	Truss
Thousand Island	U.S.A.	1938	800	Plate girder
Deer Isle	U.S.A.	1939	1080	Plate girder
Bronx-Whitestone	U.S.A.	1939	2300	Plate girder
Long's Creek	Canada	1967	713	Plate girder

* After F. B. Farquharson et al., ''Aerodynamic Stability of Suspension Bridges,'' University of Washington Bulletin 116, parts I through V. 1949–1954.

caution should be used, because these records may have been attained at a point some distance from the site, such as the local airport or federal building. Engineers should also be aware of differences in terrain features between the wind instrumentation site and the structure site that may have an important bearing on data interpretation. Data required are wind velocity, direction, and frequency. From these data, it is possible to predict high wind speeds, expected wind direction and probability of occurrence.

The aerodynamic forces that wind applies to a bridge depend on the velocity and direction of the wind and on the size, shape, and motion of the bridge. Whether resonance will occur under wind forces depends on the same factors. The amplitude of oscillation that may build up depends on the strength of the wind forces (including their variation with amplitude of bridge oscillation), the energy-storage capacity of the structure, the structural damping, and the duration of a wind capable of exciting motion.

The wind velocity and direction, including vertical angle, can be determined by extended observations at the site. They can be approximated with reasonable conservatism on the basis of a few local observations and extended study of more general data. The choice of the wind conditions for which a given bridge should be designed may always be largely a matter of judgment.

At the start of aerodynamic analysis, the size and shape of the bridge are known. Its energy-storage capacity and its motion, consisting essentially of natural modes of vibration, are determined completely by its mass, mass distribution, and elastic properties and can be computed by reliable methods.

The only unknown element is that factor relating the wind to the bridge section and its motion. This factor cannot, at present, be generalized but is subject to reliable determination in each case. Properties of the bridge, including its elastic forces and its mass and motions (determining its inertial forces), can be computed and reduced to model scale. Then, wind conditions bracketing all probable conditions at the site can be imposed on a section model. The motions of such a dynamic section model in the properly scaled wind should duplicate reliably the motions of a convenient unit length of the bridge. The wind forces and the rate at which they can build up energy of oscillation respond to the changing amplitude of the motion. The rate of energy change can be measured and plotted against amplitude. Thus, the section-model test measures the one unknown factor, which can then be applied by calculation to the variable amplitude of motion along the bridge to predict the full behavior of the structure under the specific wind conditions of the test. These predictions are not precise but are about as accurate as some other features of the structural analysis.

15.21.2 Criteria for Aerodynamic Design

Because the factor relating bridge movement to wind conditions depends on specific site and bridge conditions, detailed criteria for the design of favorable bridge sections cannot be written until a large mass of data applicable to the structure being designed has been accumulated. But, in general, the following criteria for suspension bridges may be used:

- A truss-stiffened section is more favorable than a girder-stiffened section.
- Deck slots and other devices that tend to break up the uniformity of wind action are likely to be favorable.
- The use of two planes of lateral system to form a four-sided stiffening truss is desirable because it can favorably affect torsional motion. Such a design strongly inhibits flutter and also raises the critical velocity of a pure torsional motion.
- For a given bridge section, a high natural frequency of vibration is usually favorable:

  For short to moderate spans, a useful increase in frequency, if needed, can be attained by increased truss stiffness. (Although not closely defined, moderate spans may be regarded

as including lengths from about 1,000 to about 1,800 ft.)

For long spans, it is not economically feasible to obtain any material increase in natural frequency of vertical modes above that inherent in the span and sag of the cable.

The possibility should be considered that for longer spans in the future, with their unavoidably low natural frequencies, oscillations due to unfavorable aerodynamic characteristics of the cross section may be more prevalent than for bridges of moderate span.

- At most bridge sites, the wind may be broken up; that is, it may be nonuniform across the site, unsteady, and turbulent. So a condition that could cause serious oscillation does not continue long enough to build up an objectionable amplitude. However, bear in mind:

  There are undoubtedly sites where the winds from some directions are unusually steady and uniform.

  There are bridge sections on which any wind, over a wide range of velocity, will continue to build up some mode of oscillation.

- An increase in stiffness arising from increased weight increases the energy-storage capacity of the structure without increasing the rate at which the wind can contribute energy. The effect is an increase in the time required to build up an objectionable amplitude. This may have a beneficial effect much greater than is suggested by the percentage increase in weight, because of the sharply reduced probability that the wind will continue unchanged for the greater length of time. Increased stiffness may give added structural damping and other favorable results.

Although more specific design criteria than the above cannot be given, it is possible to design a suspension bridge with a high degree of security against aerodynamic forces. This involves calculation of natural modes of motion of the proposed structure, performance of dynamic-section-model tests to determine the factors affecting behavior, and application of these factors to the prototype by suitable analysis.

Most long-span bridges built since the Tacoma bridge failure have followed the above procedures and incorporated special provisions in the design for aerodynamic effects. Designers of these bridges usually have favored stiffening trusses over girders. The second Tacoma Narrows, Forth Road, and Mackinac Straits Bridges, for example, incorporate deep stiffening trusses with both top and bottom bracing, constituting a torsion space truss. The Forth Road and Mackinac Straights Bridges have slotted decks. The Severn Bridge, however, has a streamlined, closed-box stiffening girder and inclined suspenders. Some designs incorporate longitudinal cable stays, tower stays, or even transverse diagonal stays (Deer Isle Bridge). Some have unloaded backstays. Others endeavor to increase structural damping by frictional or viscous means. *All have included dynamic-model studies as part of the design.*

15.21.3 Wind-Induced Oscillation Theories

Several theories have been advanced as models for mathematical analysis to develop an understanding of the process of wind excitation. Among these are the following.

Negative-Slope Theory. When a bridge is moving downward while a horizontal wind is blowing (Fig. 15.66*a*), the resultant wind is angled upward (positive angle of attack) relative to the bridge. If the lift coefficient C_L, as measured in static tests, shows a variation with wind angle α such as that illustrated by curve *A* in Fig. 15.66*b*, then, for moderate amplitudes, there is a wind force acting downward on the bridge while the bridge is moving downward. The bridge will therefore move to a greater amplitude than it would without this wind force. The motion will, however, be halted and reversed by the action of the elastic forces. Then, the vertical component of the wind also reverses. The angle of attack becomes negative, and the lift becomes positive, tending to increase the amplitude of the rebound. With increasing velocity, the amplitude will increase indefinitely or until the bridge is de-

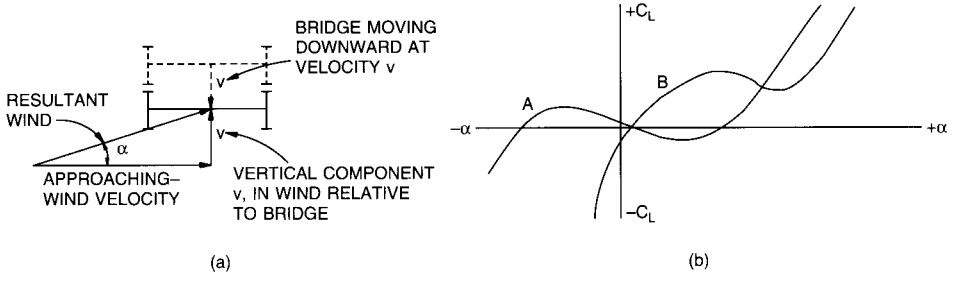

FIGURE 15.66 Wind action on a cable-stayed bridge. (*a*) Downward bridge motion develops upward wind component. (*b*) Lift coefficient C_L depends on angle of attack α of the wind.

stroyed. A similar, though more complicated situation, would apply for torsional or twisting motion of the bridge.

Vortex Theory. This attributes aerodynamic excitation to the action of periodic forces having a certain degree of resonance with a natural mode of vibration of the bridge. Vortices, which form around the trailing edge of the airfoil (bridge deck), are shed on alternating sides, giving rise to periodic forces and oscillations transverse to the deck.

Flutter Theory. The phenomenon of flutter, as developed for airfoils of aircraft and applied to suspension-bridge decks, relates to the fact that the airfoil (bridge deck) is supported so that it can move elastically in a vertical direction and in torsion, about a longitudinal axis. Wind causes a lift that acts eccentrically. This causes a twisting moment, which, in turn, alters the angle of attack and increases the lift. The chain reaction becomes catastrophic if the vertical and torsional motions can take place at the same coupled frequency and in appropriate phase relation.

F. Bleich presented tables for calculation of flutter speed v_F for a given bridge, based on flat-plate airfoil flutter theory. These tables are applicable principally to trusses. But the tables are difficult to apply, and there is some uncertainty as to their range of validity.

A. Selberg has presented the following formula for flutter speed:

$$v_F = 0.88\omega_2 b \sqrt{\left[1 - \left(\frac{\omega_1}{\omega_2}\right)^2\right] \frac{\sqrt{v}}{\mu}} \tag{15.57}$$

where v = mass distribution factor for specific section = $2r^2/b^2$ (varies between 0.6 and 1.5, averaging about 1)
μ = $2\pi\rho b^2/m$ (ranges between 0.01 and 0.12)
m = mass per unit length
b = half width of bridge
ρ = mass density of air
ω_1 = circular vertical frequency
ω_2 = circular torsional frequency
r = mass radius of gyration

Selberg has also published charts, based on tests, from which it is possible to approximate the critical wind speed for any type of cross section in terms of the flutter speed.

Applicability of Theories. The vortex and flutter theories apply to the behavior of suspension bridges under wind action. Flutter appears dominant for truss-stiffened bridges, whereas vortex action seems to prevail for girder-stiffened bridges. There are mounting indications, however, these are, at best, estimates of aerodynamic behavior. Much work has been done

and is being done, particularly in the spectrum approach and the effects of nonuniform, turbulent winds.

15.21.4 Design Indices

Bridge engineers have suggested several criteria for practical design purposes. O. H. Ammann, for example, developed two analytical-empirical indices that were applied in the design of the Verrazano Narrows Bridge, a vertical-stiffness index and a torsional-stiffness index.

Vertical-Stiffness Index S_v. This is based on the magnitude of the vertical deflection of the suspension system under a static downward load covering one-half the center span. The index includes a correction to allow for the effect of structural damping of the suspended structure and for the effect of different ratios of side span to center span.

$$S_v = \left(8.2\,\frac{W}{f} + 0.14\,\frac{I}{L^4}\right)\left(1 - 0.6\,\frac{L_1}{L}\right) \tag{15.58}$$

where W = weight of bridge, lb per lin ft
f = cable sag, ft
I = moment of inertia of stiffening trusses and continuous stringers, in^2 by ft^2
L = length of center span, in thousands of feet
L_1 = length of side span, in thousands of feet

Torsional-Stiffness Index S_t. This is defined as the maximum intensity of sinusoidal loads, of opposite sign in opposite planes of cables, on the center span and producing 1-ft deflections at quarter points of the main span. This motion simulates deformations similar to those in the first asymmetric mode of torsional oscillations.

$$S_t = \left(\frac{B}{A} + 1\right)\frac{\pi^2}{4}\,\frac{W}{f} \tag{15.59}$$

where $A = \dfrac{b^2}{2}\,\dfrac{H_w}{E}$

$B = \dfrac{2bd(A_v U_v A_h U_h)}{(b/d)A_v U_v + (d/b)A_h U_h}$

W = weight of bridge, lb per lin ft
f = cable sag, ft
H_w = horizontal component of cable load due to dead load (half bridge), kips
b = distance between centerlines of cables, or centerlines of pairs of cables, ft
d = vertical distance between top and bottom planes of lateral bracing, ft
E = modulus of elasticity of truss steel, ksf
A_v = area of the diagonals in one panel of vertical truss, ft^2
A_h = area of diagonals in one panel of horizontal lateral bracing (two members for X or K bracing), ft^2
$U_v = \sin^2 \gamma_v \cos \gamma_v$
$U_h = \sin^2 \gamma_h \cos \gamma_h$
γ_h = angle between diagonals and chord of horizontal truss
γ_v = angle between diagonals and chord of vertical truss

Typical values of these indices are listed in Table 15.13 for several bridges.

Other indices and criteria have been published by D. B. Steinman. In connection with these, Steinman also proposed that, unless aerodynamic stability is otherwise assured, the

TABLE 15.13 Stiffness Indices and First Asyymmetric Mode Natural Frequencies*

Bridge	Structural parameters									Vertical motions		Torsional motions	
	L, ft	L_1, ft	f, ft	W, lb per ft	I, in^2 ft^2	b, ft	d, ft	A, ft^4	B, ft^4	Stiffness index	Frequency, cycles per min	Stiffness index	Frequency, cycles per min
Verrazano Narrows Bridge	4,260	1,215	390	36,650	180,000	101.25	24	130.8	144.5	702	6.2	448	11.9
George Washington, Bridge, 8-lane single deck complete	3,500	650	319	28,570	168	106	—	—	—	654	6.7	221	8.2
George Washington Bridge, 14-lane double deck complete	3,500	650	326	40,000	66,000	106	30	126.5	163.7	950	6.7	694	13.2
Golden Gate Bridge with upper lateral system only	4,200	1,125	475	21,300	88,000	90	—	—	—	342	5.6	111	7.0
Golden Gate Bridge with double lateral system	4,200	1,125	475	22,800+	88,000	90	25	51.3	75.5	364	5.6	292	11.0
Tacoma Narrows original with 2-lane single deck (very unfavorable aero-dynamic characteristics)	2,800	1,100	232	5,700	2,567	39	—	—	—	158	8.0	61	10.0

* From M. Brumer, H. Rothman, M. Fiegen, and B. Forsyth, ''Verrazano-Narrows Bridge: Design of Superstructure,'' *Journal of the Construction Division,* vol. 92, no. CO2, March 1966, American Society of Civil Engineers.

depth, ft, of stiffening girders and stiffening trusses should be at least $L/120 + (L/1{,}000)^2$, where L is the span, ft. Furthermore, EI of the stiffening system should be at least $bL^4/120\sqrt{f}$, where b is the width, ft, of the bridge and f the cable sag, ft.

15.21.5 Natural Frequencies of Suspension Bridges

Dynamic analyses require knowledge of the natural frequencies of free vibration, modes of motion, energy-storage relationships, magnitude and effects of damping, and other factors.

Two types of vibration must be considered: bending and torsion.

Bending. The fundamental differential equation [Eq. (15.22)] and cable condition [Eq. (15.26)] of the suspension bridge in Fig. 15.46 can be transformed into

$$EI\eta'''' - H\eta'' = \omega^2 m\eta + H_p y'' \tag{15.60}$$

$$\frac{H_p L_c}{E_c A_c} + y'' \int_0^L \eta \, dx = 0 \tag{15.61}$$

where ω = circular natural frequency of the bridge
η = deflection of stiffening truss or girder
m = bridge mass = w/g
y = vertical distance from cable to the line through the pylon supports
w = dead load, lb per lin ft
g = acceleration due to gravity = 32.2 ft/s^2

From these equations, the basic Rayleigh energy equation for bending vibrations can be derived:

$$\int EI\eta''^2 \, dx + H \int \eta'^2 \, dx + \frac{E_c A_c}{L_c} \left(y'' \int \eta \, dx \right)^2 = \omega^2 \int m \, \eta^2 \, dx \tag{15.62}$$

Symbols are defined in "Torsion," following. After ω has been determined from this, the natural frequency of the bridge $\omega/2\pi$, Hz, can be computed.

Torsion. The Rayleigh energy equations for torsion are

$$EC_s \int \phi''^2 \, dx + \left(GI_T + \frac{b^2 H}{2} \right) \int \phi'^2 \, dx + \frac{E_c A_c}{2L_c} \left(y'' b \int \phi \, dx \right)^2 + EI_y y_M \int \eta'' \phi'' \, dx = \omega^2 I_p \int \phi^2 \, dx \tag{15.63}$$

$$EI_y y_M \int \phi'' \eta'' \, dx + EI_y \int \eta''^2 \, dx = \omega^2 m \int \eta^2 \, dx \tag{15.64}$$

where ϕ = angle of twist, radians
E = modulus of elasticity of stiffening girder, ksf
G = modulus of rigidity of stiffening girder, ksf
I_T = polar moment of inertia of stiffening girder cross section, ft^4
I_p = mass moment of inertia of stiffening girder per unit of length, kips-sec^2
I_v = moment of inertia of stiffening girder about its vertical axis, ft^4
C_s = warping resistance of stiffening girder relative to its center of gravity, ft^6
b = horizontal distance between cables, ft
H = horizontal component of cable tension, kips

A_c = cross-sectional area of cable, ft^2
E_c = modulus of elasticity of cable, ksf
L_c = $\int \sec^3 \alpha \, dx$
α = angle cable makes with horizontal, radians
y_M = ordinate of center of twist relative to the center of gravity of stiffening girder cross section, ft
ω = circular frequency, radians per sec
$m = m(x)$ = mass of stiffening girder per unit of length, kips-sec^2/ft^2

Solution of these equations for the natural frequencies and modes of motion is dependent on the various possible static forms of suspension bridges involved (see Fig. 15.9). Numerous lengthy tabulations of solutions have been published.

15.21.6 Damping

Damping is of great importance in lessening of wind effects. It is responsible for dissipation of energy imparted to a vibrating structure by exciting forces. When damping occurs, one part of the external energy is transformed into molecular energy, and another part is transmitted to surrounding objects or the atmosphere. Damping may be internal, due to elastic hysteresis of the material or plastic yielding and friction in joints, or Coulomb (dry friction), or atmospheric, due to air resistance.

15.21.7 Aerodynamics of Cable-Stayed Bridges

The aerodynamic action of cable-stayed bridges is less severe than that of suspension bridges, because of increased stiffness due to the taut cables and the widespread use of torsion box decks. However, there is a trend towards the use of the composite steel-concrete superstructure girders (Fig. 15.16) for increasingly longer spans and to reduce girder dead weight. This configuration, because of the long spans and decreased mass, can be relatively more sensitive to aerodynamic effects as compared to a torsionally stiff box.

15.21.8 Stability Investigations

It is most important to note that the validation of stability of the completed structure for expected wind speeds at the site is mandatory. However, this does not necessarily imply that the most critical stability condition of the structure occurs when the structure is fully completed. A more dangerous condition may occur during erection, when the joints have not been fully connected and, therefore, full stiffness of the structure has not yet been realized. In the erection stage, the frequencies are lower than in the final condition and the ratio of torsional frequency to flexural frequency may approach unity. Various stages of the partly erected structure may be more critical than the completed bridge. The use of welded components in pylons has contributed to their susceptibility to vibration during erection.

Because no exact analytical procedures are yet available, wind-tunnel tests should be used to evaluate the aerodynamic characteristics of the cross section of a proposed deck girder, pylon, or total bridge. More importantly, the wind-tunnel tests should be used during the design process to evaluate the performance of a number of proposed cross sections for a particular project. In this manner, the wind-tunnel investigations become a part of the design decision process and not a postconstruction corrective action. If the wind-tunnel evaluations are used as an after-the-fact verification and they indicate an instability, there is the distinct risk that a redesign of a retrofit design will be required that will have undesirable ramifications on schedules and availability of funding.

(F. Bleich and L. W. Teller, ''Structural Damping in Suspension Bridges,'' *ASCE Transactions,* vol. 117, pp. 165–203, 1952.

F. Bleich, C. B. McCullough, R. Rosecrans, and G. S. Vincent, ''The Mathematical Theory of Vibration of Suspension Bridges,'' Bureau of Public Roads, Government Printing Office, Washington, D.C.

F. B. Farquharson, ''Wind Forces on Structures Subject to Oscillation,'' *ASCE Proceedings,* ST4, July, 1958.

A. Selberg, ''Oscillation and Aerodynamic Stability of Suspension Bridges,'' *Acta Polytechnia Scandinavica,* Civil Engineering and Construction Series 13, Trondheim, 1961.

D. B. Steinman, ''Modes and Natural Frequencies of Suspension Bridge Oscillations,'' *Transactions Engineering Institute of Canada,* vol. 3, no. 2, pp. 74–83, 1959.

D. B. Steinman, ''Aerodynamic Theory of Bridge Oscillations,'' *ASCE Transactions,* vol. 115, pp. 1180–1260, 1950.

D. B. Steinman, ''Rigidity and Aerodynamic Stability of Suspension Bridges,'' *ASCE Transactions,* vol. 110, pp. 439–580, 1945.

''Aerodynamic Stability of Suspension Bridges,'' 1952 Report of the Advisory Board on the Investigation of Suspension Bridges, *ASCE Transactions,* vol. 120, pp. 721–781, 1955.)

R. L. Wardlaw, ''A Review of the Aerodynamics of Bridge Road Decks and the Role of Wind Tunnel Investigation,'' U. S. Department of Transportation, Federal Highway Administration, Report No. FHWA-RD-72-76.

A. G. Davenport, ''Buffeting of a Suspension Bridge by Storm Winds,'' *ASCE Journal of the Structural Division,* vol. 115, ST3, June 1962.

''Guidelines for Design of Cable-Stayed Bridges,'' ASCE Committee on Cable-Stayed Bridges.

W. Podolony, Jr., and J. B. Scalzi, ''Construction and Design of Cable-Stayed Bridges,'' 2d ed., John Wiley & Sons, Inc., New York.

E. Murakami and T. Okubu, ''Wind-Resistant Design of a Cable-stayed Bridge,'' International Association for Bridge and Structural Engineering, Final Report, 8th Congress, New York, September 9–14, 1968.)

15.21.9 Rain-Wind Induced Vibration

Well known mechanisms of cable vibration are vortex and wake galloping. Starting in approximately the mid-1980's, a new phenomenon of cable vibration has been observed that occurs during the simultaneous presence of rain and wind, thus, it is given the name ''rain-wind vibration,'' or rain vibration.

The excitation mechanism is the formation of water rivulets, at the top and bottom, that run down the cable oscillating tangentially as the cables vibrate, thus changing the aerodynamic profile of the cable (or the enclosing HDPE pipe). The formation of the upper rivulet appears to be the more dominant factor in the origin of the rain-wind vibration.

In the current state-of-the-art, three basic methods of rain-wind vibration suppression are being considered or used:

- Rope ties interconnecting the cable stays in the plane of the stays, Fig. 15.67*a*
- Modification of the external surface of the enclosing HDPE pipe, Fig. 15.67*b*
- Providing external damping

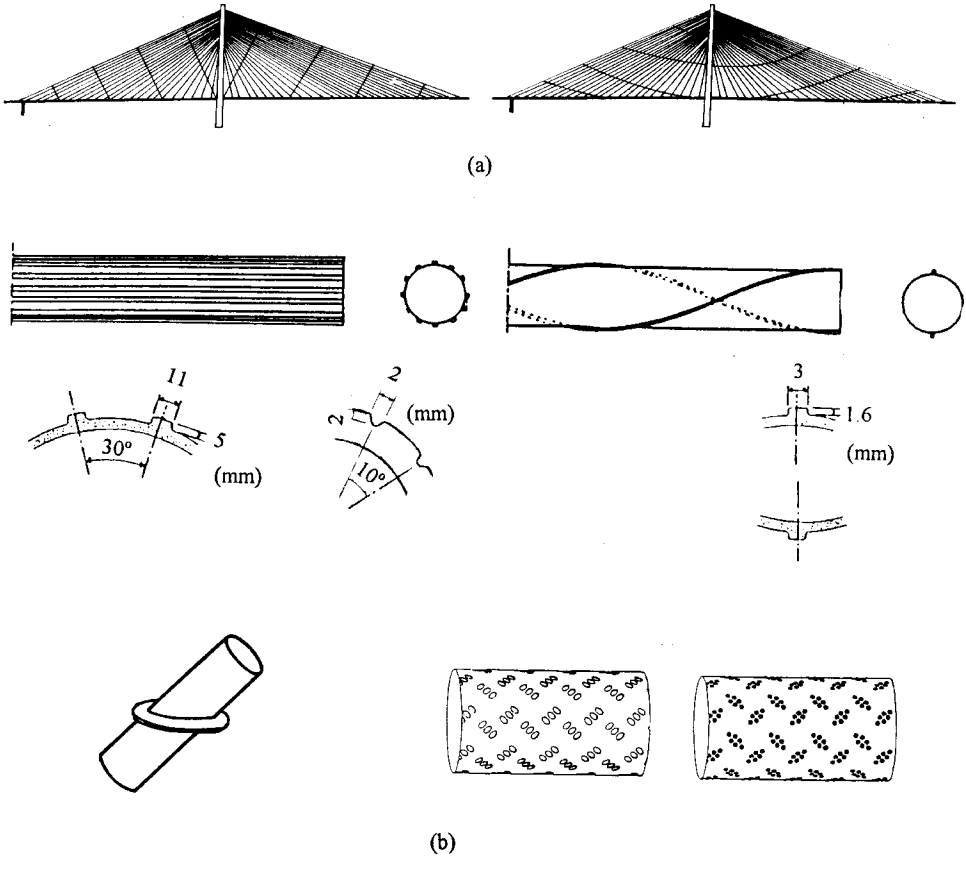

FIGURE 15.67 Methods of rain-wind vibration suppression. (*a*) Rope ties. (*b*) Modification of external surface.

The interconnection of stays by rope ties produces node points at the point of connection of the secondary tie to the cable stays. The purpose is to shorten the free length of the stay and modify the natural frequency of vibration of the stay. The modification of the surface may be such as protuberances that are axial, helical, elliptical or circular or grooves or dimples. The intent is to discourage the formation of the rivulets and/or its oscillations. Various types of dampers such as viscous, hydraulic, tuned mass and rubber have also been used to suppress the vibration.

The rain-wind vibration phenomenon has been observed during construction prior to grout injection which then stabilizes after grout injection. This may be as a result of the difference in mass prior to and after grout injection (or not). It also has been noticed that the rain-wind vibration may not manifest itself until some time after completion of the bridge. This may be the results of a transition from initial smoothness of the external pipe to a roughness, sufficient to hold the rivulet, resulting from an environmental or atmospheric degradation of the surface of the pipe.

The interaction of the various parameters in the rain-wind phenomenon is not yet well understood and an optimum solution is not yet available. It should also be noted that under

similar conditions of rain and wind, the hangars of arch bridges and suspenders of suspension bridges can also vibrate.

(Y. Hikami and N. Shiraishi, ''Rain-Wind Induced Vibrations of Cable in Cable Stayed Bridges,'' *Journal of Wind Engineering and Industrial Aerodynamics,* 29 (1988) pp. 409–418, Elsevier Science Publishers B. V., Amsterdam.

Matsumoto, M., Shiraishi, N., Kitazawa, M., Kinsely, C., Shirato, H., Kim, Y. and Tsujii, ''Aerodynamic Behavior of Inclined Circular Cylinders—Cable Aerodynamics,'' *Journal of Wind Engineering* (Japan), no. 37, October 1988, pp. 103–112.

Matsumoto, M., Yokoyama, K., Miyata, T., Fujno, Y. and Yamaguchi, H., ''Wind-Induced Cable Vibration of Cable-Stayed Bridges in Japan,'' Proc. of Canada-Japan Workshop on Bridge Aerodynamics, Ottawa, 1989, pp. 101–110.

Matsumoto, M., Hikami, Y. and Kitazawa, M., ''Cable Vibration and its Aerodynamic/Mechanical Control,'' Proc. Cable-Stayed and Suspension Bridges, Deauville, France, October 12–15, 1994, vol. 2, pp. 439–452.

Miyata, T., Yamada, H. and Hojo, T., ''Aerodynamic Response of PE Stay Cables with Pattern-Indented Surface,'' Proc. Cable-Stayed and Suspension Bridges, Deauville, France, October 12–15, 1994, vol. 2, pp. 515–522.)

15.22 SEISMIC ANALYSIS OF CABLE-SUSPENDED STRUCTURES

For short-span structures (under about 500 ft) it is commonly assumed in seismic analysis that the same ground motion acts simultaneously throughout the length of the structure. In other words, the wavelength of the ground waves are long in comparison to the length of the structure. In long-span structures, such as suspension or cable-stayed bridges, however, the structure could be subjected to different motions at each of its foundations. Hence, in assessment of the dynamic response of long structures, the effects of traveling seismic waves should be considered. Seismic disturbances of piers and anchorages may be different at one end of a long bridge than at the other. The character or quality of two or more inputs into the total structure, their similarities, differences, and phasings, should be evaluated in dynamic studies of the bridge response.

Vibrations of cable-stayed bridges, unlike those of suspension bridges, are susceptible to a unique class of vibration problems. Cable-stayed bridge vibrations cannot be categorized as vertical (bending), lateral (sway), and torsional; almost every mode of vibration is instead a three-dimensional motion. Vertical vibrations, for example, are introduced by both longitudinal and lateral shaking in addition to vertical excitation. In addition, an understanding is needed of the multimodal contribution to the final response of the structure and in providing representative values of the response quantities. Also, because of the long spans of such structures, it is necessary to formulate a dynamic response analysis resulting from the multisupport excitation. A three-dimensional analysis of the whole structure and substructure to obtain the natural frequencies and seismic response is advisable. A qualified specialist should be consulted to evaluate the earthquake response of the structure.

(''Guide Specifications for Seismic Design of Highway Bridges,'' American Association of State Highway and Transportation Officials; ''Guidelines for the Design of Cable-Stayed Bridges,'' ASCE Committee on Cable-Stayed Bridges.

A. M. Abdel-Ghaffar, and L I. Rubin, ''Multiple-Support Excitations of Suspension Bridges,'' *Journal of the Engineering Mechanics Division,* ASCE, vol. 108, no. EM2, April, 1982.

A. M. Abdel-Ghaffar, and L. I. Rubin, ''Vertical Seismic Behavior of Suspension Bridges,'' *The International Journal of Earthquake Engineering and Structural Dynamics,* vol. 11, January–February, 1983.

A. M. Abdel-Ghaffar, and L. I. Rubin, ''Lateral Earthquake Response of Suspension Bridges,'' *Journal of the Structural Division,* ASCE, vol. 109, no ST3, March, 1983.

A. M. Abdel-Ghaffar, and J. D. Rood, ''Simplified Earthquake Analysis of Suspension Bridge Towers,'' *Journal of the Engineering Mechanics Division,* ASCE, vol. 108, no. EM2, April, 1982.)

15.23 ERECTION OF CABLE-SUSPENDED BRIDGES

The ease of erection of suspension bridges is a major factor in their use for long spans. Once the main cables are in position, they furnish a stable working base or platform from which the deck and stiffening truss sections can be raised from floating barges or other equipment below, without the need for auxiliary falsework. For the Severn Bridge, for example, 60-ft box-girder deck sections were floated to the site and lifted by equipment supported on the cables.

Until the 1960s, the field process of laying the main cables had been by spinning (Art. 15.12.3). (this term is actually a misnomer, for the wires are neither twisted nor braided, but are laid parallel to and against each other.) The procedure (Fig. 15.68) starts with the hanging of a catwalk at each cable location for use in construction of the bridge. An overhead cableway is then installed above each catwalk. Loops of wire (two or four at a time) are carried over the span on a set of grooved spinning wheels. These are hung from an endless hauling rope of the cableway until arrival at the far anchorage. There, the loops are pulled off the spinning wheels manually and placed around a semicircular strand shoe, which connects them by an eyebar or bolt linkage to the anchorage (Fig. 15.33). The wheels then start back to the originating anchorage. At the same time, another set of wheels carrying wires starts out from that anchorage. The loops of wire on the latter set of wheels are also placed manually around a strand shoe at their anchorage destination. Spinning proceeds as the wheels shuttle back and forth across the span. A system of counterweights keeps the wires under continuous tension as they are spun.

The wires that come off the bottom of the wheels (called dead wires) and that are held back by the originating anchorage are laid on the catwalk in the spinning process. The wires passing over the wheels from the unreelers and moving at twice the speed of the wheels, are called *live wires.*

As the wheels pass each group of wire handlers on the catwalks, the dead wires are temporarily clipped down. The live wires pass through small sheaves to keep them in correct order. Each wire is adjusted for level in the main and side spans with come-along winches, to ensure that all wires will have the same sag.

The cable is made of many strands, usually with hundreds of wires per strand (Art. 15.12). All wires from one strand are connected to the same shoe at each anchorage. Thus, there are as many anchorage shoes as strands. At saddles and anchorages, the strands maintain their identity, but throughout the rest of their length, the wires are compacted together by special machines. The cable usually is forced into a circular cross section of tightly bunched parallel wires.

The usual order of erection of suspension bridges is substructure, pylons and anchorages, catwalks, cables, suspenders, stiffening trusses, floor system, cable wrapping, and paving.

Cables are usually coated with a protective compound. The main cables are wrapped with wire by special machines, which apply tension, pack the turns tightly against one another, and at the same time advance along the cable. Several coats of protective material, such as paint, are then applied For alternative wrapping, see Art. 15.14.

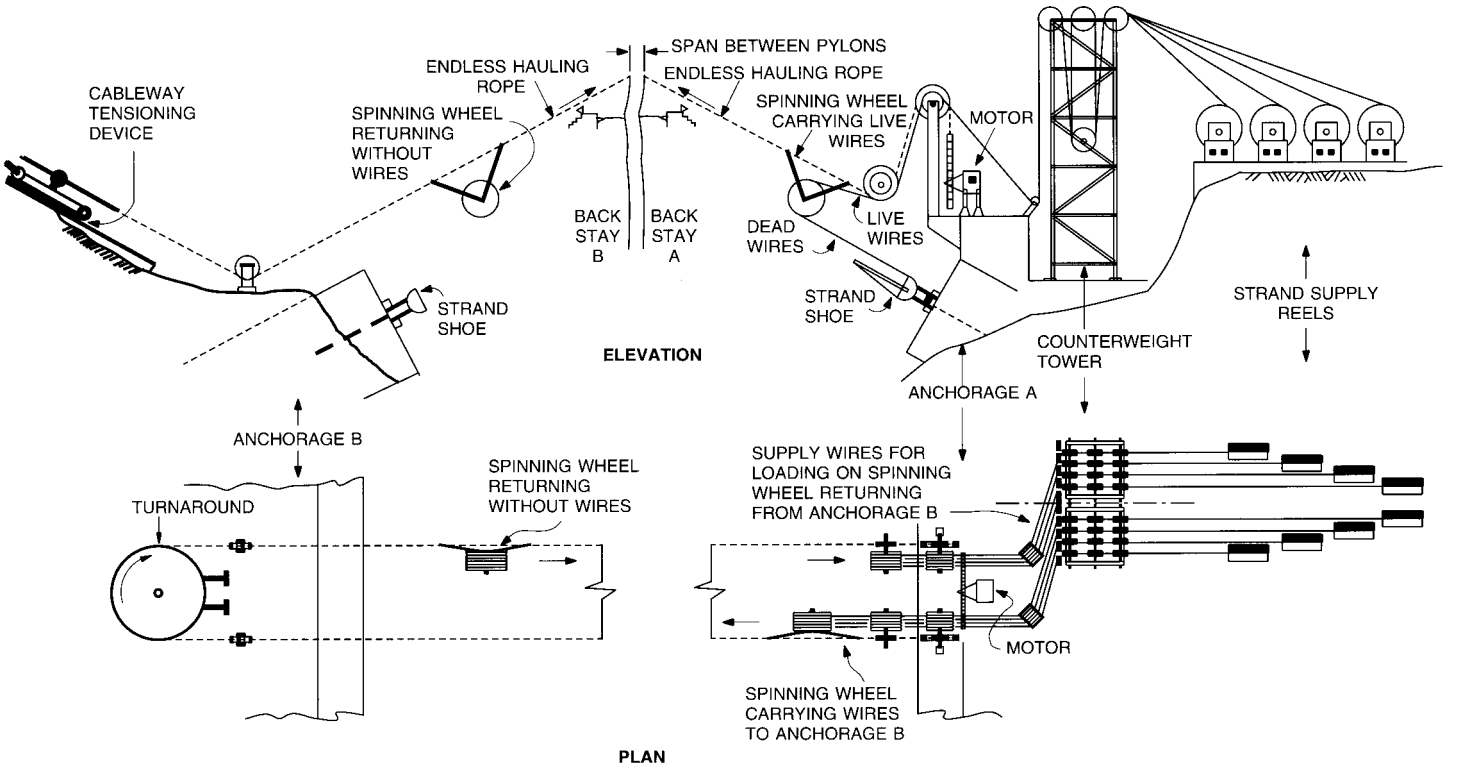

FIGURE 15.68 Scheme for spinning four wires at a time for the cables of the Forth Road Bridge.

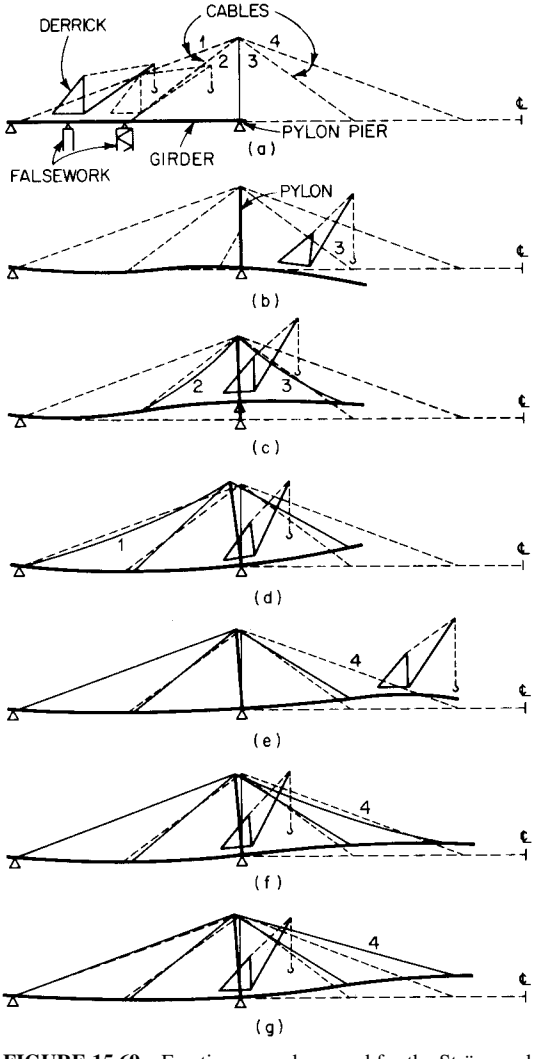

FIGURE 15.69 Erection procedure used for the Strömsund Bridge. (*a*) Girder, supported on falsework, is extended to the pylon pier. (*b*) Girder is cantilevered to the connection of cable 3. (*c*) Derrick is retracted to the pier and the girder is raised, to permit attachment of cables 2 and 3 to the girder. (*d*) Girder is reseated on the pier and cable 1 is attached. (*e*) Girder is cantilevered to the connection of cable 4. (*f*) Derrick is retracted to the pier and cable 4 is connected. (*g*) Preliminary stress is applied to cable 4. (*h*) Girder is cantilevered to midspan and spliced to its other half. (*i*) Cable 4 is given its final stress. (*j*) The roadway is paved, and the bridge takes its final position. (*Reprinted with permission from H. J. Ernst, "Montage Eines Seilverspannten Balkens im Grossbrucken-bau," Stahlbau, vol. 25, no. 5, May 1956.*)

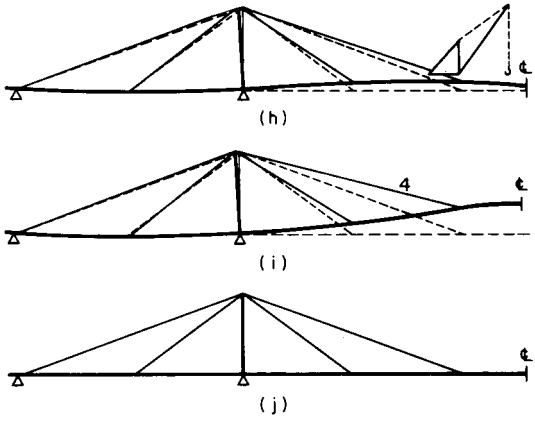

FIGURE 15.69 (*Continued*)

Typical cable bands are illustrated in Figs. 15.39 and 15.40. These are usually made of paired, semicylindrical steel castings with clamping bolts, over which the wire-rope or strand suspenders are looped or attached by socket fittings.

Cable-stayed structures are ideally suited for erection by cantilevering into the main span from the piers. Theoretically, erection could be simplified by having temporary erection hinges at the points of cable attachment to the girder, rendering the system statically determinate, then making these hinges continuous after dead load has been applied. The practical implementation of this is difficult, however, because the axial forces in the girder are larger and would have to be concentrated in the hinges. Therefore, construction usually follows conventional tactics of cantilevering the girder continuously and adjusting the cables as necessary to meet the required geometrical and statical constraints. A typical erection sequence is illustrated in Fig. 15.69.

Erection should meet the requirements that, on completion, the girder should follow a prescribed gradient; the cables and pylons should have their true system lengths; the pylons should be vertical, and all movable bearings should be in a neutral position. To accomplish this, all members, before erection, must have a deformed shape the same as, but opposite in direction to, that which they would have under dead load. The girder is accordingly cambered, and also lengthened by the amount of its axial shortening under dead load. The pylons and cable are treated in similar manner.

Erection operations are aided by raising or lowering supports or saddles, to introduce prestress as required. All erection operations should be so planned that the stresses during the erection operations do not exceed those due to dead and live load when the structure is completed; otherwise loss of economy will result.